Spring 2016

Study of heat transfer phenomenon during natural convection

Muhammad Yousaf

STUDY OF HEAT TRANSFER PHENOMENON DURING NATURAL CONVECTION

by

MUHAMMAD YOUSAF

A DISSERTATION

Presented to the Faculty of the Graduate School of the

MISSOURI UNIVERSITY OF SCIENCE AND TECHNOLOGY

In Partial Fulfillment of the Requirements for the Degree

DOCTOR OF PHILOSOPHY

in

NUCLEAR ENGINEERING

2016

Approved by:
Shoaib Usman, Advisor
Ayodeji B. Alajo
Joshua P. Schlegel
Joseph D. Smith
Muthanna H. Al-Dahhan

PUBLICATION DISSERTATION OPTION

This dissertation has been prepared in the style utilized by International Journal of Heat and Mass Transfer. These pages consist of three separate papers (i.e. Paper I (4-46), Paper II (Pages 47-79), and Paper III (Pages 80-117)). Papers I and II have been submitted for publication, while Paper III has been published in the said journal.

ABSTRACT

The purpose of the present study was to numerically investigate the effects of the roughness elements on the heat transfer during natural convection. A computational algorithm was developed based on the Lattice Boltzmann method to conduct numerical study in two-dimensional rectangular cavities and Rayleigh-Bénard cell. A single relaxation time Bhatnagar-Gross-Krook model of Lattice Boltzmann method was used to solve the coupled momentum and energy equations in two-dimensional lattices. Computational model was validated against previous benchmark solutions, and a good agreement was found to exist. A Newtonian fluid of Prandtl (Pr) number 1.0 was considered for this numerical study. The range of Ra numbers was investigated from 10^3 to 10^6. The roughness was introduced in the form of sinusoidal elements on a hot, cold, and both the hot and cold walls of the cavities and Rayleigh-Bénard cell. The frequency or number of the roughness elements and the dimensionless amplitude (h/H) were varied from 2 to 10 and 0.015 to 0.15 respectively. Numerical results showed that thermal and hydrodynamic behaviors of the fluid were considerably affected in the presence of the roughness elements. A dimensionless amplitude of approximately 0.025 has no significant effects on the average heat transfer. In contrast, a dimensionless amplitude of ≥ 0.05 cause a degradation in the average heat transfer and delay in the onset of natural convection. The maximum reduction in the average heat transfer was calculated to be approximately 51 percent in the Rayleigh-Bénard convection when the roughness was present on both the hot and cold walls with a dimensionless amplitude of 0.15 and the number of roughness elements equal to 10.

ACKNOWLEDGMENTS

In the name of Allah Almighty, the most merciful and beneficial

The author cannot thank enough to Allah Almighty, for his abundant blessings upon him, and his guidance without which it would be impossible to be here today.

The author deems it a real privilege to express his sincere appreciation and thanks to his advisor, Shoaib Usman, PhD, for his financial, and moral support, and encouragement throughout this study. His valuable suggestions and guidance helped me to accomplish this goal. The author is also very grateful to all dissertation committee members for their valuable suggestions and guidance to improve this work, and their careful review of this dissertation. The author is also thankful to high performance computing department of Missouri S & T for their help and support.

The author may not be able to thank his beloved parents for their efforts, struggle and the most importantly their prayers to make this journey possible. The author gratefully appreciates the moral support, prayers and encouragement of his siblings, which always make him look forward, and without their support, it would not be possible for me to accomplish this goal. The author cannot forget to express special thanks and appreciations to his wife for her moral support, encouragement, and prayers and my adorable daughter Aiza. The author greatly appreciates all graduate students and my friends in Rolla for making my stay memorable and pleasurable.

Finally, the author, wishes to dedicate this dissertation to his parents.

TABLE OF CONTENTS

LIST OF ILLUSTRATIONS

PAPER III

LIST OF TABLES

SECTION

1. INTRODUCTION

1.1 MOTIVATION AND OBJECTIVES

Heat transfer through buoyancy induced natural convection has attracted a considerable attention due to its inherent reliability and diverse applications in engineering and technology. This is the most commonly studied aspect of heat transfer phenomenon not only because of its applications but a dynamical system rich in its characteristics. Natural convection phenomenon is studied to explore some complex aspects of fluid flow and heat transport like: transition from laminar to turbulent, boundary layer phenomenon, and different flow patterns.

The main focus of the heat transfer research is the enhancement of the heat transfer. This is not possible without understanding the role of surface characteristics. Because most of the flows in industry and in our environment from micro-scale devices to macro-scale are over surfaces with some degrees of the roughness present. Also, surface roughness is considered as the most effective method to augment the heat transfer. Therefore, a fundamental understanding of the role of surface roughness is necessary for energy efficient design of cooling systems from buildings to large scale nuclear reactors.

A literature survey showed that many studies were conducted experimentally, theoretically, and computationally in the presence of partitions, fins, and roughness elements. But these studies were limited to rectangular, square, and V-shaped groves of partitions and roughness elements respectively. Moreover, natural convection studies performed in the presence of the roughness elements have conflicting results. A rational conclusion may not be possible without investigating the role of all commercially available shapes of roughness elements in a laminar as well as turbulent region of flow.

Therefore, the main purpose of the present study, was to investigate the role of sinusoidal roughness elements. The sinusoidal roughness elements of varying dimensionless amplitude and frequency were located on isothermal walls. Different cases were studied by introducing the roughness elements on a hot, a cold, and both the hot and cold walls in a rectangular cavity of aspect ratio (H/L) 1.0 and 2.0, and Rayleigh-Bénard

cell. The investigation was performed keeping the dimensionless amplitude constant while varying the number of roughness elements and vice versa. Thermal and hydrodynamic behaviors of a Newtonian fluid were studied by analyzing streamlines, isotherms, and the average Nusselt number. Besides the traditional numerical techniques, studies were conducted by using an algorithm based on a single relaxation time Bhatnagr-Gross and Krook (BGK) model of LBM. The studies were performed in a two-dimensional geometries in a laminar region of flow.

1.2 LATTICE BOLTZMANN METHOD

The analysis of fluid flow and heat transfer phenomena with the help of numerical techniques using computer, is known as computational fluid dynamics (CFD). CFD is under constant development since its use in 1960 [1]. There are two basic approaches to solve transport equations namely: continuum and particle based [2]. Earlier numerical techniques using continuum approach are based on finite element (FEM) and finite difference methods (FDM) [3]. Other numerical technique which can be formulated by using FEM or FDM is known as finite volume method (FVM). This scale is called macro-scale.

Second approach, which is based on the assumption that the medium consists of a collection of small particles called atoms or molecules. This scale is called micro-scale and method to solve the equations with this assumption is known as molecular dynamics. The MD method is very useful to treat complex boundaries. But the only issue with this method is the lack of large computational resources [2]. MD is also the most suitable method for nano-scale fluid systems [4].

There is another method which lies in between two extremes known as macro and micro scale. This is called Lattice Boltzmann method (LBM). In this method, instead of individual particle, a collective behavior of particles known as distribution function is solved in lattice units (lu). This scale is known as meso-scale [2].

LBM basically originated from lattice gas automata (LGA) and was first introduced as a computational method by McNamara and Zannetti [4, 5]. The main challenge for the solution of collision terms was first introduced by Bhatnagr-Gross and Krook (BGK) model in 1954, which paved the way for extensive use in the field of CFD. A

kinetic theory based LBM simulates the fluid flow and heat transport by tracking a collection of particle represented by distribution function. This method has proven ability particularly for simulating interfacial dynamics and phenomena involving complex geometries. Being a mesoscopic method, inter particle forces are naturally incorporated [6]. Macroscopic Navier-Stokes equation can be deduced from LBM by using Chapman-Enskog expansion developed by Chapman and Enskog [2, 4].

There is no need to mention that LBM has achieved a great success in few decades, and has proved itself to be an alternative to traditional numerical methods [2]. It does have many advantages including: easy to implement on complex boundaries, easy to treat boundaries in the porous medium or irregular structures, solution of single and multiphase processes, evaporation and condensation. It is inherently easy to adapt for parallel computing. There is no need to solve Laplace equation at every time step [2, 4, 7]. Besides, many advantages, LBM also has some stability challenges especially for highly turbulent flows.

PAPER

I. INFLUENCE OF SURFACE ROUGHNESS ON HEAT TRANSFER DURING NATURAL CONVECTION

M. Yousaf, S. Anwar, and S. Usman

ABSTRACT: The influence of surface roughness on the flow field and heat transfer within a fluid trapped between two parallel horizontal plates was investigated. A single relaxation time Bhatnagr-Gross and Krook (BGK) model of the Lattice Boltzmann method (LBM) was used to solve coupled momentum and energy equations for 2D natural convection. A computational model was validated against well-established benchmark studies, and a good agreement was found for both square cavity and horizontal parallel plates. The range of Rayleigh numbers from 10^3 to $5x10^5$ was investigated for a Newtonian fluid of Prandtl number 1.0. Surface roughness in the form of sinusoidal roughness elements was introduced on hot wall, cold wall, and both walls simultaneously. The number of sinusoidal roughness elements was varying from 2 to 10, and dimensionless amplitude from 0.025 to 0.15. Both the hydrodynamic and the thermal behavior of fluid between two horizontal parallel plates with roughness present on boundaries, were studied by analyzing isotherms, velocity streamlines, and average heat transfer. The numerical results showed that a sinusoidal roughness amplitude above 0.025 impacts a fluid's hydrodynamics and thermal behavior even at a low Ra number. While a sinusoidal roughness of 0.025 or smaller seems to have no significant effects on heat transfer. A maximum reduction in heat transfer was found when roughness was present on both walls simultaneously. Presence of roughness also causes a delay in onset of natural convection, for example no natural convection was observed for a roughness of amplitude 0.15 on the Top/bottom plate even up to Ra = $5x10^3$.

Keywords: Natural convection, Nusselt number, Bénard convection, Laminar

1. Introduction

Rayleigh-Bénard, convection in which a fluid is trapped between two horizontal smooth plates, has been extensively studied most commonly and carefully in the flied of non-linear physics [8, 9]. Henri Bénard [10] was first who experimentally observed the formation of convection cells when a thin layer of fluid was heated from bottom. In fact, Bénard studied surface tension and thermo capillary convection which was later known as Bénard-Marangoni convection. First attempt to explain this cell formation theoretically was made by Lord Rayleigh [11] who studied convection due to thermally induced buoyancy force. There is a transition from conduction to natural convection when buoyancy force overcomes the viscous force which is represented by a non-dimensional number Rayleigh number (Ra) as shown in Equation 1[12].

$$Ra_H = \frac{g\beta\Delta T H^3}{\nu\alpha} \quad (1)$$

Because of its diverse applications in engineering and science, Rayleigh-Bénard convection research spans over a century [13]. One of the main focus of research is to find out ways to enhance heat transfer, which in turn results in efficient cooling systems and cost reduction[14]. This is not possible without a better understanding of surface topography and its effects on convective heat transfer as most of the flows are over surfaces other than smooth. In general, role of surface roughness is considered negligible during natural convection because of low flow velocities. However, a review study showed an increase in free convective heat transfer coefficient up to 100 percent for fluids like air, water, and oils [15]. Some general example of flows over rough surfaces can be found in oceanography, geophysics and geology, meteorology, and atmosphere [16].

A large volume of theoretical and experimental [17-20] studies have identified a relationship between the amount of heat transfer and Ra number for Rayleigh-Bénard convection with smooth top and bottom plates. The amount of heat transferred is quantified by “Nusselt Number (Nu)”, [21, 22]. These two governing dimensionless numbers Nu, and Ra have a power law relation [18, 21].

$$Nu = A(Ra)^B \quad (2)$$

The value of '*B*' provided by dimensional analysis is approximately 1/3 for Ra number > $5x10^4$, whereas, different studies reported slightly different values for smooth surfaces for the two coefficients [14, 16, 18, 23]. As surface roughness is one of the possible way to augment heat transfer, the studies regarding scaling or power law relation of Nu and Ra for such surfaces is limited to some simple shapes of roughness. Reported effects of surface roughness are conflicting in that there is no general agreement regarding enhancement or degradation of heat transfer due to surface roughness [16]. Praslov [24] experimentally studied effects of distributed roughness elements on surface of horizontal cylinder for Ra number 3×10^3 to 3×10^6 with air as a working fluid. He found a significant increase in heat transfer due to turbulization caused by the roughness. Chinnappa [25] performed experimental studies to observe role of V-grooves on free convection and proposed his best values for the coefficients in equation 2. He reported values of '*B*' and '*A*' as 0.36 and 0.054 respectively for $10^4 < Gr < 8 \times 10^4$, and 0.278 and 0.139 for $8 \times 10^4 < Gr < 10^6$ respectively. ElSherbiny et al. [26] experimentally studied the effects of V-shaped roughness elements on heat transfer with air as a working fluid for both horizontal and inclined cavities of aspect ratio greater than 12 and inclination from 0 to 60 degree. The range of Ra number in their study was < $4x10^6$, and dimensionless amplitude (h/H) of roughness elements as 1, 2.5, and 4. They found that V-corrugation delays onset of natural convection and causes a degradation in average heat transfer up to 50 percent. Saidi et al. [27] performed both numerical and experimental studies to find the role of sinusoidal rough surface on fluid flow and heat transfer. They concluded that vortex formation in shadow of roughness element significantly affect streamlines and isotherm behavior. Amin [28] numerically studied role of the rectangular roughness elements of varying amplitude in a square cavity by using finite element based code. He applied isothermal boundary conditions on horizontal, and adiabatic on vertical walls with a fluid of Pr number 10.0 and Ra number from 10^3 to 10^5. He concluded that onset of convection is delayed by the presence of roughness. He also observed a higher heat transfer for low Ra number region as compared to high Ra number. He observed a maximum decrement in heat transfer to be 61 percent for Ra number of 3×10^4.

Shen et al. [29] studied the role of V-shaped roughness of 3.175 mm height with a spacing of 6.35 mm on hot wall of a cylinder with aspect ratio (diameter/height) of 0.5

and 1 and filled with water. They found an increase in heat flux up to 20 percent due to presence of roughness which causes production of thermal plumes in the gap between grooves. They also reported that role of roughness depends on relative height of roughness to thickness of boundary layer. Villermaux [30] concluded that roughness can increase the value of '*B*' in equation 2 above for rough surface as compared to smooth when thickness of thermal boundary layer is smaller than roughness height. Du and Tong [31] experimentally studied effects of V-groove roughness elements with amplitude of 9.0 mm and spacing 18 mm on heat transfer in a cylindrical cell in turbulent region. An increase of over 76% in heat transfer was observed. The height of roughness in the case of Du and Tong [26] larger than thickness of thermal boundary layer. Ciliberto and Laroche [32] performed experiment to study the effects of randomly distributed roughness on bottom plate of cell. They concluded that the effect of roughness on scaling law depends on the dimension of the roughness compared with the thickness of boundary layer.

Prétot et al. [33] performed experimental and numerical studies to observe effects of sinusoidal bottom plate with uniform heat flux using finite difference method in laminar region of free convection for air and water. They found formation of eddies in the shadows of roughness elements with increasing amplitude of corrugation. A decrease of heat transfer as compared to smooth surface was reported when roughness amplitude is increased. Das and Mahmud [34] performed numerical studies using finite volume method for a cavity with an aspect ratio (L/H) 2 having wavy horizontal walls and straight vertical walls. They observed no significant effect of waviness on heat transfer. Stringano et al. [14] performed direct numerical simulations of a fluid of Pr number 0.7 in a cylinder with an aspect ratio (diameter/height) of 0.5 with 0.025h ('*h*' is height of cylinder) V-grooves of amplitude on the hot plate. They found an increase in heat transfer when thickness of thermal boundary layer was smaller than roughness height. They pointed out the role of eddies formation leading to heat transfer enhancement in turbulent region. Tisserand et al. [35] studied Rayleigh-Bénard convection experimentally with smooth cold wall and hot bottom wall with square roughness elements of height 2.0 mm. They found an increase in heat transfer up to 60 percent and concluded that increase in heat transfer is not only due to additional surface area of

roughness but also due to near wall phenomenon. Hasan et al. [36] studied the effects of sinusoidal top wall with uniform heat flux and isothermal vertical walls using finite element method with air as working fluid and aspect ratio of 0.5 to 2 in laminar flow region. They observed that an increase in frequency causes an increase in heat transfer. Recently, Shishkina and Wagner [16] numerically studied effects of rectangular roughness elements on hot and cold walls with amplitude larger than thermal boundary layer thickness with finite volume method. They derived analytical relation and incorporated roughness height in Nusselt number formula. Numerical simulations were performed for a fluid of Pr number 1.0 in the range of $10^7 \leq Ra \leq 10^8$. They concluded that Nusselt number for rough cell can be found by knowing the Nusselt number for smooth cell within an accuracy of 6 percent.

Heat transfer through natural convection is critical for nuclear reactors or fuel rods. Recent trend of nuclear industry is to rely on passive safety systems based on natural convection [37-39]. Although, it causes an increase in friction factor and hence pressure drop but the presence of rough ribs enhance turbulence and hence heat transfer enhancement [40]. Donne and Meyer [40] used two dimensional rectangular roughness elements and derived an empirical correlation for heat transfer and friction factor based on experimental study. Firth and Meyer [41] experimentally studied thermal performance of various types of rough ribs like square, trapezoidal, and helical etc. They concluded that overall heat transfer enhancement is better than the two dimensional roughness.

A comprehensive study of Rayleigh-Bénard convection is required with incorporation of rough surfaces which could offer more clues to many complex aspects of natural convection [16]. This may be able to answer some critical questions like what is minimum roughness amplitude that would have no significant effects on heat transfer, can presence of surface roughness cause transition from stable to unstable (convective)? And the fundamental question regarding the effect of roughness; does it increase or decrease heat transfer? Presence of surface roughness on channel walls cause surface-fluid interactions, which are not easy to understand analytically [42]. Impact of surface roughness on heat transfer may not be well explained without exploring all available shapes of roughness like rectangular, semi-circular, sinusoidal, square, and V-shaped both in laminar and turbulent flow region. Most of the studies cited above considered the

role of V-shaped groove in laminar and turbulent flow [26, 31, 43] with majority in turbulent region, and rectangular roughness elements [16, 28] to observe role of roughness, and some considered whole wall as sinusoidal [33]. Therefore, in the present study, Rayleigh-Bénard convection which is being simple and rich in its dynamic behavior [44] has been considered with sinusoidal roughness elements on hot and cold walls with varying amplitude and frequency instead of smooth parallel plates. Although, Rayleigh-Bénard convection with smooth plates has been studied to validate numerical algorithms by Shan, Xu and lui, Zhou et al. [44-46]. But studies of Rayleigh-Bénard convection with single relaxation time LBM model with rough surfaces and for Ra number > $5x10^4$ are rare. Therefore, in present case, two dimensional study of Rayleigh-Bénard convection with sinusoidal roughness present on hot and cold walls has been carried out up to Ra up to $5x10^5$ to find numerical stability of algorithm. Thermal and hydrodynamic behavior of fluid has been analyzed by average Nusselt number, isotherms and velocity streamlines.

Nomenclature

A	Dimensionless Amplitude (h/H)	T_{ref}	Reference Temperature (K)
g	Gravitational acceleration (ms^{-2})	ts	Time step
H	Height of cavity (m)	U	Horizontal velocity component (ms^{-1})
h	Height of Roughness Element (m)	V	Vertical velocity component (ms^{-1})
K	Thermal conductivity ($Wm^{-1}k^{-1}$)	x	Coordinate parallel to the wall (m)
L	Length of cavity (m)	y	Coordinate normal to the wall (m)
lu	Lattice unit		
Nu	Nusselt number	**Greek symbols**	
n	Number of Roughness Elements		
Pr	Prandtl number	α	Molecular thermal diffusivity (m^2s^{-1})
Ra	Rayleigh Number	β	Coefficient of thermal expansion (K^{-1})
ΔT	Temperature difference (K)	θ	Dimensionless temperature
T_c	Temperature of cold wall (K)	ν	Molecular kinematic viscosity (m^2s^{-1})
T_h	Temperature of hot wall (K)	ρ	Density ($Kg.m^{-3}$)

2. Mathematical modelling

Rayleigh-Bénard convection with initial perturbation in thermal field and in presence of sinusoidal roughness elements with varying frequency and amplitude has been considered in the present study. Coupled momentum and energy equations has been solved by using numerical technique based on lattice Boltzmann method (LBM) [2, 7]. Geometry for the present study is shown in the Figure 2-1 with corresponding isothermal boundary conditions for top and bottom walls, and periodic boundary conditions for sides during simulations. Sinusoidal roughness has been applied on bottom and top walls to observe its influence on heat transfer and fluid flow but with varying dimensionless amplitude (h/H) '*A*' from 0.025 to 0.15 and frequency (number of roughness elements) from 02 to 10. Solid roughness elements are at same boundary conditions as corresponding walls. When roughness was present on both top and bottom walls, roughness elements were in phase. A two dimensional numerical study of Newtonian fluid of Prandtl number 1.0 has been carried out in laminar region Ra number 10^3 to $5x10^5$. Navier-Stokes and energy equations have been solved with negligible viscous dissipation and compression work and assuming negligible radiative heat transfer [36, 47]. External force which is in present case is buoyancy force has been applied using Boussinesq approximation as shown in Equation 3, by assuming other properties as constant [48].

$$\rho - \rho_{\infty} = \rho_{\infty} \beta \Delta T \tag{3}$$

Navier-Stokes and energy equations are coupled in case of free convection, and with assumption of negligible viscous and compression work, this coupling is through external force using Boussinesq approximation given by [49];

$$F_{ext} = \rho g \beta \left(T - T_{ref} \right) \tag{4}$$

The governing parameters or dimensionless numbers used to solve Navier-Stokes and energy equations and to analyze fluid flow and heat transfer during numerical study are given as [48, 50];

$$Ra_{H} = \frac{g \beta \Delta T H^{3}}{\upsilon \alpha} \tag{5}$$

$$P_r = \frac{\upsilon}{\alpha} \tag{6}$$

$$\theta = \frac{T - T_{ref}}{T_h - T_c} \tag{7}$$

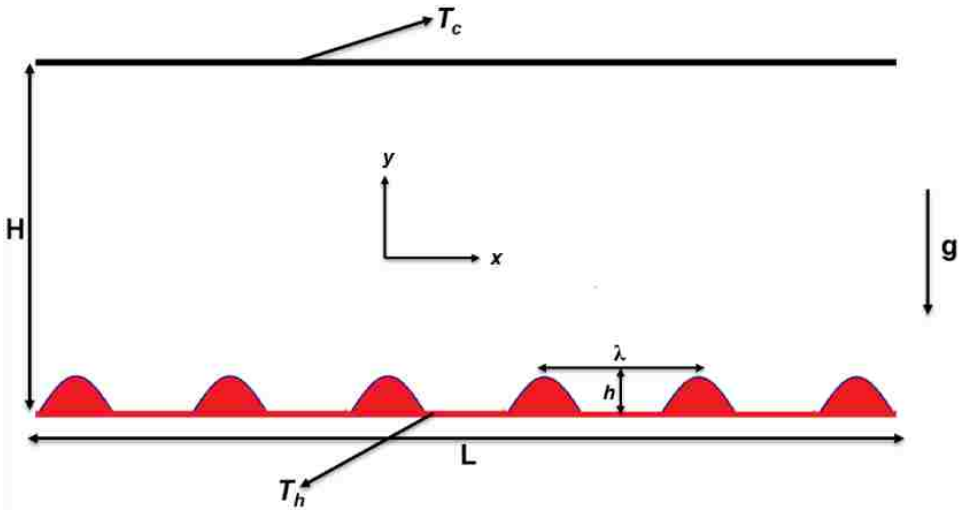

Figure 2-1: Schematic for Simulation of Rayleigh-Bénard Convection with Roughness

Nusselt number (Nu) has been used to calculate amount of Heat transfer both for a whole domain and at hot and cold walls and is given as [49, 51];

$$Nu_{av} = 1 + \frac{< V.\theta > H}{k\Delta\theta} \tag{8}$$

$$Nu_{av} = \frac{H}{L}\int_0^L \left(\frac{\partial\theta}{\partial y}\right) dx \tag{9}$$

Here, 'V' is the vertical component of velocity, < > shows a quantity averaged over Whole volume domain, and [redacted] is temperature gradient in y-direction normal to hot wall. No- slip boundary condition has been implemented on horizontal walls with side walls as periodic. Isothermal boundary conditions for horizontal walls are $\theta_h = 1$ at bottom and $\theta_c = 0$ at cold/top wall respectively.

3. Numerical method

Thermal and hydrodynamic equations in present study have been solved by adapting single relaxation time Bhatnagr-Gross and Krook (BGK) model of LBM [7]. LBM has become one of the most promising numerical tool to analyze single, and multiphase flow, condensation, evaporation, and other complex phenomenon. This method is based on a model of lattice gas automata (LGA) which solve dynamics of a hypothetical particle [44]. Although, LBM has achieved a significant success in simulation of fluid flow and heat transfer problems, but still has some challenges for numerical stability for highly turbulent flows [51]. But it does have many other advantages like ease of algorithm, parallel computing, and treatment of complex boundary conditions with relative ease compared to other available traditional methods. There is no need to solve Laplace equation as in other numerical schemes at every step [2, 7]. Solution of both momentum and energy equations is performed independently by using two separate distribution function. The energy equation is solved by considering temperature as a passive scalar [52]. Passive scalar approach assumes that temperature at macroscopic level behaves as passive scalar if viscous dissipation and compression works are neglected. Because of a better numerical stability, this approach has been preferred compared with other schemes [53].

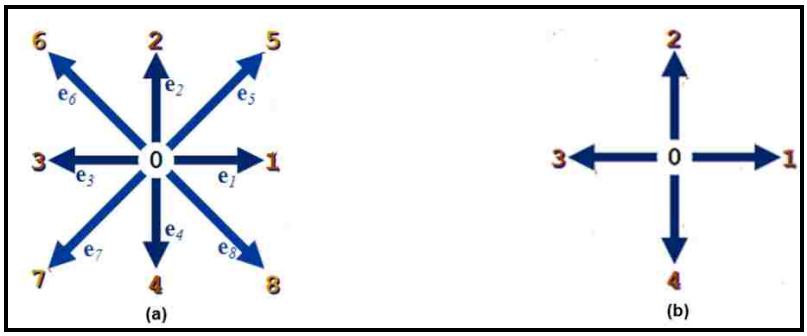

Figure 3-1: D2Q9 and D2Q5 Model for Velocity and Temperature respectively [7]

A standard D2Q9 model for nine velocities and D2Q5 for passive scalar has been used for solution of Navier-Stokes and energy equation as shown in Figure 3-1. The main equation used for solution based on single relaxation time BGK model of LBM with external force term is given by [49];

$$f_i\left(x + e_i\Delta t, t + \Delta t\right) = f_i\left(x,t\right) - \frac{\left(f_i\left(x,t\right) - f_i^{eq}\left(x,t\right)\right)}{\tau} + \Delta t F_{ext} \tag{10}$$

Corresponding equilibrium distribution function can be calculated as;

$$f_i^{eq} = w_i \rho\left[1 + 3\left(c_i.u\right) + 4.5\left(c_i.u\right)^2 - 1.5\left(u.u\right)\right] \tag{11}$$

Where, W_i = 4/9, 1/9, 1/9, 1/9, 1/9, 1/36, 1/36, 1/36, 1/36, respectively for i= 0 to 8. In a similar manner, distribution function equation for solution of passive scalar is given as;

$$g_j^{eq} = w_j T\left[1 + 3\left(c_i.u\right)\right] \tag{12}$$

Here, Wj = 1/3, 1/6, 1/6, 1/6, 1/6, respectively for j= 0 to 4. The relaxation time for both energy and momentum equations can be calculated by using value of kinematic viscosity and thermal diffusivity in lattice terms as shown in Equation 11-12 [2].

$$\upsilon = \frac{1}{3}\left(\tau_f - \frac{1}{2}\right) \tag{13}$$

$$\alpha = \frac{1}{3}\left(\tau_{energy} - \frac{1}{2}\right) \tag{14}$$

Macroscopic variables can be calculated by using distribution functions as;

$$\rho = \sum_{i=0}^{8} f_i \quad u = \frac{1}{\rho}\sum_{i=0}^{8} c_i f_i \text{ and } T = \sum_{i=0}^{4} g_i \tag{15}$$

One of the most significant element which causes a great success for LBM is its treatment of complex boundary conditions [54]. Boundary conditions are essential for a better convergence of a solution both at macro and micro level. In case of LBM, we need to transform macro level boundary conditions which are suitable to both energy and momentum equations in solving with distribution functions [4]. To implement no-slip boundary conditions at solid wall and roughness elements, we implemented half-way or mid-plane bounce back scheme as explained in Mohamad [2] and Sukop and Thorne [7].

These half-way bounce back boundary condition has proven ability to produce simulation results of second order accuracy for simple flows [54]. Thermal boundary conditions for isothermal or adiabatic walls are implemented as explained by Mohamad [2]. As we adapted a well-established single relaxation time BGK model of LBM without any modification, so details related all other recent models is omitted and is referred to Yang et al. [55], Shan [44], and Guo and Shu [4] for more explanation.

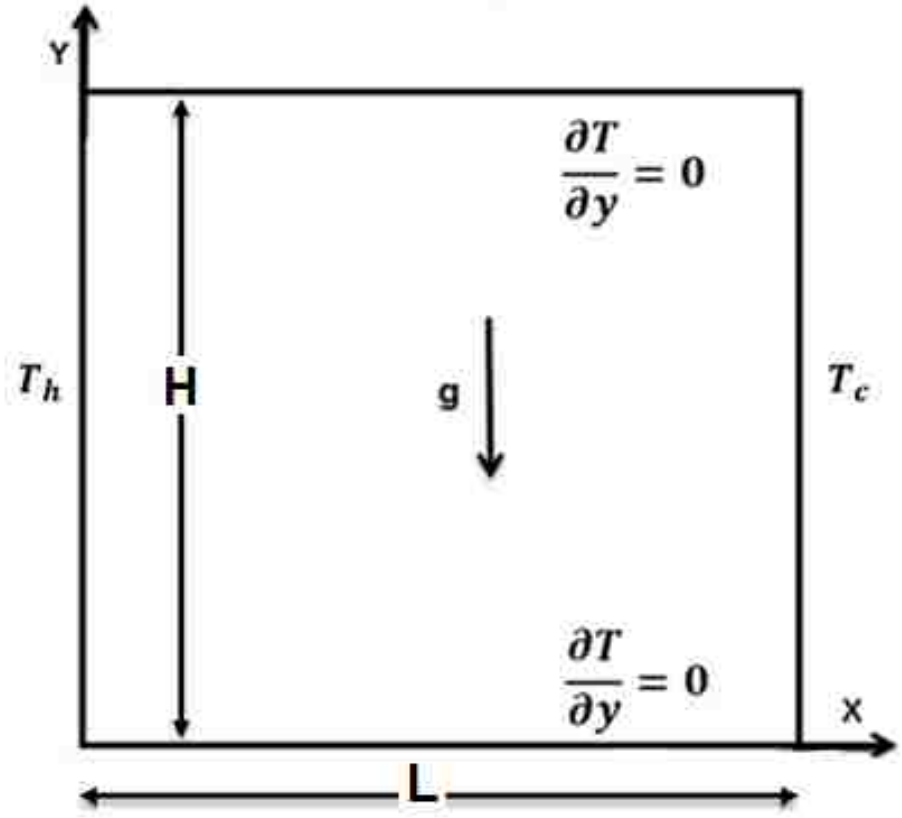

Figure 3-2: Square Cavity with Isothermal and Adiabatic Walls

4. Results and discussion

Lattice Boltzmann Method (LBM) based code is developed to solved Navier-Stokes equation coupled with energy equation to simulate Rayleigh-Bénard convection. Solution for Newtonian fluid of *Pr* number 1.0 was implemented for laminar in 2D. The degree of accuracy of results produced by the code has been verified first, by finding grid independence, and then by comparing simulation results with benchmark solution performed by Davis [56] for square cavity with side wall heating, and with Clever & Busse [57] for Rayleigh-Bénard convection with smooth bottom and top plates. The geometry for differentially heated square cavity is shown in Figure 3-2 with corresponding boundary conditions. For Rayleigh-Bénard convection case, geometry is same as shown in Figure 2-1, except all walls are smooth for benchmarking. The simulation results for grid independence are shown for both square cavity and Rayleigh-Bénard convection in Table 4-1. The maximum and minimum error for square cavity is 0.8 and 0.2 % respectively whereas, for Rayleigh-Bénard convection, it is 1.1 and 0.99% respectively. Therefore, for accurate results, a mesh size of 700x350 for Ra number $1x10^4$ in Rayleigh-Bénard convection and 350x350 for Ra number $1x10^4$ and larger for large Ra numbers has been chosen for present study which ensure better accuracy.

Table 4-1: Grid Independence Results of Average Nusselt Number

Ra	H	Present	% Error
Rayleigh-Bénard Convection with Clever & Busse [57]			
$1.0x10^4$	250	2.6298	1.1725
	300	2.6325	1.0710
	350	2.6346	0.9921
Differentially Heated Square Cavity with Davis [56]			
$1.0x10^4$	200	2.2241	0.8426
	250	2.2306	0.5528
	350	2.2381	0.2185

A quantitative and qualitative comparison of numerical results for square cavity and Rayleigh-Bénard convection with smooth hot and cold plates in two dimensions are

also made with Davis [56] and Clever & Busse [57] for a range of Ra number as shown in Figure 4-1 and Figure 4-2. A comparison of the results from present code with Davis [56] for a differentially heated square cavity demonstrated good agreement for Nusselt number. For case of square cavity average Nusselt number has been calculated at each hot and cold walls by using Equation 9 in order to further validate computational results produced by the code. This requires that difference between average Nusselt number at both vertical isothermal walls should not have a difference of more than 0.05% [58].

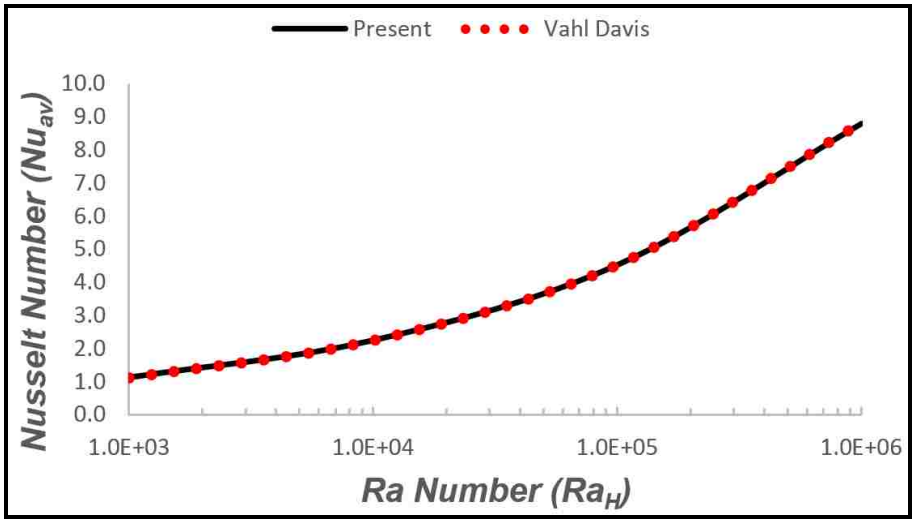

Figure 4-1: A Comparison of Present and Davis [59] Results of Nu_{av} for a Differentially Heated Square Cavity

For Rayleigh-Bénard convection, comparison with benchmark solution of Clever & Busse [57] and Xu and Lui [45] using LBM is shown below in Figure 4-2, our results are in good agreement with both solutions. A small perturbation in thermal field in form of initial condition has been applied to study natural convection [44]. At high Ra number $> 2x10^4$ value of average Nusselt number calculated in present results is less than their corresponding values reported by Clever & Busse. But in good agreement with Xu and

Lui [45] for entire range of Rayleigh number is observed. This slight difference in results produced by computational method based on LBM has been reported by the previous studies performed by Shan [44], and He et al.[6]. A qualitative comparison of isotherms produced in present study has been performed with previous studies to further validate our results for Rayleigh-Bénard convection as shown in Figure 4-3 at two different Ra number 10^4 and $5x10^4$. Both results are in good agreement with well-established results, further validating the quality of the present code.

A comparison of present numerical code with previous benchmark solutions performed with two different numerical schemes both quantitatively and qualitatively shows that computational code can produce reliable and grid independent results for free convection heat transfer.

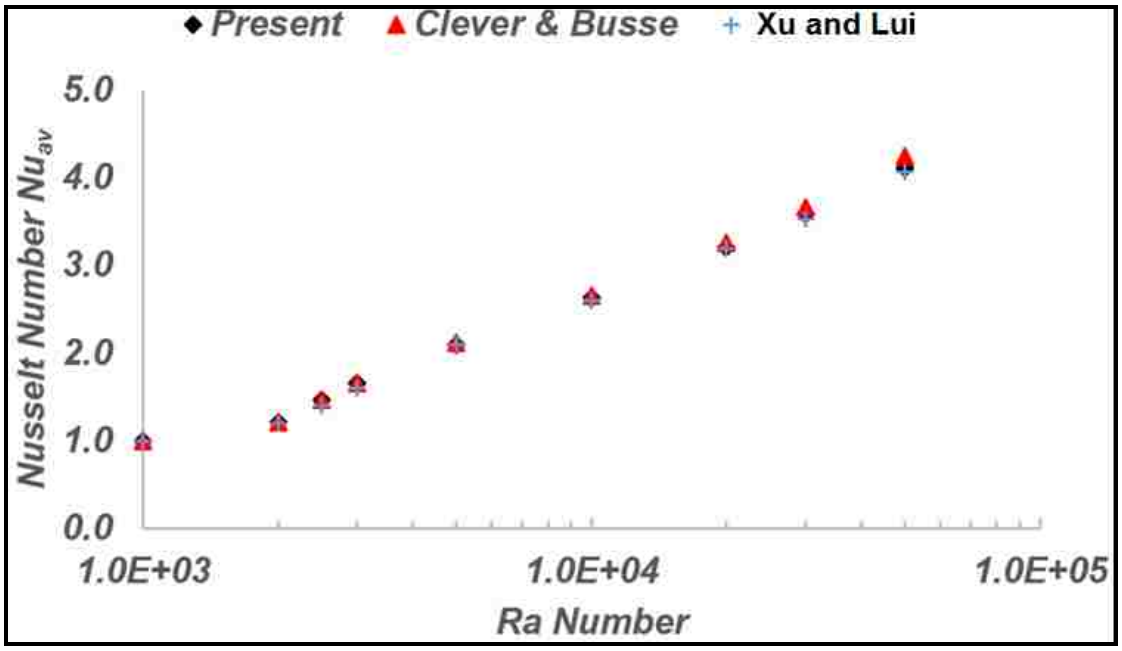

Figure 4-2: A Comparison of Present Results with Clever & Busse [57] and Xu and Lui [45] for Nu_{av} of Rayleigh-Bénard Convection

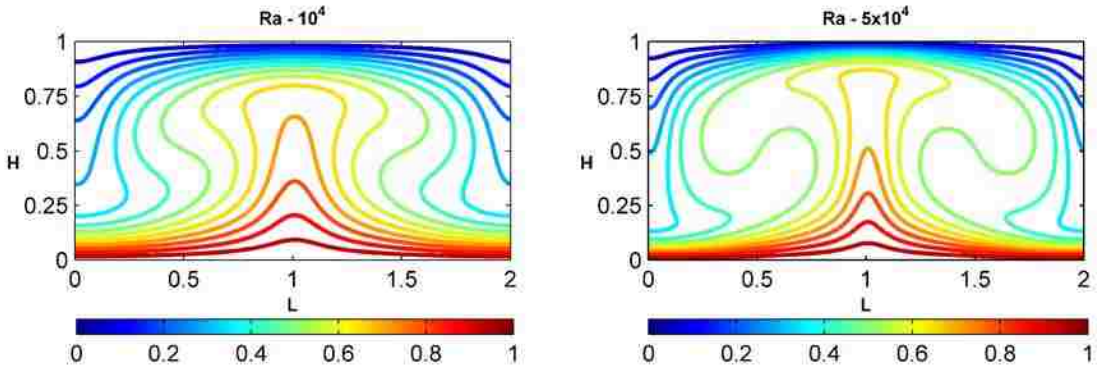

Figure 4-3: A Comparison of Isotherms Produced by Present Study

After performing grid independence and validation studies, Rayleigh-Bénard convection was simulated with and without sinusoidal roughness elements on hot wall with top wall as smooth in laminar region for Ra number in the range of 10^3 to $5x10^5$. The geometry and boundary conditions used during these simulations is shown in Figure 2-1. Thermal and hydrodynamic behavior of Newtonian fluid in two dimensions has been observed by keeping amplitude of roughness elements constant and varying the number of roughness elements and similarly by keeping number of elements constant as 8 or 10 and varying the amplitude from very small 0.025 to 0.15. Isothermal boundary conditions are used for top and bottom walls with periodic boundary conditions on sides. Results have been produced for analysis in terms of volume averaged Nusselt number, velocity streamlines and isotherms. Effects of variation of amplitude and frequency of sinusoidal roughness elements have been analyzed in terms of calculating volume averaged Nu as compared to previous studies performed using different shapes of roughness by Shishkina and Wagner [16], Tissernad et al.[35] , and Stringano et al. [14]. Physical phenomenon are studied which can play their role in affecting heat transfer and fluid flow behavior.

In the first step, simulations for Rayleigh-Bénard convection with smooth bottom and top walls have been carried out beyond Ra number $5x10^4$ in order to verify numerical stability of computational code for higher Ra number. Some interesting feature of Rayleigh-Bénard convection have been observed during this study. Numerical

simulations of two different cases of Rayleigh-Bénard convection have been carried out; thermal perturbation as initial condition, thermal perturbation with roughness present on hot wall, and no thermal perturbation but only roughness present on hot wall. Numerical results in the form of average heat transfer (not presented here) showed no significant difference when only thermal perturbation was applied and when a combination of thermal perturbation and sinusoidal roughness present on hot wall.

Figure 4-4 shows value of average *Nu* calculated through whole fluid domain. Results are plotted against benchmark solution of Clever & Busse [57] to make a comparison up to Ra number $5x10^4$. There is a slight difference at higher values of Ra which is discussed earlier. Average Nusselt number is a function of Pr, Ra number and aspect ratio. Two-dimensional simulations were performed with periodic boundary condition on sides, hence aspect ratio effects are negligible [60]. As studied by Kao and Yang [60], Nu number was almost independent of Pr number in the range of 0.7 to 70.

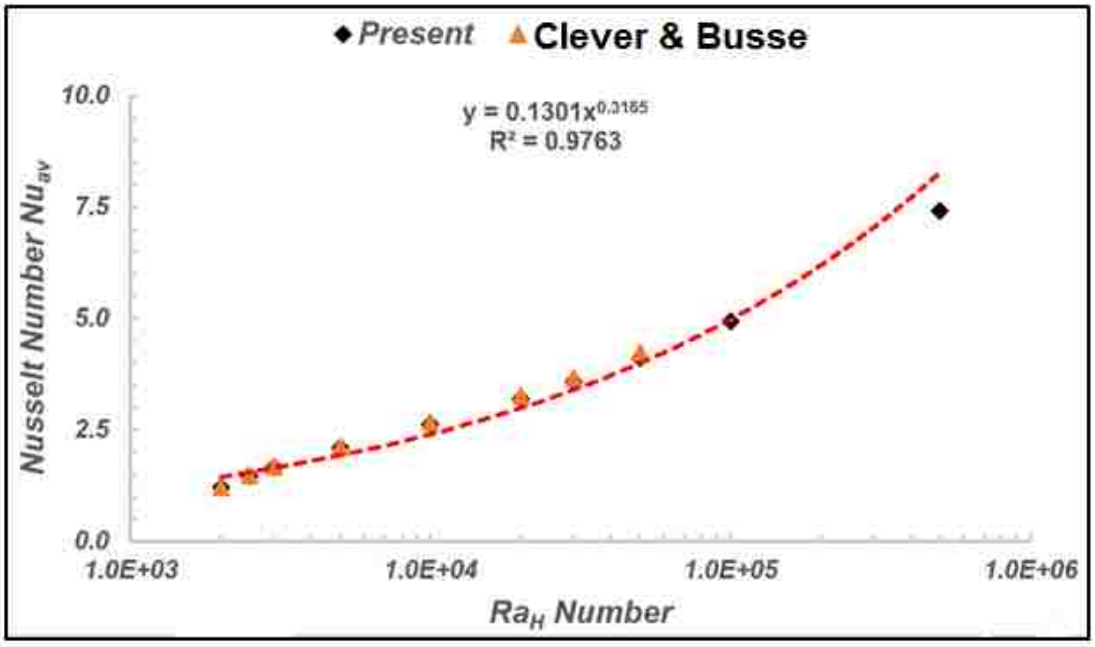

Figure 4-4: Rayleigh-Bénard convection for Ra_H Number up to $5x10^5$ with Smooth Top and Bottom Walls

Therefore, simulations were carried out for only Pr number 1.0. A power law relation found in the present study between Nu and Ra number as shown in the Figure 4-4. Experimental and numerical investigations of Nu and Ra relation in Rayleigh-Bénard convection showed a value of 0.2 to 0.386, whereas, in most cases this value lies close to 0.3. In present study, value of exponent found was 0.31, which is close to previous studies. Isothermal and velocity streamlines are plotted against roughness cases to provide qualitative comparison. Single relaxation time BGK model of LBM [2, 7] was found stable even at this high Ra number up to $5x10^5$, as bottom heating systems are inherently unstable as discussed by Amin [28], therefore simulations are limited up to value of Ra $5x10^5$ and also due to available computational resources.

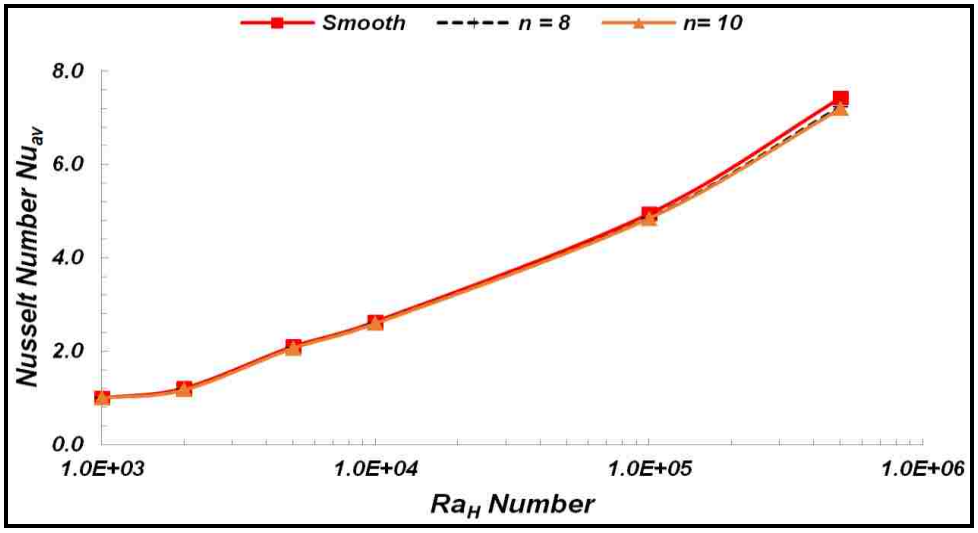

Figure 4-5: Average Nu Number for Roughness Amplitude 0.025 as Compared to Smooth Surface at Bottom Plate

Simulations were performed with only sinusoidal roughness present on the hot wall with varying frequency and no thermal perturbation. It is interesting to note that average Nu calculated with dimensionless roughness amplitude of only 0.025 present on

hot wall is almost same as in case of only thermal perturbation present as an initial condition with smooth walls. A comparison of average Nu of roughness amplitude of 0.025 for 8 and 10 elements present on hot wall is shown in Figure 4-5. It is very clear from these results that a dimensionless amplitude of sinusoidal roughness elements of 0.025 has no significant effects on heat transfer except a slight decrease in heat transfer at Ra number $> 10^5$. Similar results have been reported by Kandlikar [42] that a roughness height less than 0.05 has no significant effects on heat transfer. The role of roughness alone will be described in detail with simulation results in next paragraphs with comparison to smooth system at the same Ra numbers for a better analysis.

In the present study, effort has been made to study numerically some fundamental and physical phenomenon affecting fluid flow and heat transfer in the presence of roughness in Rayleigh-Bénard convection. Previous studies [14, 16, 28, 33, 43, 61] of natural convection heat transfer has mentioned some major elements causing increase or decrease in average heat transfer like formation of eddies or vortices in the wake of roughness elements, effective distance between hot and cold walls in the presence of roughness, reduction in volume of heat transfer medium, and additional heat transfer area due to incorporation of surface roughness. All these elements will be discussed along with numerical results for different cases. There were many simulations performed in present study but some prominent results are presented here.

4.1 Heat transfer

Average heat transfer has been calculated by using Nu value given by Equation 8 for all the cases with roughness. Values of average Nu are presented along with case of smooth plates for a better comparison to understand role of surface roughness. Figure 4-6 - Figure 4-9 show the variation of average Nu for roughness present on different walls with different amplitude and frequency. A comparison of these results showed that as number of roughness elements and their amplitude is increased, amount of average heat transfer decreased in all cases. Figure 4-6 shows that decrease in heat transfer is more when the number of roughness elements are increased to 10. A maximum decrease in heat transfer was observed to be 15% at Ra number $5x10^5$. Another interesting observation is made based on value of average Nu that when number of roughness elements is increased up to 10, it causes a delay in the onset of free convection.

In another simulation, amplitude of sinusoidal roughness elements is increased while fixing the number of roughness elements on bottom hot wall to 8. Results for average Nu are shown in Figure 4-7. For a dimensionless roughness amplitude of 0.025, no significant effect on heat transfer was observed. Also when amplitude of roughness is increased, amount of heat transfer was observed to decrease. As amplitude is increased ≥ 0.1, it causes delay in the onset of natural convection in Rayleigh-Bénard convection. A minimum and maximum heat transfer reduction was calculated as 14.8 to 21.4 % respectively at an amplitude of 0.15. The degradation in the average Nu increases as compared to smooth walls becomes more pronounced as the Ra number increases, and for Ra number > 10^4 for all amplitudes of roughness except amplitude of 0.025 show a notable degradation in heat transfer.

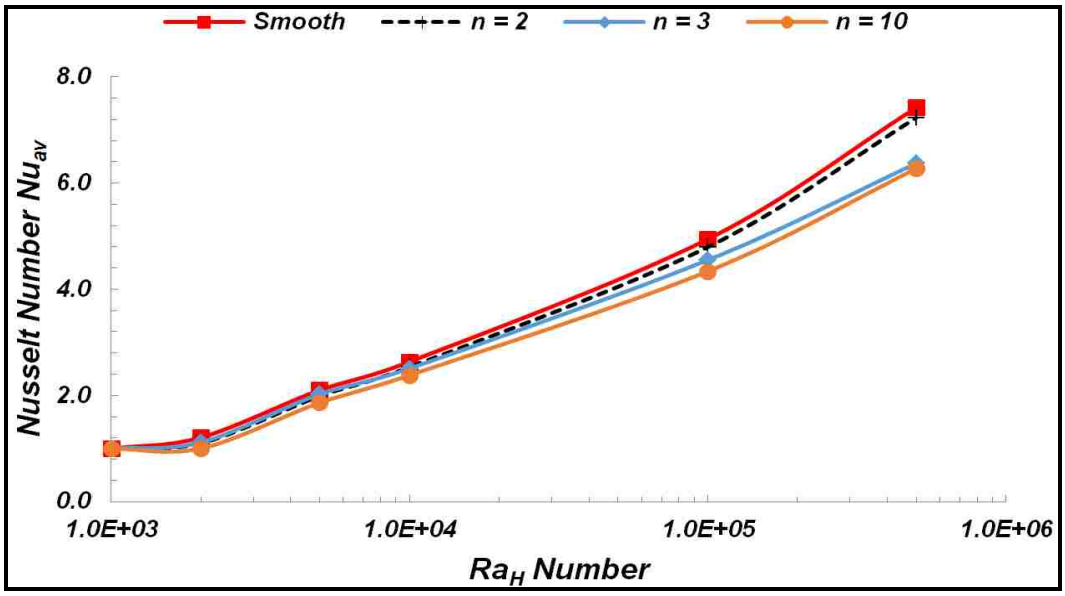

Figure 4-6: Average Values of Nu for Rough and Smooth Systems with Constant Amplitude of 0.1 at Bottom Plate

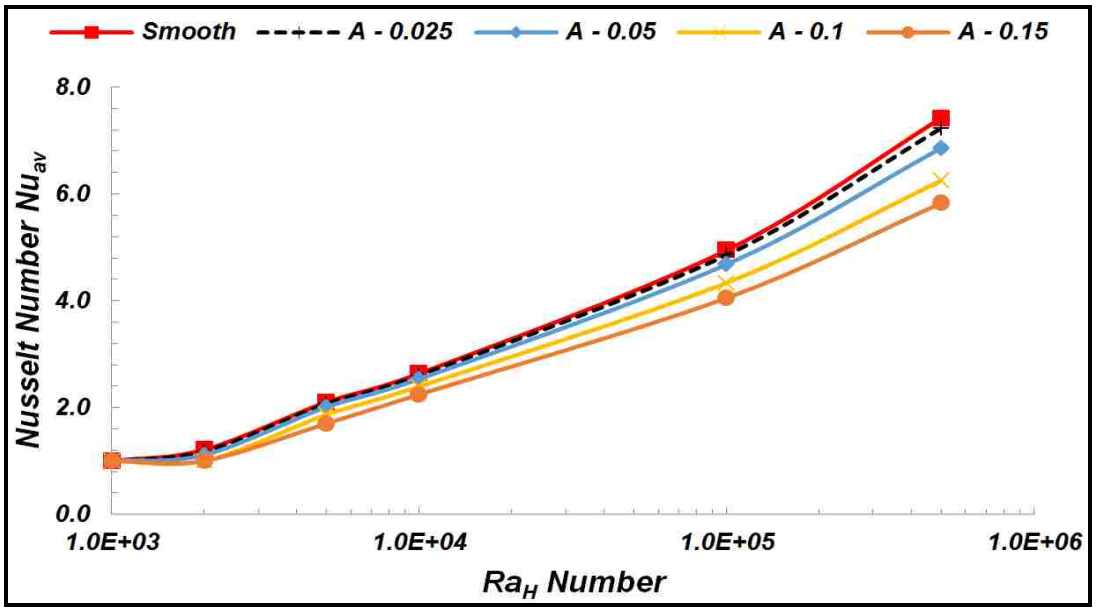

Figure 4-7: Average Values of Nu for Rough and Smooth Systems with variation of Amplitude and Roughness Elements of 8 at Bottom Plate

Figure 4-8 shows results of numerical simulations of Rayleigh-Bénard convection when sinusoidal roughness is present on both hot and cold walls simultaneously and roughness elements are in phase; meaning roughness elements on the top surface is exactly aligned with the bottom surface roughness element. The amplitude of roughness was varied while keeping number of elements fixed at 10. Average Nu values showed that as amplitude is increased at both bottom and top walls, transition from purely conductive state to convective state is delayed. This delay in onset is maximum at 0.15, the maximum roughness amplitude simulated. Likewise, the effect is more prominent as the Ra increases. For the case of both sides roughness, the effect of roughness of smallest amplitude of 0.025 is more than the previous results when roughness was present only on hot wall. It causes a decrease in heat transfer as Ra number is increased beyond 10^5. Reduction in heat transfer was more at low Ra number as compared to high Ra number, as reduction in heat transfer at $5x10^3$ was 51% and 37% at Ra number $5x10^5$.

Two cases of roughness present only on top or cold wall were studied to observe any effect on average heat transfer with amplitude of 0.05 and 0.1 and number of roughness elements equal to 8. Roughness elements are at same temperature as cold wall. As amplitude of roughness elements is increased, average value of Nu decreased as shown in the Figure 4-9. One important observation is when roughness is only present at top wall decrease in average heat transfer is less than the case when the roughness is present only on hot wall.

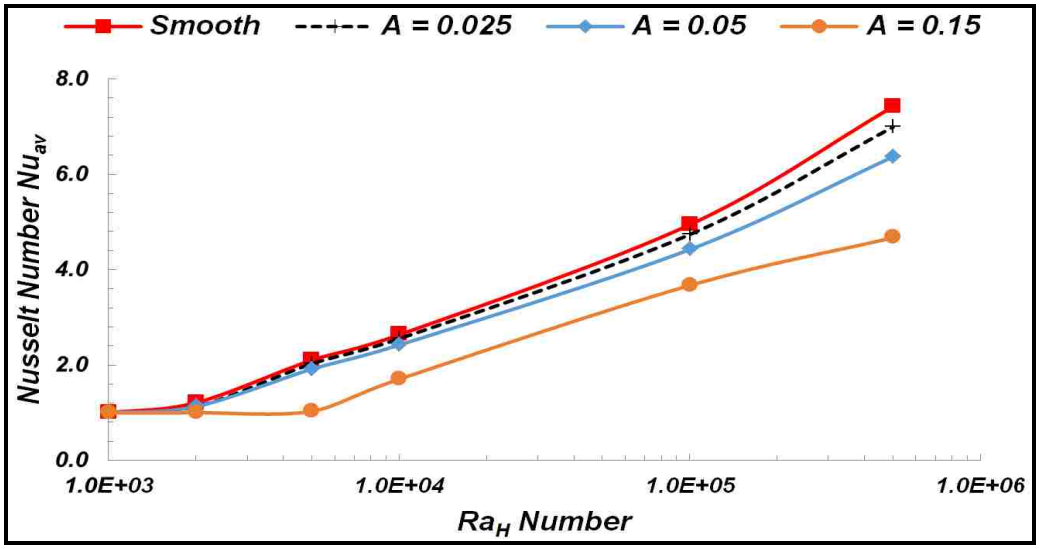

Figure 4-8: Average Values of Nu for Rough and Smooth Systems with variation of Amplitude and Roughness Elements of 10 at Top and Bottom Plates

In all the cases when either roughness is present on one wall or both walls, amount of heat transfer calculated decreases with increasing roughness amplitude. There are some factors which may play their role in reduction of heat transfer in presence of roughness. For example, when roughness is present on any wall or both, an effective distance between two walls decreases as compared to smooth system. This decrease in distance causes a relative decrease in Ra number and hence heat transfer is reduced. Also,

a decrease in distance between cold and hot wall causes an increase in conductive flux which cause a delay in the onset of free convection. This delay in onset of convection results in reduction of heat transfer. Similar results have been reported by Amin [28] with rectangular roughness elements on bottom hot wall and ElSherbiny et al. [26] with V-shaped roughness elements.

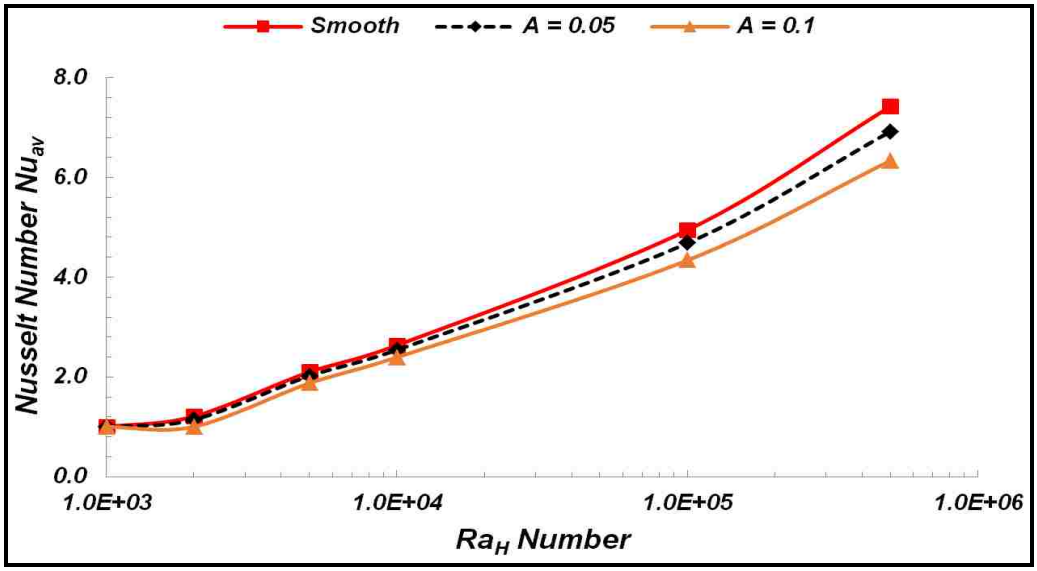

Figure 4-9: Average Values of Nu for Rough and Smooth Systems with Variation of Amplitude and Roughness Elements of 8 at Top Plate

Another possible reason for decrease of average heat transfer as reported by Amin [47] with rectangular roughness elements may be due to reduction of the heat transfer medium when roughness is incorporated in the system. A close look at present results of average heat transfer for different amplitude shows that decrease in heat transfer is more in case of roughness present on both walls simultaneously as compared to case when roughness is present only on one wall either hot or cold. This shows that a reduction in fluid volume due to the presence of roughness may be one of the reason for a decrease in heat transfer.

When roughness of any shape is introduced in a channel or cavity, more area is added for heat transfer as compared to smooth surface. Shakerin et al. [62] performed experimental studies to observe effects of rectangular roughness elements present at vertical isothermal wall on heat transfer in a square cavity. They observed that an addition of surface area due to presence of rough element may be balanced by a deceleration or obstruction in the flow velocity during natural convection and hence no significant enhancement in heat transfer was observed. Similarly, in the present case when sinusoidal roughness elements are introduced on either hot or cold wall or both, heat transfer is decreased. This presence of roughness elements caused a deceleration in the velocity during free convection and hence a reduction in the heat transfer. This effect is more pronounced when roughness is present on both walls. Ji et al. [63] with rectangular roughness, Zhang et al. [64] with three different shapes of roughness in micro channels, and Amin [47] with rectangular roughness elements also reported similar results due to increase in amplitude of roughness.

Most significant phenomenon that can alter heat transfer in the presence of roughness is formation of 'eddies or vortices' in the interstices of roughness elements of any shape as reported by Kandlikar [42], Saidi et al. [27], Du and Tong [31], Prétot et al. [33], Stringano et al. [14], and Olga and Clause [16]. The velocity streamlines behavior for different number of roughness elements and amplitude may be helpful in understanding the physics behind this decrease in average heat transfer. Figure 4-10 and Figure 4-11 show that for roughness elements 2 and 6 with an amplitude of 0.1 at hot bottom wall at Ra number of 10^4, there is no formation of eddies or circulation in the interstices of roughness elements. But as number of roughness elements are increased at same Ra number of 10^4, formation of vortices/eddies in the shadow of roughness elements are observed. When Ra number is increased to $5x10^5$, eddies are also seen for 6 roughness elements as shown in Figure 4-11. These vortices get stronger and flatter or elongated as the Ra number is increased from 10^4 to $5x10^5$. These circulations cause detachment of main fluid from flat portion of the hot wall and hence reduced heat transfer. Figure 4-9 shows a decrease in heat transfer when roughness is present on both walls is more as compared to smooth and others cases of roughness. A comparison of streamlines shows that eddies are formed in the shadows of roughness elements at low Ra

number of $5x10^3$ when roughness is present on both walls simultaneously as compared to other cases where there is no formation of eddies up to Ra number 10^4. These eddies causes flow blockage phenomenon that causes thermally inactive regions on both sides of roughness elements and hence cause a reduction in heat transfer [61]. As Ra number is increased, presence of eddies for 6 roughness elements further causes a reduction in heat transfer as compared to Ra number 10^4. Therefore, decrease in heat transfer at larger Ra number is more as compared to small Ra number of 10^4.

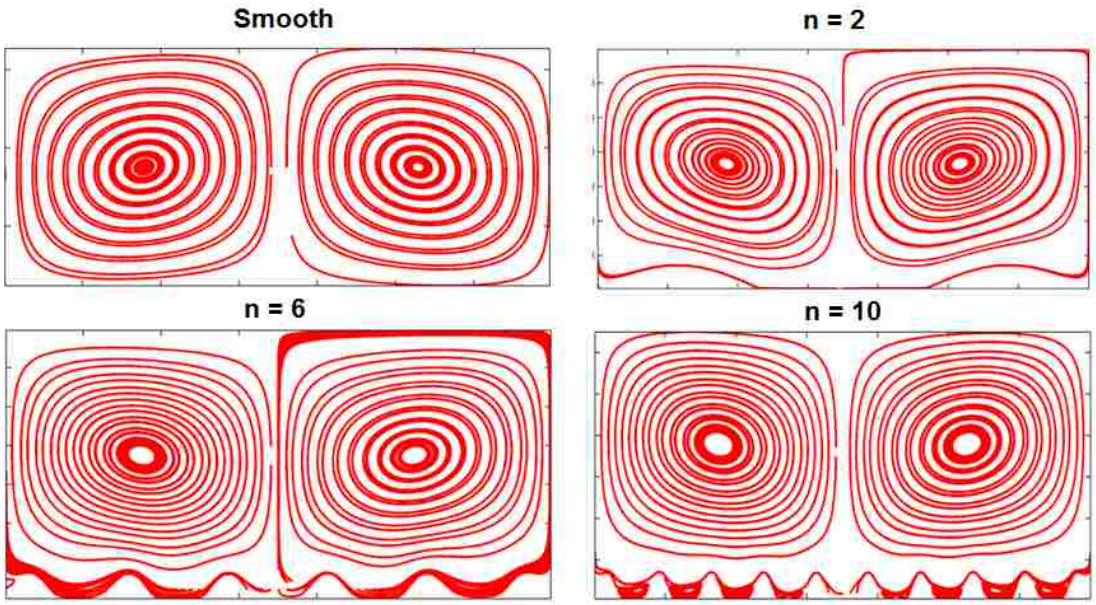

Figure 4-10: Velocity Streamlines for A = 0.1 and Different Number of Roughness Elements for Ra – 10^4

Vijiapurapu and Cui [65] also reported such kind of phenomenon of eddies formation both for rectangular and square roughness in the interstices of roughness elements that causes a detachment and reattachment of main fluid depends on the spacing between roughness elements. Prètot et al. [33] in their experimental study with sinusoidal wall showed that as amplitude increases, eddies formed are more noticeable and hence

cause a reduction in heat transfer. Amin [28] in his study of free convection with rectangular roughness elements evenly spaced did not mention such phenomenon of eddies formation in a square cavity. The velocity streamlines for different cases under study are shown separately later in this section.

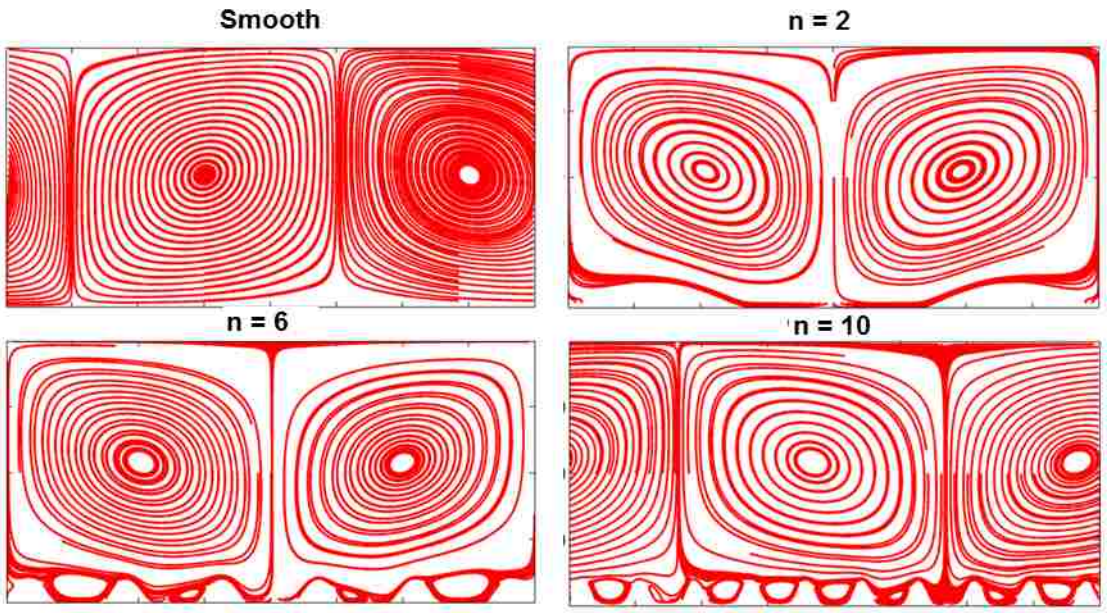

Figure 4-11: Velocity Streamlines for A = 0.1 and Different Number of Roughness Elements at Ra – $5x10^5$

Another very interesting feature was observed during this study with varying amplitude and frequency at both top and bottom walls simultaneously. As will be shown in the Figure 4-15, for Ra number 10^4 with all other cases and Ra numbers. It is very clear that the fluid in the cavity in all cases including smooth is bi-cellular for all Ra numbers and amplitude of roughness elements except when roughness is present on both walls simultaneously at Ra number 10^4 at an amplitude of 0.15. But when sinusoidal roughness elements are present on both top and bottom walls with amplitude of 0.15 and 10 roughness elements, a bi-cellular flow is transformed into a quadru-cellular flow and

remains divided into four cells up to Ra number 10^5. Fluid flow in presence of roughness divides whole cell into four symmetric cells instead of two like other cases of roughness. This may cause a further decrease in the heat transfer as compared to smooth geometry. Amin [28] performed numerical studies for a square cavity and isothermal rectangular roughness elements and reported a transformation of bi-cellular flow into quadru-cellular flow at an amplitude of 0.125.

4.2 Streamlines and isotherms

The main purpose of the present study was to observe effects of sinusoidal roughness elements on heat transfer and fluid flow in Rayleigh-Bénard convection as compared to smooth plates. Presence of roughness is found to significantly affect fluid flow behavior during free convection. Fluid flow rises from central region of the cavity towards the cold wall and making a counter clockwise and clockwise rotation returned to bottom wall. The flow remains stagnant unless a certain value of Ra number is reached. Once the value of the Ra number is increased beyond this limit, buoyancy force takes over the viscous force and cause an onset of free convection and formation of vortex cells. Before the onset of convection, fluid remains stagnant with no cell formation of velocity present in the cell, and hence no deviation in isothermal lines. Flow rises in the upward direction from the center of hot plate and divides the cell into two symmetric cells. When Ra number is increased, strong buoyancy force causes transformation of bi-cellular flow into quadru-cellular flow. Most significant results for velocity streamlines for roughness present on bottom, top, and both top and bottom walls with varying number of roughness elements and amplitude from 0.025 to 0.15 are presented here.

Figure 4-12 and Figure 4-13 show the results for roughness present on bottom wall with fixed number of elements 8, and varying amplitude. No circulation or eddies are present for amplitude of 0.05 for Ra number of 10^4 and $5x10^5$. At Ra number 10^4, some small eddies are present for an amplitude of 0.1, but much larger in size for amplitude of 0.15. When Ra number is increased up to $5x10^5$, large eddies or circulations are present at an amplitude of 0.1 and get stronger and flatter in size as amplitude is further increased as shown in Figure 4-13.

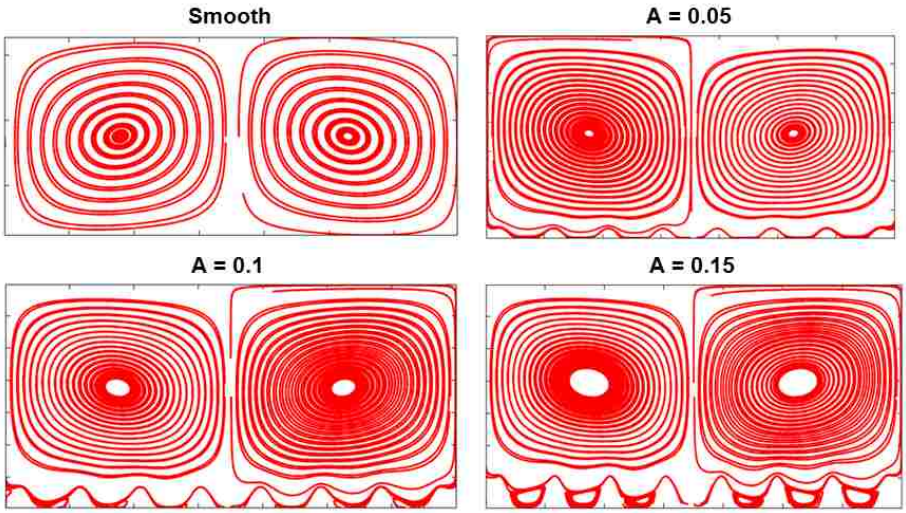

Figure 4-12: Velocity Streamlines for Different Amplitude and Constant Number of Roughness Elements of 8 at Bottom Wall for Ra – $1x10^4$

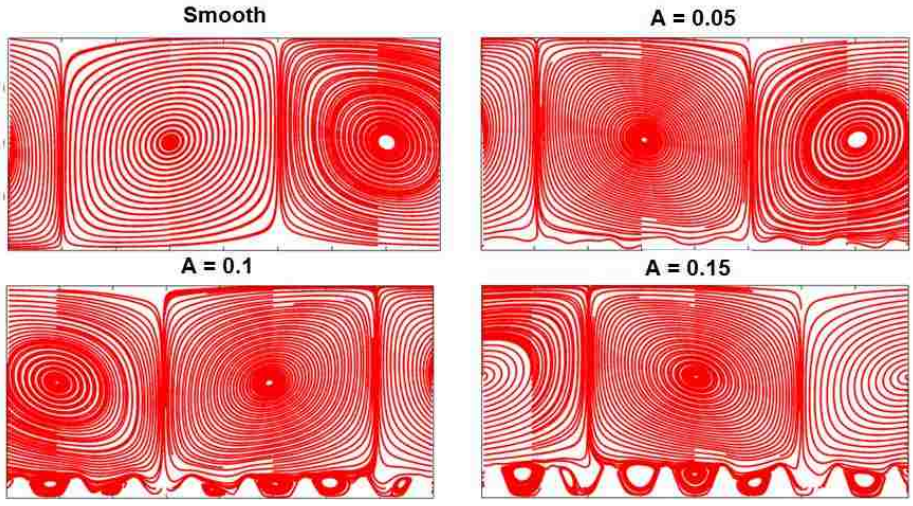

Figure 4-13: Velocity Streamlines for Different Amplitude and Constant Number of Roughness Elements of 8 at Bottom Wall for Ra – $5x10^5$

The results for roughness amplitude of 0.025 are not presented, because no eddies or circulation formation was observed even at large Ra number $5x10^5$. Fluid flow behaves in the same manner when roughness is present on top wall rather than on the bottom or hot wall.

Some interesting and somewhat different streamlines behavior was observed in Rayleigh-Bénard convection with sinusoidal roughness present on both hot and cold walls simultaneously. Amplitude of sinusoidal roughness has been varied from 0.025 to 0.15 by keeping number of roughness elements equal to 10. There is no formation of eddies or circulations for any roughness amplitude for Ra number < 10^4. But eddies or circulations are present when roughness is present on both hot and cold walls for an amplitude of 0.15 even at Ra number $5x10^3$ as shown in the Figure 4-14. A comparison of streamlines for roughness present on hot and cold wall with streamlines of roughness present on both hot and cold walls shows a very clear difference at Ra number equal to 10^4 and amplitude of 0.15. In all the cases studied with roughness and smooth surface, flow is bi-cellular for all Ra number except for Ra number 10^4 with an amplitude of 0.15 where flow is converted to quadru-cellular as shown in Figure 4-15. In all cases studied, flow divides entire cavity into two symmetrical cells from center line. But in the case of Figure 4-15, flow divides the whole flow domain into four symmetrical cells, like two halves of cavity are further divided into two. This division into four equal cells causes a stronger reduction in the heat transfer in the cell. This flow remains divided into four cells for Ra number up to 10^5. But when Ra number is increased to $5x10^5$, flow again converted to bi-cellular. Hence, in present results a quadru-cellular formation was present from 10^4 to 10^5, this range of quadru-cellular formation may extend beyond these Ra numbers. Flow remains parallel to roughness elements at top of eddies or vortices. When Ra number is increased, it causes a stronger buoyancy force and hence stronger convective effects. This strong buoyancy force causes circulation or eddies formation in the wake of roughness elements. Hasan et al. [36] performed numerical studies in a cavity with different aspect ratio and sinusoidal top wall at uniform heat flux. They also reported formation of eddies in the wake of sinusoidal elements at larger Ra number. These vortices are responsible for the overall heat transfer degradation.

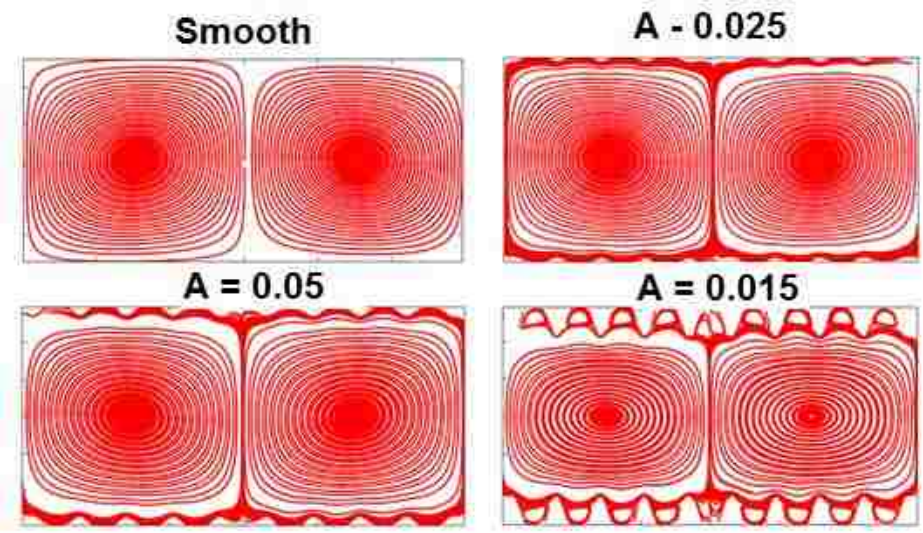

Figure 4-14: Streamlines for Roughness Elements of 10 on Top and Bottom Walls with Varying Amplitude for Ra – $5x10^3$

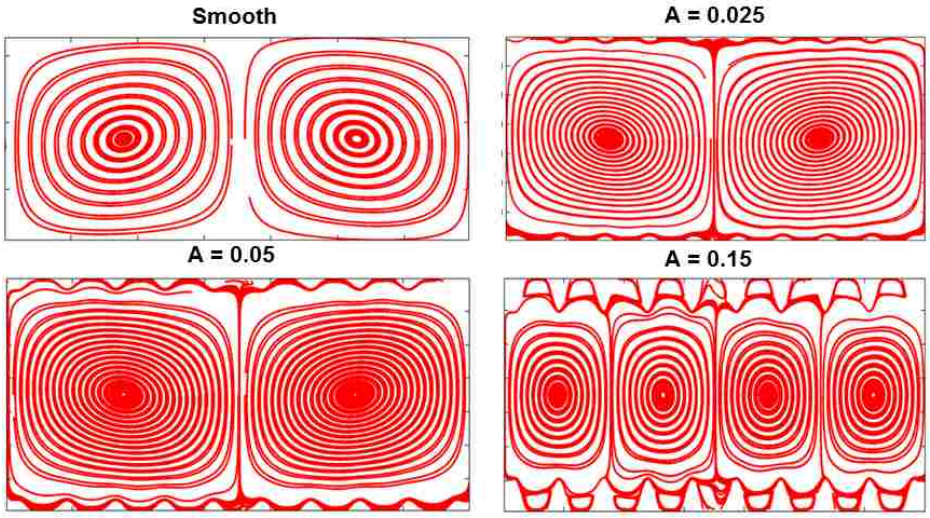

Figure 4-15: Streamlines for Roughness Elements of 10 on Top and Bottom Walls with Varying Amplitude for Ra – $1x10^4$

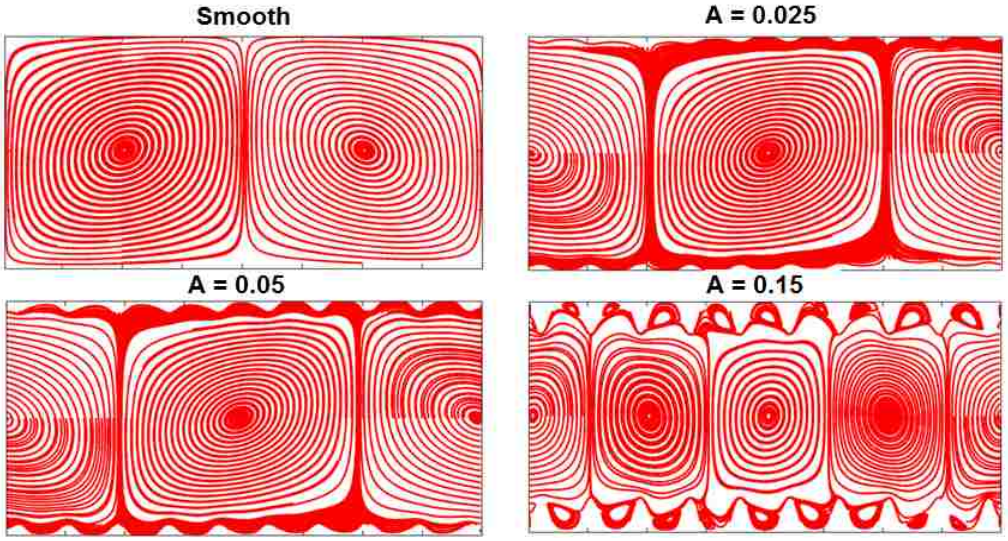

Figure 4-16: Streamlines for Roughness Elements of 10 on Top and Bottom Walls with Varying Amplitude for Ra – $1x10^5$

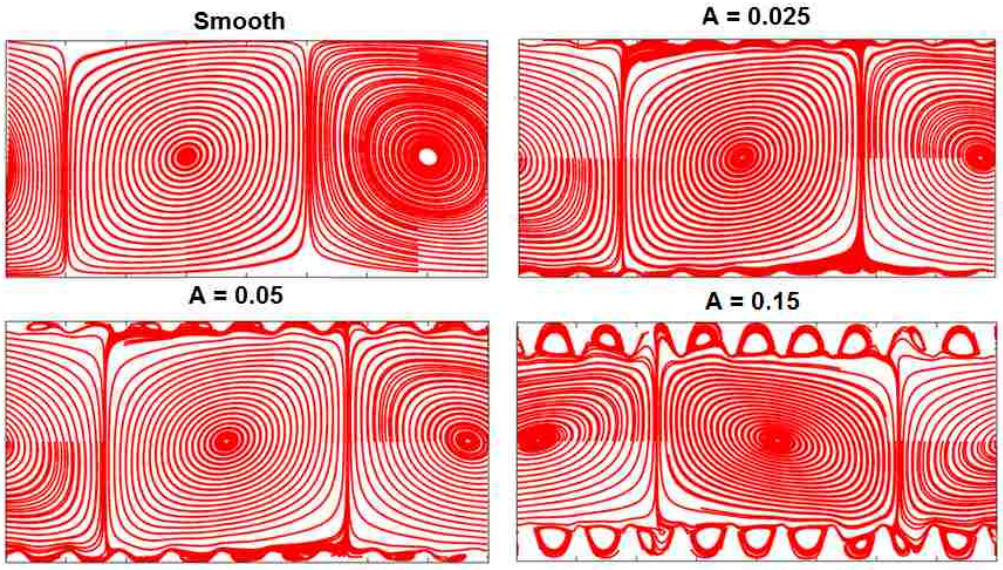

Figure 4-17: Streamlines for Roughness Elements of 10 on Top and Bottom Walls with Varying Amplitude for Ra – $5x10^5$

Thermal behavior of Newtonian fluid has been observed in the form of isotherms both in smooth as well as in the presence of roughness. Isotherms for all cases with Ra number < 10^4 behaves in same way in almost all cases except otherwise mentioned. Therefore, thermal behavior of fluid is presented here for Ra number ≥ 10^4, where roughness effects are more pronounced.

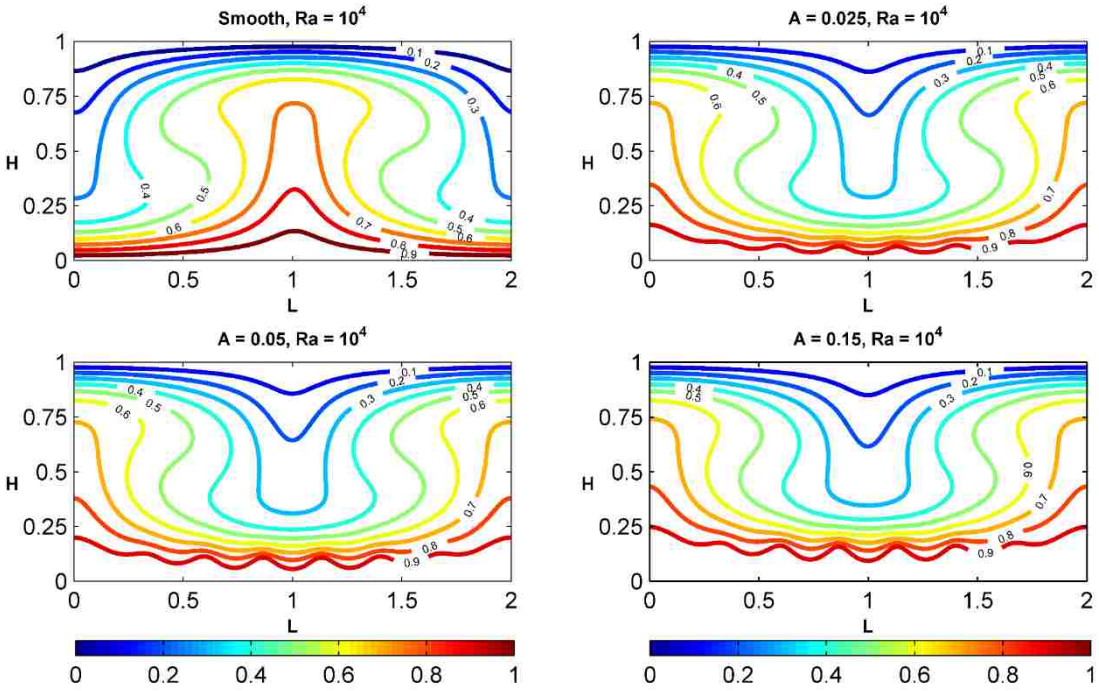

Figure 4-18: Isothermal Lines for constant Roughness Elements of 8 at Bottom Wall and Varying of Roughness Elements for Ra – 1x10^4

To have a better understanding of isothermal lines, dimensionless temperature contours are shown. All the values of dimensionless temperature lies in between 0 and 1, where 0 and 1 is temperature of cold and hot wall respectively. All contours are shown by an interval of 0.1 for all cases. Thermal behavior of fluid when roughness is present on bottom hot wall by varying frequency of elements and amplitude is shown in Figure 4-18

- Figure 4-23. For low Ra number, when buoyancy force is weak, all isothermal lines are almost parallel at the top of roughness elements and in smooth system. Isothermal lines are not showing any constriction or shrinking of thermal lines in the rough elements wakes. When Ra number is increased $\geq 5x10^3$, it causes an increase in the buoyancy force and hence results in strong convection. Deviation of isotherms starts from bottom hot wall in the upward direction approximately at the center of wall. This upward deviation results in the swirling of isothermal lines and hence cell is divided into two or more symmetric cells. This phenomenon is also clear from velocity streamlines behavior discussed before. With further increase in Ra number and hence increase in buoyancy force, convection effects are enhanced which causes stratification or distortion in isotherms and shrinking towards the hot and cold walls and also in the interstices of roughness elements, showing strong effects of convection. Shrinking or large local concentration of isothermal lines at bottom hot wall generate a hot spot at bottom wall. A close look at isotherms showed that in absence of roughness spreading for the fluid more than the case of roughness. This observation is clear from isotherm labeled as 0.5 in Figure 4-19. This spreading gets weaker as amplitude of roughness elements is increased and is more clearly shown in Figure 4-19 for Ra number $5x10^5$. This shrinking of isotherms also manifest as a decrease in the heat transfer from hot wall to cold. The cavity is divided by two symmetric cells as also shown by streamlines, therefore, a point where flow is rising upward isotherms are parallel to roughness peaks with no confinement in wakes, and in contrast, a point where flow is moving downwards, isotherms are strongly confined into the wakes. This aspect is more pronounced at higher amplitude as shown in Figure 4-19.

Figure 4-21 shows isotherms behavior when amplitude of roughness is constant equal to 0.1 and number of elements is increased from 2 to 10. Isotherms show a reattachment of fluid to flat surface in case when only two roughness elements are present as compared to other cases of higher number of elements. At low Ra number, there is no constriction of isothermal lines in the wakes but as Ra number is increased past 10^4, isotherms are packed together close to the boundary restricted by the shape of the roughness. In both cases of Ra number 10^4 and $5x10^5$ with two roughness elements, fluid expansion is slightly higher as compared to case of more elements present on the

wall. This slightly less expansion shows that presence of only two roughness elements does not significantly affect heat transfer.

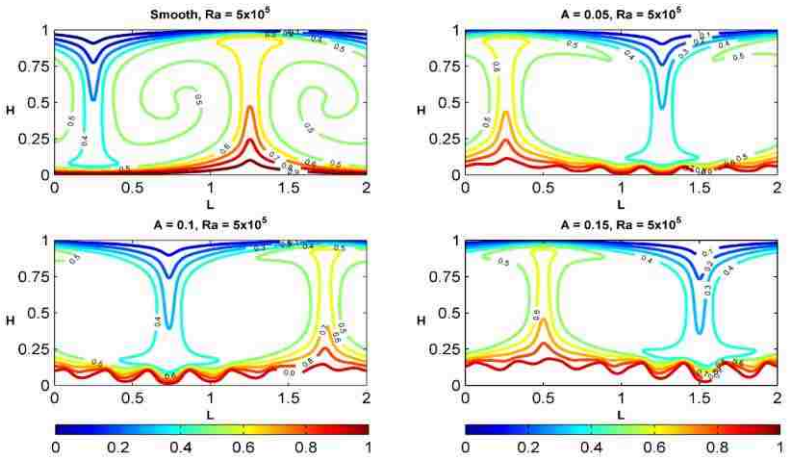

Figure 4-19: Isothermal Lines for Constant Roughness Elements of 8 at Bottom Wall and Varying of Roughness Elements for Ra – $5x10^5$

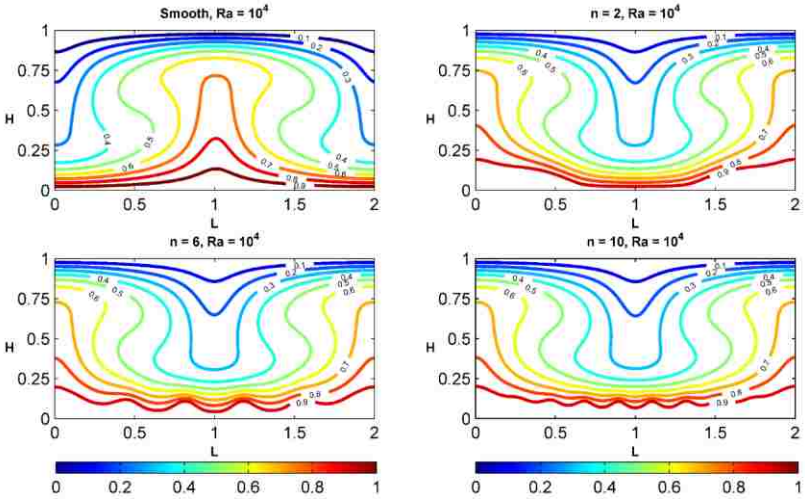

Figure 4-20: Isothermal Lines for Constant Roughness Amplitude of 0.1 at Bottom Wall and Varying number of Roughness Elements for Ra – $1x10^4$

Sinusoidal roughness elements present on top or cold wall also affect thermal behavior of fluid in same manner as roughness on both hot and bottom wall but slightly modification. Isotherms for top roughness with amplitude of 0.1 and 8 roughness elements is shown for Ra number 10^4 and $5x10^5$. Isotherms are suppressed like in case of bottom roughness and there is confinement of isothermal lines in wakes of roughness elements but as roughness is present on top or cold wall, therefore, effects of roughness is slightly less pronounced as compared to case when roughness is present on hot wall. This behavior is also delineated in the Figure 4-9.

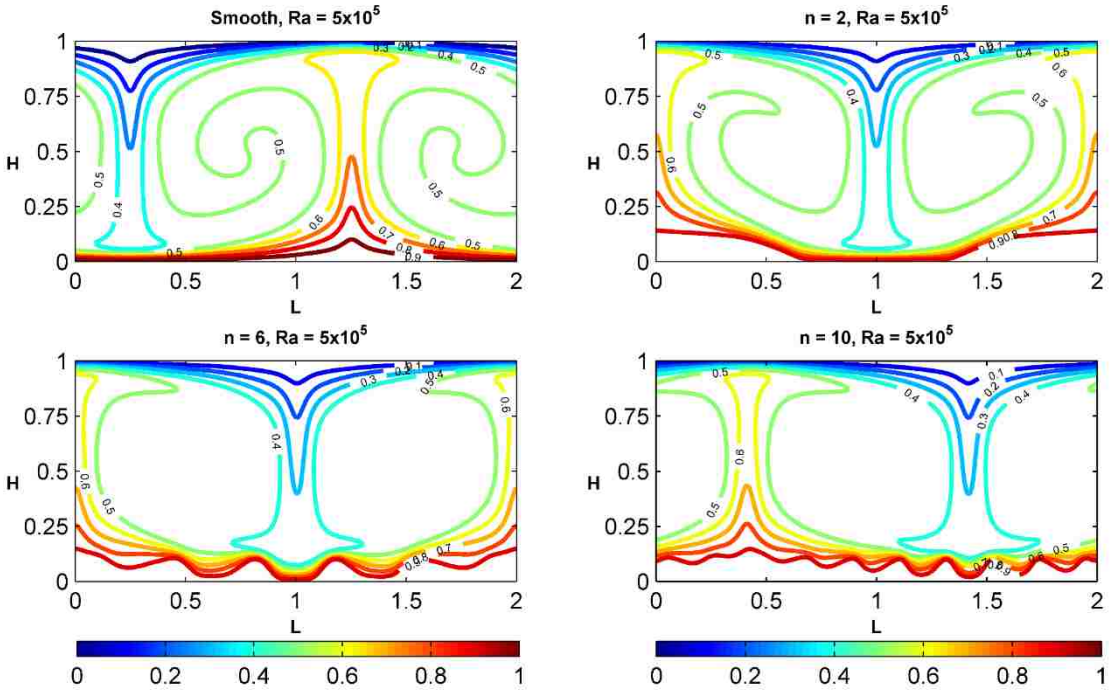

Figure 4-21: Isothermal Lines for Constant Roughness Amplitude of 0.1 at Bottom Wall and Varying Number of Roughness Elements for Ra – $5x10^5$

Behavior of isotherms in case of roughness present on both top and bottom walls is somewhat different than other cases of only top or bottom roughness. Figure 4-23

shows behavior of isothermal lines for roughness elements equal to 10 and varying amplitude of 0.025, 0.05 and 0.15. At Ra number 10^4, with the amplitude of roughness 0.025, and 0.05, isotherms behave in same manner as in the case of smooth. But when amplitude is further increased to 0.15, a quadru-cellular flow generates periodic swirling of isothermal lines. For all cases isotherms are parallel at peak of roughness and change shape with shape of roughness elements. This phenomenon persists up to Ra number of 10^5. When Ra number is further increased to $5x10^5$, a quadru-cellular flow is converted to bi-cellular flow. Also, at high Ra number of $5x10^5$, hot spots get elongated and occupy more area of hot wall. Similar behavior of isothermal lines has been reported by a numerical study performed by Das and Mahmud [34] in a cavity of sinusoidal top and bottom walls.

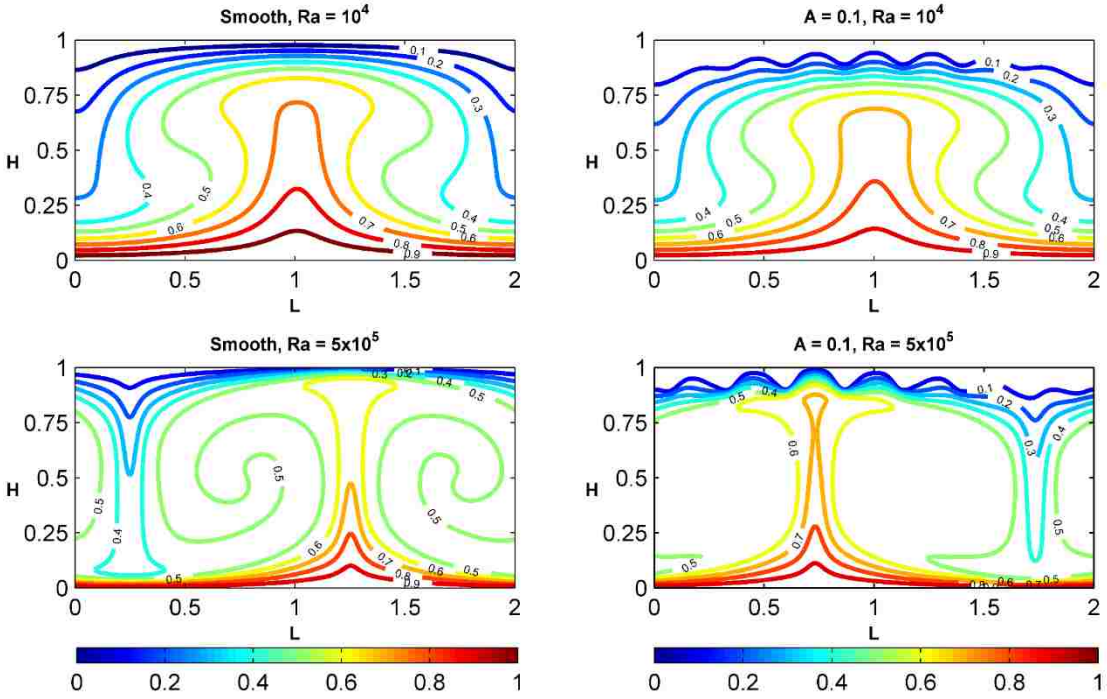

Figure 4-22: Isothermal Lines for Constant Roughness Amplitude of 0.1 at Top Wall and 8 Roughness Elements

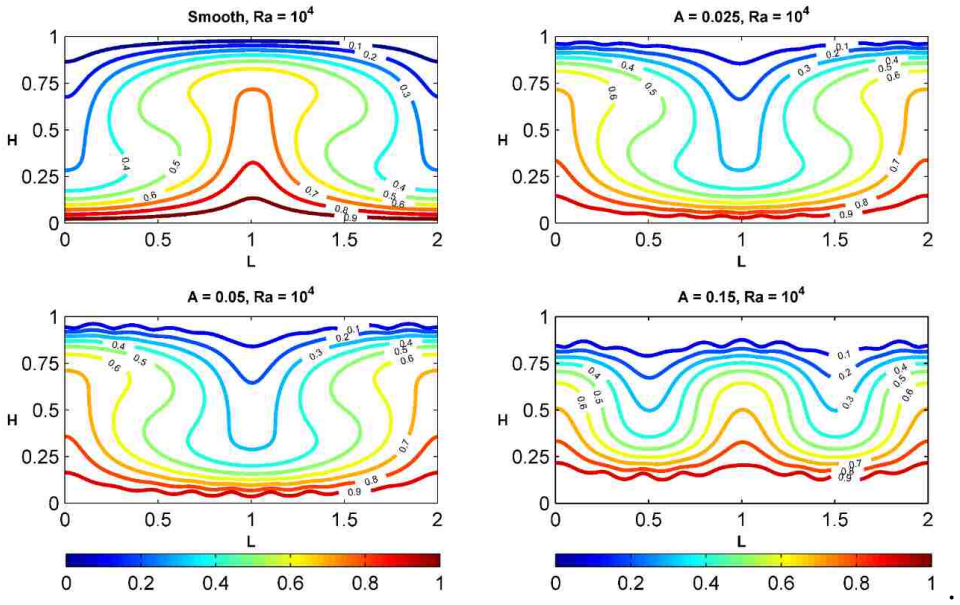

Figure 4-23: Isotherms for Constant Roughness Elements of 10 and Varying Amplitude

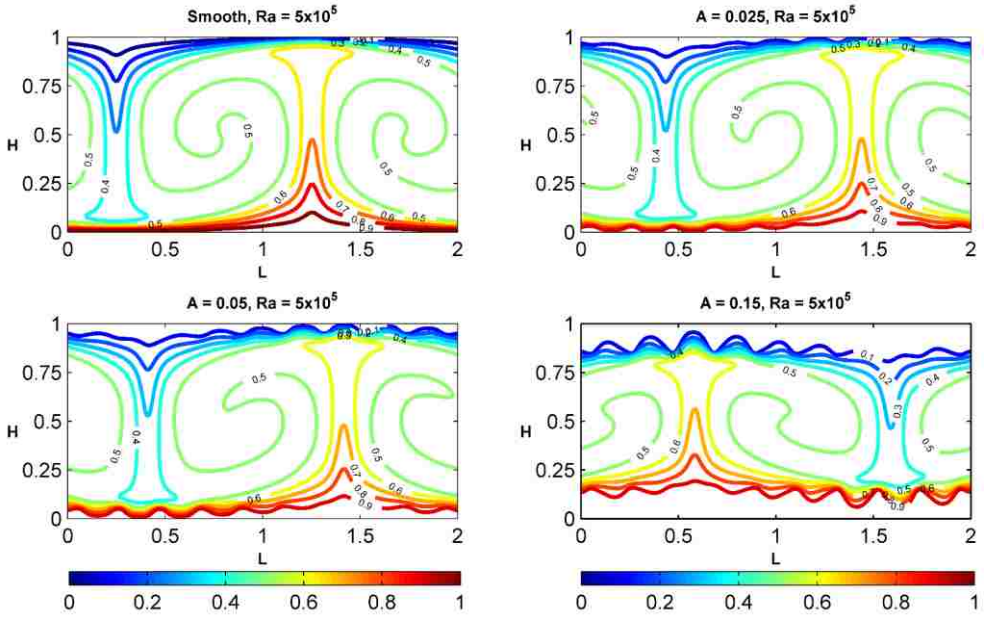

Figure 4-24: Isotherms for Constant Roughness Elements of 10 and Varying Amplitude

5. Conclusion

The general view that roughness does not play any significant role during laminar or low Ra number in natural convection has been investigated numerically in classical Rayleigh-Bénard convection. Numerical study of Rayleigh-Bénard convection with sinusoidal roughness elements present on boundaries has been performed using single relaxation time BGK model of LBM satisfying criteria of incompressibility. Qualitative as well as quantitative analysis have been performed to explore the role of surface roughness on average heat transfer up to Ra number $5x10^5$. Following are the significant conclusions of this study;

i. A numerical scheme based on single relaxation time BGK model of LBM was found stable up to Ra number of $5x10^5$ in Rayleigh-Bénard convection with smooth and as well as rough walls.

ii. A small roughness of dimensionless amplitude of 0.025 present on bottom hot and/or top cold wall does not have any significant effects on average heat transfer. This result suggest that there may be a critical roughness amplitude for a given Ra number which will impact the flow as well as heat transfer of the system.

iii. An increase in the amplitude of roughness elements enhances reduction in the average heat transfer increasing Ra number.

iv. The degradation was observed at $5x10^5$ to be 21% for roughness amplitude of 0.15 with 8 elements. Presence of sinusoidal roughness elements on top and bottom walls simultaneously with amplitude of 0.15 and 10 roughness elements cause a reduction in the heat transfer of 51% and 37% for Ra number $5x10^3$ and $5x10^5$ respectively.

v. Roughness causes a delay in the onset of natural convection. This delay increases with increase in amplitude of sinusoidal roughness elements.

vi. In all cases with and without roughness, isotherms and streamlines remain bi-cellular except in the case when roughness is present on both walls simultaneously with amplitude of 0.15. At this amplitude and Ra number 10^4, flow is transformed into quadru-cellular flow with a further increase in Ra to $5x10^5$, it is transformed to bi-cellular again.

vii. Some physical phenomenon were studied causing degradation in heat transfer with most significant is formation of eddies or vortices in the wake of roughness elements. These vortices prevent the main body of the fluid from interacting with the wall and hence degradation in heat transfer is observed.

References

[1] P. Le Gal, V. Croquette, Appearance of a square pattern in a Rayleigh–Bénard experiment, Physics of Fluids (1958-1988), 31(11) (1988) 3440-3442.

[2] A.V. Getling, Rayleigh-Bénard Convection, World Scientific, 1998.

[3] H. Bénard, Les tourbillons cellulaires dans une nappe liquide.-Méthodes optiques d'observation et d'enregistrement, J. Phys. Theor. Appl., 10(1) (1901) 254-266.

[4] L. Rayleigh, LIX. On convection currents in a horizontal layer of fluid, when the higher temperature is on the under side, The London, Edinburgh, and Dublin Philosophical Magazine and Journal of Science, 32(192) (1916) 529-546.

[5] M. Latif, Heat convection, in, Berlin: Springer-Verlag, 2006.

[6] O. Turgut, N. Onur, An experimental and three-dimensional numerical study of natural convection heat transfer between two horizontal parallel plates, International communications in heat and mass transfer, 34(5) (2007) 644-652.

[7] G. Stringano, G. Pascazio, R. Verzicco, Turbulent thermal convection over grooved plates, Journal of Fluid Mechanics, 557 (2006) 307-336.

[8] W.M. Rohsenow, J.P. Hartnett, E.N. Ganic, Handbook of heat transfer applications, New York, McGraw-Hill Book Co., 1985, 973 p. No individual items are abstracted in this volume., 1 (1985).

[9] O. Shishkina, C. Wagner, Modelling the influence of wall roughness on heat transfer in thermal convection, Journal of Fluid Mechanics, 686 (2011) 568-582.

[10] G. Ahlers, Experiments with Rayleigh-Bénard convection, in: Dynamics of Spatio-Temporal Cellular Structures, Springer, 2006, pp. 67-94.

[11] T. Chu, R. Goldstein, Turbulent convection in a horizontal layer of water, Journal of Fluid Mechanics, 60(01) (1973) 141-159.

[12] J.W. Deardorff, A numerical study of two-dimensional parallel-plate convection, Journal of the Atmospheric Sciences, 21(4) (1964) 419-438.

[13] E. Bodenschatz, W. Pesch, G. Ahlers, Recent developments in Rayleigh-Bénard convection, Annual review of fluid mechanics, 32(1) (2000) 709-778.

[14] E.D. Siggia, High Rayleigh number convection, Annual review of fluid mechanics, 26(1) (1994) 137-168.

[15] E. Koschmieder, S. Pallas, Heat transfer through a shallow, horizontal convecting fluid layer, International Journal of Heat and Mass Transfer, 17(9) (1974) 991-1002.

[16] J.S. Malkus, G. Witt, The evolution of a convective element: A numerical calculation, The atmosphere and the sea in motion, (1959) 425-439.

[17] R. Praslov, On the effects of surface roughness on natural convection heat transfer from horizontal cylinders to air, Inzhenerno Fizicheskii Zhurnal (in Russian), 4 (1961) 3-7.

[18] J. Chinnappa, Free convection in air between a 60 vee-corrugated plate and a flat plate, International Journal of Heat and Mass Transfer, 13(1) (1970) 117-123.

[19] S. Elsherbiny, K. Hollands, G. Raithby, Free convection across inclined air layers with one surface V-corrugated, Journal of Heat Transfer, 100(3) (1978) 410-415.

[20] C. Saidi, F. Legay-Desesquelles, B. Prunet-Foch, Laminar flow past a sinusoidal cavity, International journal of heat and mass transfer, 30(4) (1987) 649-661.

[21] M. Ruhul Amin, Natural convection heat transfer and fluid flow in an enclosure cooled at the top and heated at the bottom with roughness elements, International journal of heat and mass transfer, 36(10) (1993) 2707-2710.
[22] Y. Shen, P. Tong, K.-Q. Xia, Turbulent convection over rough surfaces, Physical review letters, 76(6) (1996) 908.
[23] E. Villermaux, Transfer at rough sheared interfaces, Physical review letters, 81(22) (1998) 4859.
[24] Y.-B. Du, P. Tong, Enhanced heat transport in turbulent convection over a rough surface, Physical review letters, 81(5) (1998) 987.
[25] S. Ciliberto, C. Laroche, Random roughness of boundary increases the turbulent convection scaling exponent, Physical review letters, 82(20) (1999) 3998.
[26] S. Pretot, B. Zeghmati, P. Caminat, Influence of surface roughness on natural convection above a horizontal plate, Advances in Engineering Software, 31(10) (2000) 793-801.
[27] P.K. Das, S. Mahmud, Numerical investigation of natural convection inside a wavy enclosure, International Journal of Thermal Sciences, 42(4) (2003) 397-406.
[28] J.-C. Tisserand, M. Creyssels, Y. Gasteuil, H. Pabiou, M. Gibert, B. Castaing, F. Chillà, Comparison between rough and smooth plates within the same Rayleigh–Bénard cell, Physics of Fluids (1994-present), 23(1) (2011) 015105.
[29] M.N. Hasan, S. Saha, S.C. Saha, Effects of corrugation frequency and aspect ratio on natural convection within an enclosure having sinusoidal corrugation over a heated top surface, International Communications in Heat and Mass Transfer, 39(3) (2012) 368-377.
[30] S. Penner, R. Seiser, K. Schultz, Steps toward passively safe, proliferation-resistant nuclear power, Progress in Energy and Combustion Science, 34(3) (2008) 275-287.
[31] T. Schulz, Westinghouse AP1000 advanced passive plant, Nuclear Engineering and Design, 236(14) (2006) 1547-1557.
[32] L. Lommers, F. Shahrokhi, J. Mayer III, F. Southworth, AREVA HTR concept for near-term deployment, Nuclear Engineering and Design, 251 (2012) 292-296.
[33] M.D. Donne, L. Meyer, Turbulent convective heat transfer from rough surfaces with two-dimensional rectangular ribs, international Journal of Heat and Mass transfer, 20(6) (1977) 583-620.
[34] R. Firth, L. Meyer, A comparison of the heat transfer and friction factor performance of four different types of artificially roughened surface, International Journal of Heat and Mass Transfer, 26(2) (1983) 175-183.
[35] S.G. Kandlikar, Exploring Roughness Effect on Laminar Internal Flow–Are We Ready for Change?, Nanoscale and Microscale Thermophysical Engineering, 12(1) (2008) 61-82.
[36] Y.-B. Du, P. Tong, Turbulent thermal convection in a cell with ordered rough boundaries, Journal of Fluid Mechanics, 407 (2000) 57-84.
[37] X. Shan, Simulation of Rayleigh-Bénard convection using a lattice Boltzmann method, Physical Review E, 55(3) (1997) 2780.
[38] K. Xu, S.H. Lui, Rayleigh-Bénard simulation using the gas-kinetic Bhatnagar-Gross-Krook scheme in the incompressible limit, Physical Review E, 60(1) (1999) 464.

[39] Y. Zhou, R. Zhang, I. Staroselsky, H. Chen, Numerical simulation of laminar and turbulent buoyancy-driven flows using a lattice Boltzmann based algorithm, International Journal of Heat and Mass Transfer, 47(22) (2004) 4869-4879.
[40] M.C. Sukop, D.T. Thorne, Lattice Boltzmann modeling: an introduction for geoscientists and engineers, Springer, 2007.
[41] A. Mohamad, Lattice Boltzmann Method, Springer, 2011.
[42] M.R. Amin, The effect of adiabatic wall roughness elements on natural convection heat transfer in vertical enclosures, International journal of heat and mass transfer, 34(11) (1991) 2691-2701.
[43] J.R. Welty, C.E. Wicks, G. Rorrer, R.E. Wilson, Fundamentals of momentum, heat, and mass transfer, John Wiley & Sons, 2009.
[44] A. Mohamad, A. Kuzmin, A critical evaluation of force term in lattice Boltzmann method, natural convection problem, International Journal of Heat and Mass Transfer, 53(5) (2010) 990-996.
[45] L.M. Jiji, L.M. Jiji, Heat convection, Springer, 2006.
[46] J. Wang, D. Wang, P. Lallemand, L.-S. Luo, Lattice Boltzmann simulations of thermal convective flows in two dimensions, Computers & Mathematics with Applications, 65(2) (2013) 262-286.
[47] J. Eggels, J. Somers, Numerical simulation of free convective flow using the lattice-Boltzmann scheme, International Journal of Heat and Fluid Flow, 16(5) (1995) 357-364.
[48] H. Dixit, V. Babu, Simulation of high Rayleigh number natural convection in a square cavity using the lattice Boltzmann method, International journal of heat and mass transfer, 49(3) (2006) 727-739.
[49] Q. Zou, X. He, On pressure and velocity boundary conditions for the lattice Boltzmann BGK model, Physics of Fluids (1994-present), 9(6) (1997) 1591-1598.
[50] Z. Guo, C. Shu, Lattice boltzmann method and its applications in engineering (advances in computational fluid dynamics), World Scientific Publishing Company, 2013.
[51] X. Yang, B. Shi, Z. Chai, Generalized modification in the lattice Bhatnagar-Gross-Krook model for incompressible Navier-Stokes equations and convection-diffusion equations, Physical Review E, 90(1) (2014) 013309.
[52] G. de Vahl Davis, Natural convection of air in a square cavity: a bench mark numerical solution, International Journal for Numerical Methods in Fluids, 3(3) (1983) 249-264.
[53] R. Clever, F. Busse, Transition to time-dependent convection, J. Fluid Mech, 65(4) (1974) 625-645.
[54] A. Nag, A. Sarkar, V. Sastri, Natural convection in a differentially heated square cavity with a horizontal partition plate on the hot wall, Computer methods in applied mechanics and engineering, 110(1) (1993) 143-156.
[55] G. de Vahl Davis, I. Jones, Natural convection in a square cavity: a comparison exercise, International Journal for numerical methods in fluids, 3(3) (1983) 227-248.
[56] X. He, S. Chen, G.D. Doolen, A novel thermal model for the lattice Boltzmann method in incompressible limit, Journal of Computational Physics, 146(1) (1998) 282-300.

[57] P.-H. Kao, R.-J. Yang, Simulating oscillatory flows in Rayleigh–Benard convection using the lattice Boltzmann method, International Journal of Heat and Mass Transfer, 50(17) (2007) 3315-3328.
[58] G. Tanda, Natural convection heat transfer in vertical channels with and without transverse square ribs, International journal of heat and mass transfer, 40(9) (1997) 2173-2185.
[59] S. Shakerin, M. Bohn, R. Loehrke, Natural convection in an enclosure with discrete roughness elements on a vertical heated wall, International journal of heat and mass transfer, 31(7) (1988) 1423-1430.
[60] Y. Ji, K. Yuan, J. Chung, Numerical simulation of wall roughness on gaseous flow and heat transfer in a microchannel, International journal of heat and mass transfer, 49(7) (2006) 1329-1339.
[61] C. Zhang, Y. Chen, M. Shi, Effects of roughness elements on laminar flow and heat transfer in microchannels, Chemical Engineering and Processing: Process Intensification, 49(11) (2010) 1188-1192.
[62] S. Vijiapurapu, J. Cui, Performance of turbulence models for flows through rough pipes, Applied Mathematical Modelling, 34(6) (2010) 1458-1466.

II. EFFECTS OF AMPLITUDE OF ROUGHNESS ELEMENTS ON HEAT TRANSFER IN A RECTANGULAR CAVITY

M. Yousaf, and S. *Usman

ABSTRACT: The Lattice Boltzmann method was used to numerically investigate the natural convection heat transfer in the presence of sinusoidal roughness elements, in a two-dimensional rectangular cavity heated at the bottom. The single relaxation time Bhatnagar-Gross-krook (BGK) model of Lattice Boltzmann method was used to solve coupled flow and energy equations in a two-dimensional lattice. A computational model was validated against previous benchmark solutions, and a very good agreement was found to exist with smooth and rough cavities. Numerical studies were performed for a Newtonian fluid with a Prandtl number (*Pr*) 1.0 in a cavity of aspect ratio (L/H) 2.0. Sinusoidal roughness elements (n = 8) were placed on hot, cold, and both hot and cold walls. The dimensionless amplitude was varied from 0.015 to 0.15 in small steps. The frequency of roughness was held constant to investigate Rayleigh number (*Ra*) from 10^3 to 10^6. Thermal and hydrodynamic behaviors were studied by analyzing isotherms, streamlines and the average heat transfer rate in presence of roughness elements in the laminar flow region. The computational results indicate that a small roughness of approximately 0.025 has no significant effects on average heat transfer. In contrast, the presence of sinusoidal roughness with an amplitude $\geq$ 0.05 causes the average heat transfer to degrade in the cavity and delay in on set of natural convection.

Keywords: Heat transfer, Natural convection, Roughness, Cavity, Laminar flow

1. Introduction

An understanding of the heat transfer through buoyancy induced flows is essential because of its immense applications [66]. These applications range from design of cooling of electronics equipment [47], energy systems for buildings [67], heat transfer in solar collectors [68], to passive heat removal systems in nuclear reactors [38, 39]. Most of the flows of natural convection heat transfer in nature and in industrial processes are over surfaces having some degree of roughness, or wavy structure like in atmosphere, ocean, and buildings [69]. Similarly, surface roughness plays a significant role in a micro-scale device's performance, where smooth surfaces are rare [70]. Therefore, a fundamental understanding is required to explore the role of surface roughness during natural convection heat transfer. A better understanding of roughness during natural convection can lead to efficient energy system design.

Natural convection in cavities has primarily been studied in three categories: smooth cavities, cavities with either single or multiple partitions, and walls with either wavy or rectangular roughness on the surface. Both the hydrodynamic and the thermal behavior present in smooth cavities have been investigated over decades with different boundary conditions on walls and has been presented in detail [66, 71-73]. EISherbiny et al. [26] experimentally investigated effects of V-corrugated plate on heat transfer. They used air as a working fluid in a cavity of aspect ratio 12 or greater with dimensionless amplitude of V-corrugation 1, 2.5, and 4. The range of Ra number was $< 4x10^6$, which was calculated using mean spacing of two plates with an inclination angle from 0 to 60 degree. They found a decrease in the heat transfer up to 50 percent as compared to smooth or flat surfaces. Bajorek and LIoyd [74] performed experimental studies to investigate the influence of insulated horizontal walls with partitions, and isothermal vertical walls on heat transfer in a square cavity of aspect ratio 1. They utilized air and carbon dioxide as working fluid. They concluded that the heat transfer decreased between 12 to 21% due to the presence of insulated partitions.

Nienchuan and Bejan [75] experimentally studied effects of the opening above partition in a rectangular enclosure with isothermal side walls and insulated horizontal walls with water as a working fluid. They found that the Nusselt number decreased as the partition height increased, up to 15%. Anderson and Bohn [68] examined effects of

roughness on heat transfer in a water filled cubical geometry at very high Ra number of 10^{10}. They found a maximum increase in the Nusselt number of up to 15%. Shaw et al. [67] used the cubic spline method to perform numerical studies within a square cavity. They focused on analyzing the effects of insulated partitions on the heat transfer. They used partitions with different heights, at varying distances from the hot wall. Horizontal walls were adiabatic and vertical walls were used as isothermals. They concluded that heat transfer decreased as partitions height increased.

Shakerin and Bohn [62] performed experiments to examine effects of the roughness with single and double rectangular roughness elements on vertical isothermal wall of square cavity. They investigated Ra number 10^6 and 10^8 with air as working fluid. Here the heat transfer increased in the presence of hot roughness elements. Yucel and Ozdem [76] investigated the effects of multiple partitions both conducting and insulating on the heat transfer that occurs in a square cavity. They found that the mean Nusselt number decreased as the number of partitions increased. Saidi et al. [27] experimentally studied the fluid flow and heat transfer behavior from a sinusoidal cavity. They found that the heat transfer from a wavy wall to a fluid decreased due to the presence of a vortex formation in a laminar region.

Amin [28] used the term ‘roughness’ when the cavity’s wall was comprised of rectangular elements. He [47] numerically found that the heat transfer decreased up to 44% within an enclosure of aspect ratio greater than 1. He used adiabatic rectangular roughness elements on the bottom wall with the vertical walls as isothermal. Amin [77] also performed numerical simulations of a cavity with aspect ratio 1and 4. He used the air as a working fluid and range of Ra number from 10^3 to 10^5. He concluded that with one vertical and horizontal walls as adiabatic and others isothermal with roughness elements, an increase in the heat transfer was 78% with higher amplitude of the roughness elements. In another study of Amin [28] with isothermal rectangular roughness elements at bottom wall and adiabatic vertical walls. He used an enclosure of aspect ratio 1.0 and investigated Ra number up to 10^5. He observed a decrease in the heat transfer up to 61% as compared to the smooth walls cavity.

Wang and Vanka [78] studied convective heat transfer in a sinusoidal wavy passage using numerical techniques in a laminar region. They found an enhancement in

heat transfer. Adjlout et al. [79] presented the results they gathered from numerical study on corrugated hot wall. They investigated effects on the heat transfer in an inclined square cavity with horizontal walls as adiabatic. They observed that fluid's thermal and hydrodynamic behavior was sensitive to a hot wall's corrugation. Ashjaee et al. [80] used both numerical studies using finite volume approach and experimental studies to analyze the effects of a vertical wavy surface on heat transfer. They found that the average heat transfer decreased as the amplitude-wavelength ratio increased.

Prétot [33] conducted both experimental and numerical studies using finite difference method to examine the effects of a sinusoidal plate's surface at uniform heat flux, in a semi-infinite medium. They found that eddies formed in the wake of roughness elements as amplitude increased. They also found that the heat transfer decreased as sinusoidal elements amplitude was increased.

Das and Mahmud [34] used finite volume approach to perform numerical studies in an attempt to analyze the influence of two wavy walls on the heat transfer and fluid flow for a fluid of Pr number 1.0. Both the bottom and top walls were sinusoidal with isothermal boundary conditions. The straight side walls were adiabatic in an enclosure with an aspect ratio of 2. They concluded that the amplitude-wavelength ratio did impact local heat transfer. But it did not significantly affect average heat transfer.

Hasan et al [36] investigated effects of sinusoidal corrugation on top wall with constant heat flux on the heat transfer in a cavity with an aspect ratio of 0.5 to 2.0. They used air as a working fluid using finite element based approach. They assumed that the vertical walls as isothermal and bottom wall insulated, and varied corrugation from 3 to 5. They carried out simulations for *Ra* number between 10^3 and 10^6. They found that the heat transfer increased as the corrugation frequency increased.

Natural convection has been an integral part of nuclear reactor heat transfer systems. It's importance was further enhanced with the incorporation of passive phenomenon in advanced and small modular reactors [38, 39]. Meyer [81] experimentally studied role of roughness elements on single rod heat transfer and pressure drop. He concluded that law of wall does not hold for rough surfaces, and the friction factor was dependent on the roughness amplitude. Harry et al. experimentally studied effects of surface characteristics like roughness, wettability, and porosity on a

boiling critical heat flux [82]. Similar studies were reported by Chang and You [83] related to role of surface structure and its effects on boiling heat transfer.

Heat transfer studies are typically conducted in an attempt to enhance the heat transfer. One of the most significant method to augment the heat transfer is to utilize surface roughness [15]. The role of roughness cannot be utilized effectively without a proper understanding of all shapes of roughness elements including circular, transvers, V-shaped and sinusoidal. Amin [28, 47, 77] examined both adiabatic and isothermal walls that contained rectangular roughness elements. Das and Mahmud [34] considered both top and bottom walls as wavy, and Hasan et al. [36] used top wall as corrugated with uniform heat flux. The effects of sinusoidal type roughness elements placed on either a smooth or a flat wall are, however rare. Present study was focused on using sinusoidal roughness elements on a wall instead of making wall as corrugated as in several previous studies. These sinusoidal roughness elements were introduced on smooth or flat bottom wall, top wall, and both top and bottom walls. The amplitude was varied so that impact of roughness elements on fluid flow and heat transfer in a rectangular cavity could be observed. Roughness elements were assumed to be at same the temperature as that of the corresponding wall. Recently developed technique based on a single relaxation time BGK model of LBM was used to perform numerical simulations. Computational work has been performed extensively using a single relaxation time based BGK model of LBM for square cavity with side heating [53, 55]. But studies with bottom heating of cavity which are inherently unstable as described by Amin [28] are rare. Therefore, the numerical stability of a single relaxation time BGK model of LBM was explored and simulations were conducted out up to Ra number 10^6.

Nomenclature

A	Dimensionless Amplitude (h/H)	T_{ref}	Reference Temperature (K)
g	Gravitational acceleration (ms^{-2})	ts	Time step
H	Height of cavity (m)	U	Horizontal velocity component (ms^{-1})
h	Height of Roughness Element (m)	V	Vertical velocity component (ms^{-1})
K	Thermal conductivity ($Wm^{-1}k^{-1}$)	x	Coordinate parallel to the wall (m)
L	Length of cavity (m)	y	Coordinate normal to the wall (m)
lu	Lattice unit		
Nu	Nusselt number	**Greek symbols**	
n	Number of Roughness Elements		
Pr	Prandtl number	α	Molecular thermal diffusivity (m^2s^{-1})
Ra	Rayleigh Number	β	Coefficient of thermal expansion (K^{-1})
ΔT	Temperature difference (K)	θ	Dimensionless temperature
T_c	Temperature of cold wall (K)	ν	Molecular kinematic viscosity (m^2s^{-1})
T_h	Temperature of hot wall (K)	ρ	Density ($Kg.m^{-3}$)

2. Computational model

In order to investigate the effects of amplitude of isothermal sinusoidal roughness elements on heat transfer and fluid flow during natural convection, a two-dimensional rectangular cavity was considered. The rectangular cavity of aspect ratio (*L/H*) 2.0 with corresponding boundary conditions is shown in Figure 2-1. Eight sinusoidal roughness elements were typically used throughout this study. The normalized amplitude (*h/H*), denoted by '*A*,' varied from very small 0.015 to 0.15. The choice of amplitude was selected to observe any small effect because of the roughness presence. Roughness elements were maintained at the same temperature as corresponding wall. A technique based on a single relaxation time BGK model of LBM was used to solve the momentum and energy equations for both the laminar flow and heat transfer of a Newtonian fluid. Viscous dissipation in energy equation was assumed negligible. The fluid was assumed to be radiatively non-participating medium, and the compression work was assumed to be negligible. Momentum and energy equations are coupled through the Boussinesq approximation [36]. All other properties were considered constant. However, density varied with the temperature and incorporated using Boussinesq approximation shown in Equation 1.[48]

$$\rho - \rho_{\infty} = \rho_{\infty} g \beta \Delta T \tag{1}$$

The following dimensionless numbers and parameters were used to solve the energy and momentum equations numerically [2, 48].

$$Ra_{H} = \frac{g \beta \Delta T H^{3}}{\upsilon \alpha} \tag{2}$$

$$P_{r} = \frac{\upsilon}{\alpha} \tag{3}$$

$$\theta = \frac{T - T_{ref}}{T_{h} - T_{c}} \tag{4}$$

Here, T_{ref} is mean, or average, temperature of cold and hot wall. The dimensionless number known as the Nusselt number (Nu) was used to calculate the heat transfer [34, 45].

$$Nu_{av} = 1 + \frac{< V . \theta > H}{k \Delta \theta} \tag{5}$$

$$Nu_{av} = \frac{H}{L}\int_0^L \left(\frac{\partial \theta}{\partial y}\right) dx \qquad (6)$$

Where '< >' is the quantity averaged over the entire fluid volume, $\Delta\theta$ is the temperature difference between the hot and cold walls, 'V' is the horizontal velocity, and  was the temperature gradient normal to the hot wall.

Both hydrodynamic and thermal boundary conditions for numerical simulations throughout this study were given as follows:

At all walls: U = V = 0, the no slip boundary conditions for velocity,

Bottom wall: $\theta_h = 1$, and top wall: $\theta_c = 0$

The side or vertical walls:  were assumed adiabatic

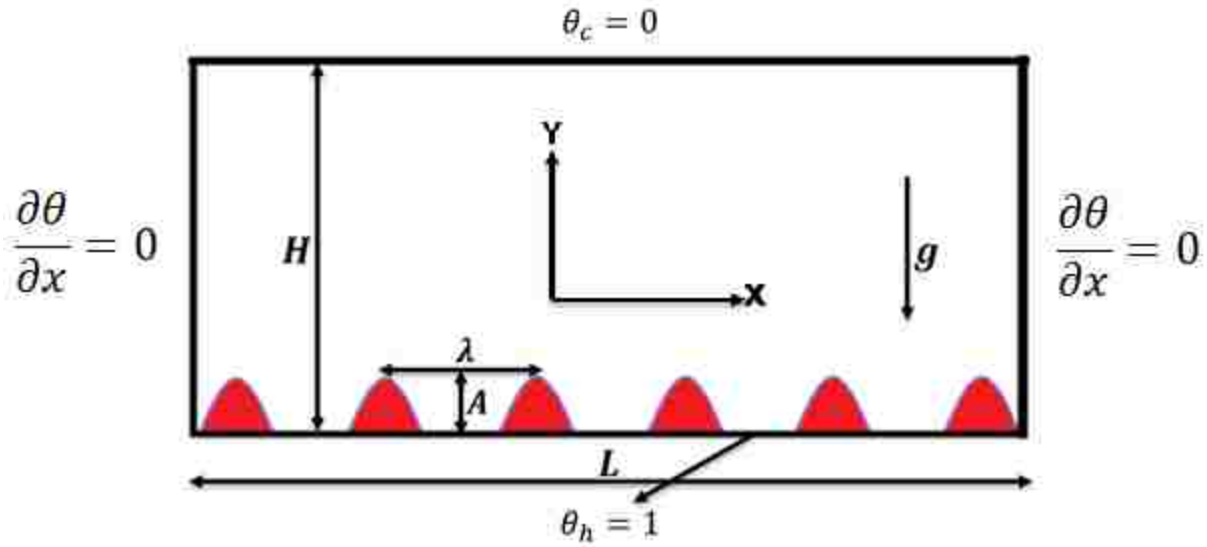

Figure 2-1 Schematic of a Rectangular Cavity with Sinusoidal Roughness Elements on both Bottom Wall and Boundary Conditions

2.1 Lattice Boltzmann method

The Lattice Boltzmann method (LBM), first introduced in 1980s, has become an alternative to traditional numerical methods that are based on finite volume, element, and finite difference method for solution of Navier-Stokes and energy equations [53, 55]. The LBM is an important tool when simulating single and two phase heat and fluid flows, buoyancy induced flows, and condensation and evaporation in complex geometries [7]. It can be used to solve the dynamics of a hypothetical particle based on the Boltzmann equation. it has many advantages like ease of algorithm, no special treatments of boundaries for velocity boundary conditions in porous and complex geometries, and solution of Laplace equation is not required at every time step [2].

Besides, its major advantages, LBM still has some challenges of stability particularly for high Ra number flows. Progress being made in overcoming these challenges. As a well-established model of LBM based on a single relaxation time model of BGK was utilized in the present study. Therefore, reader is referred for a complete and detailed discussion of all previous models presented to date, to improve its stability to Yang [55], Mohamad [2] and Guo [4].

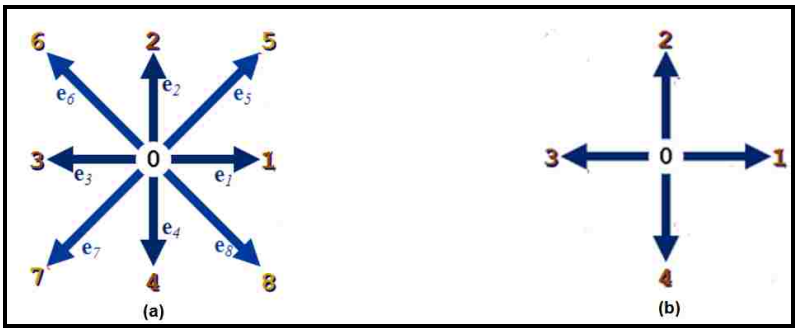

Figure 2-2: D2Q9 Lattice Velocity and D2Q5 Temperature Model for LBM [7]

A general D2Q9 and D2Q5 model with nine velocity and five temperature components is illustrated in Figure 2-2. D2Q9 model was used in this study to solve the

Navier-Stokes equation and D2Q5 with five temperature components to solve the energy equation as a passive scalar [7]. The basic equation used to solve the Navier-Stokes and energy equations, based on the Bhatnagar-Gross-krook model, and external force, and with a single relaxation time, is given as [2];

$$f_i(x + e_i\Delta t, t + \Delta t) = f_i(x,t) - \frac{\left(f_i(x,t) - f_i^{eq}(x,t)\right)}{\tau} + \Delta t F_{ext} \quad (7)$$

Where *'e_i'* and *'Δt'* are the lattice velocity and the time, respectively, '$\boldsymbol{F_{ext}}$' is the external force, and '$\boldsymbol{\tau}$' is relaxation time. The equilibrium distribution function for the Navier-Stokes and energy equation is shown in [49];

$$f_i^{eq} = w_i \rho \left[1 + 3(c_i.u) + 4.5(c_i.u)^2 - 1.5(u.u)\right] \quad (8)$$

Where w_i = 4/9, 1/9, 1/9, 1/9, 1/9, 1/36, 1/36, 1/36, 1/36, respectively for i= 0 to 8. For the energy equation;

$$g_j^{eq} = w_j T \left[1 + 3(c_i.u)\right] \quad (9)$$

w_j = 1/3, 1/6, 1/6, 1/6, 1/6, respectively for j= 0 to 4.

Here, 'u' is the velocity of fluid that has both vertical (V) and horizontal (U) components, and *'g'* and *'f'* are the distribution functions of energy and momentum equation, respectively. The external force which was the buoyancy force in this study can be introduced either during the collision function calculation or during the calculation of equilibrium function in velocity term [2]. The external force in this study was introduced as [7];

$$V = V + g\beta\tau_f \left(T - T_{ref}\right) \quad (10)$$

Where '$\boldsymbol{\tau_f}$' is the relaxation time for momentum equation. The macroscopic variables corresponding values calculated as [7];

$$\rho = \sum_{i=0}^{8} f_i \quad u = \frac{1}{\rho}\sum_{i=0}^{8} c_i f_i \quad \text{and} \quad T = \frac{1}{\rho}\sum_{i=0}^{4} g_i \quad (11)$$

Viscosity and thermal diffusivity were used to calculate the relaxation time for the Navier-Stokes and energy equation [49].

$$\upsilon = \frac{1}{3}\left(\tau_f - \frac{1}{2}\right) \tag{12}$$

$$\alpha = \frac{1}{3}\left(\tau_{energy} - \frac{1}{2}\right) \tag{13}$$

Boundary conditions are an essential part in solving the Navier-Stokes and energy equations (e.g. velocity and temperature). It is necessary to transform the density, velocity, and temperature boundary conditions for LBM to solve in terms of distribution function. As these boundary conditions have a direct effects on accuracy, stability and convergence [4]. In order to implement no slip boundary condition of the velocity, bounce back boundary conditions which is referred as "half-way wall bounce back" in Sukop and Thorne [7] are generally used in LBM for complex and porous geometries for a better accuracy up to second order. The only requirement is to characterize solid nodes and then no special programming algorithm is needed to implement boundary conditions. In the present study, mid plane or half-way bounce back approach was used for the hydrodynamic in order to achieve higher order accuracy. This also omit calculation of distribution function on solid boundaries but streaming process is carried out [2]. A detailed discussion of these boundary conditions and their implementation can be found in Sukop and Thorne [7] and Mohamad [2]. Results were produced up to a higher Ra number of 10^6 for a cavity with bottom heating, and the model was found to be numerically stable.

2.2 Benchmarking

The governing equations of fluid flow and heat transfer have been solved by using a computational code based on LBM of a Newtonian fluid of *Pr* number 1. The method's accuracy was examined and verified in two steps. In the first step, assessment of grid independence of results produced was verified for different meshes for Ra number 10^4 both for a square and rectangular cavity. Results are shown in Table 2-1 and corresponding geometries are shown in Figure 2-3 and Figure 2-4.

Table 2-1: Grid Independence Study for Natural Convection in Square and Rectangular Cavity using Average Nusselt Number (Nu_{av})

Ra	H	Present	% Error
Square Cavity Comparison with Davis and Jones[59]			
10^4	200	2.2241	0.8426
	250	2.2306	0.5528
	350	2.2381	0.2185
Rectangular Cavity Comparison with Hollands et al.[84]			
10^4	100	2.3707	0.8532
	200	2.3835	0.3178
	300	2.3896	0.0627

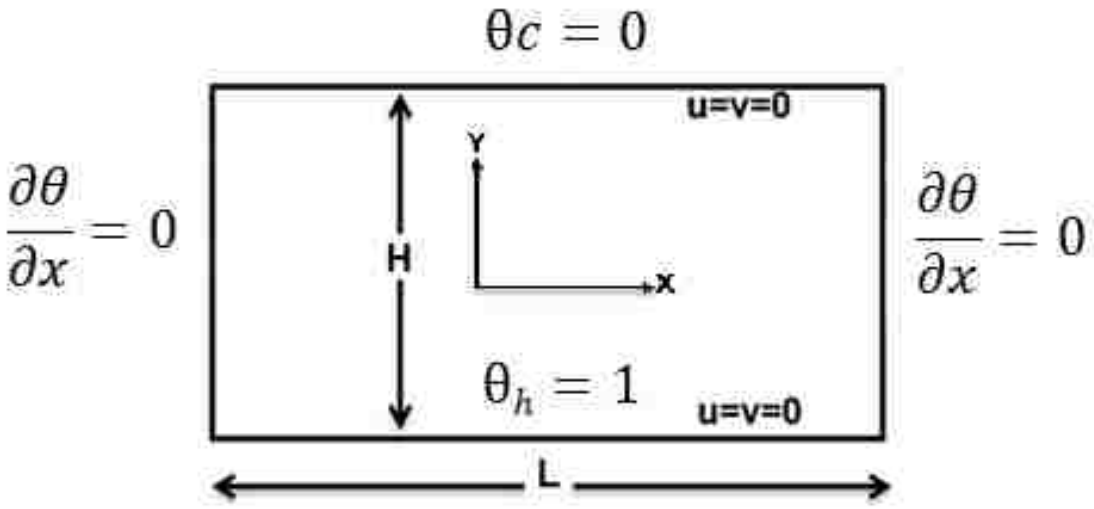

Figure 2-3: A Smooth Rectangular Cavity with an Aspect ratio of 2.0

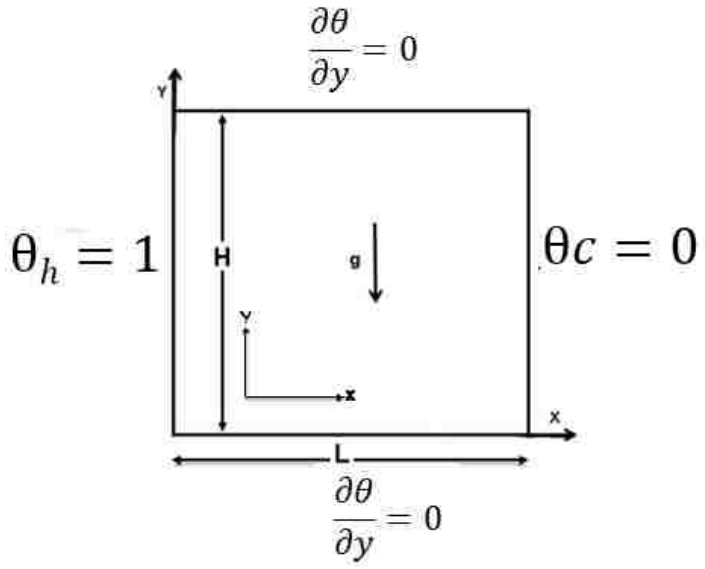

Figure 2-4: A Smooth Square Cavity with Side Heating and Insulated Bottom and Top Walls

The results with different number of grids were compared with benchmark solution of Davis and Jones [59] for square cavity and with Hollands et al. [84] for rectangular cavity heated at the bottom with aspect ratio 2. The error decreased as the number of grid points were increased. The minimum and maximum error calculated for the rectangular cavity was 0.06% and 0.85%, respectively. Therefore, a mesh of 600x300 was selected for the numerical simulation of Ra equal to 10^4 for better accuracy and larger mesh size for larger Ra number. This comparison indicates that code was able to produce results taken to be mesh independent.

In the second step of validation of numerical method, our results were compared with previous studies performed by Davis and Jones [59] for square cavity as shown in Figure 2-5 and with Ozisik [72] as shown in Figure 2-6. The results collected during this study were in good agreement with those collected by Davis and Jones and Ozisik [72]. In comparison with Ozisik [72], the amount of heat transfer at a high Ra number 10^6 was smaller in this study than it was in Ozisik [72] study. This may be due to reason that at a

high Ra number, LBM has less heat transfer for bottom heating cases and same was mentioned in earlier studies performed by Kun [45] and Shan [44].

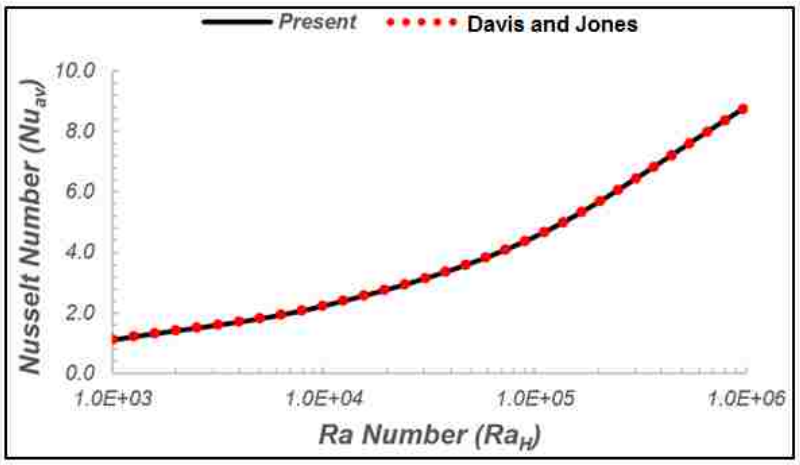

Figure 2-5: A Comparison of Present Results of Square Cavity with Davis and Jones [59]

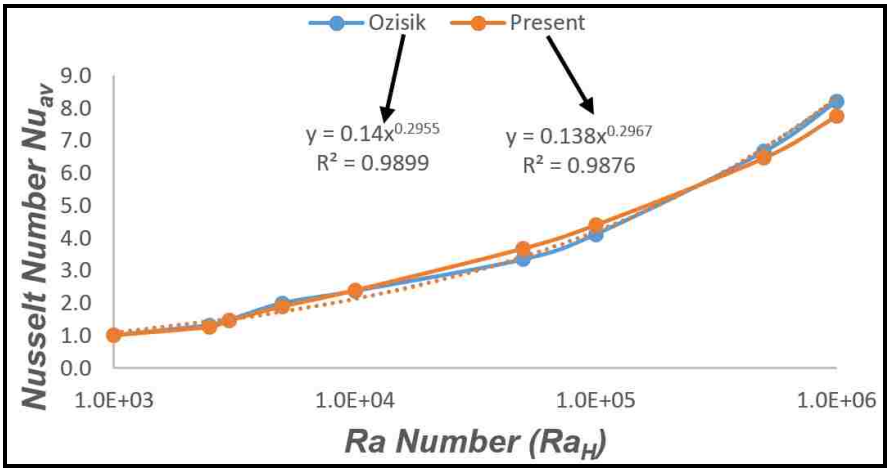

Figure 2-6: A Comparison of the Present Results Nu_{av} of Rectangular Cavity with Bottom Heating with Ozisik [72]

In order to further validate computational code for the case of natural convection in a square cavity with partition, simulations were performed for Ra number 10^4 to 10^6 for a cavity shown in Figure 2-7. The corresponding results for average Nu are shown in Figure 2-8. Our results were in good agreement with those collected by Shaw et al. [67]. As in case of square cavity, both top and bottom walls were adiabatic, thus the energy coming from one wall must be equal to the energy leaving another wall. This was confirmed by measuring the average Nusselt number along both hot and cold walls to further validate computational code. The convergence and steady state was verified by calculating average Nusselt number along both hot and cold walls of cavity.

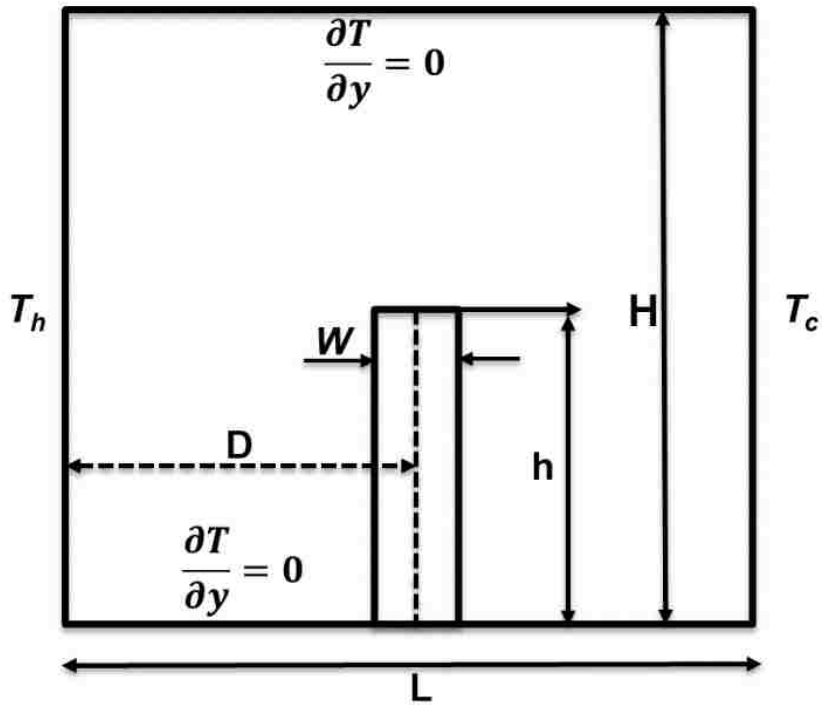

Figure 2-7: A Square Cavity with a Partition for Comparison

These comparisons with both the smooth and rough cavities, proved that the computational code can be used to produce reliable results with different boundary conditions. As natural convection in rectangular cavity with bottom heating has an inherent unstability of flows as prescribed by the Amin [28], therefore, our simulations were limited up to Ra number of 10^6 for rectangular cavity with bottom heating in the present case and due to availability of computational resources. All these results are therefore, in the Ra number range within the laminar fluid flow region and heat transfer.

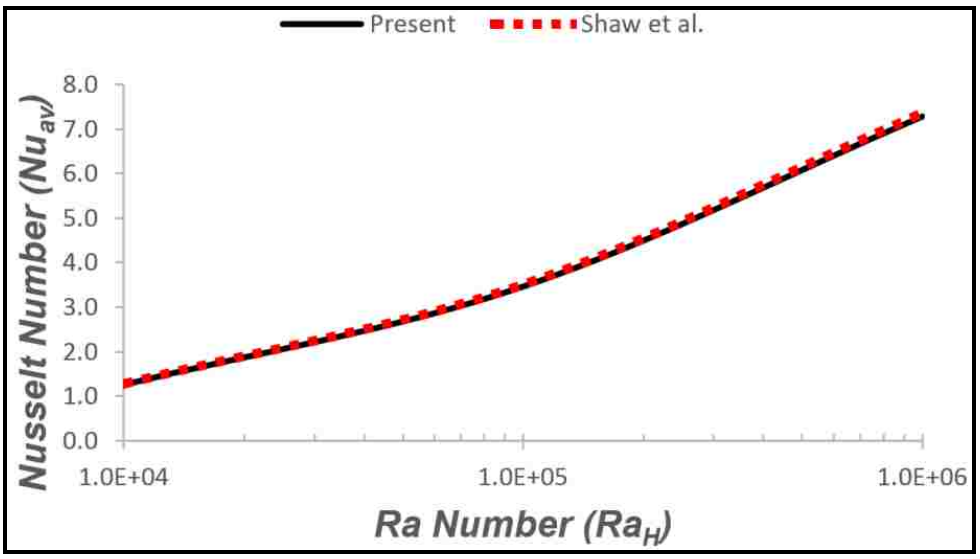

Figure 2-8: A Comparison of Results of this study of a Square Cavity with a Partition Compared with those gathered by Shaw et al. [67]

3. Results and discussion

A computational algorithm based on single relaxation time BGK model of LBM was used to perform numerical simulations of a 2-D rectangular cavity with an aspect ratio of 2. The range of *Ra* number examined was from 10^3 to 10^6. As mentioned in Amin [47] who carried out numerical studies in a cavity with *Pr* from 0.7 to 4.52 and concluded that *Pr* has no significant effects on heat transfer, therefore, simulations were performed for Newtonian fluid of *Pr* number 1.0. A dimensionless amplitude of sinusoidal roughness elements from 0.015 to 0.15, and a fixed number of roughness elements 'n' equal to 8 were studied. The results presented here include a varying amplitude of roughness elements for three different cases: roughness elements on a hot wall, roughness elements on a cold wall, and roughness elements on both cold and hot walls with same thermal boundary conditions as corresponding wall. These elements were introduced in phase when roughness was present on both hot and cold walls simultaneously.

3.1 Heat transfer

This study focused on analyzing the rate of heat transfer in a rough cavity as compared to that in a smooth cavity by calculating volume averaged *Nu* given by Equation 5. The primary factors affecting both fluid flow and heat transfer due to the presence of roughness elements include the thermal resistance and the effective distance between hot and cold walls, the amplitude of roughness, the addition in heat transfer area due to roughness elements, either the local recirculation or eddies formed in the wakes of roughness elements, and the reduction in the volume of fluid due to incorporation of roughness [42, 47, 77, 85]. In the present case, heat transfer was taking place from hot to cold wall while remaining two sides or vertical walls were insulated. Therefore, variation in the area of either cold or hot wall due to the presence of roughness elements can affect the heat transfer rate. The role of these elements will be discussed and explored in more details in next paragraphs.

More than 70 cases of varying amplitude and roughness location were conducted in an attempt to investigate the natural convection phenomenon that occurs within a laminar region. Some notable observations were reported here. The effects of the amplitude of roughness elements on the volume averaged heat transfer in three different cases are shown in Figure 3-1 and Figure 3-3. The average Nu was plotted against the

smooth cavity so that cavities with different roughness amplitude could be compared to one another. In all three figures, the average heat transfer as compared to smooth cavity for any location of roughness either on a hot or a cold wall and boundary condition decreases. Also, when dimensionless amplitude of roughness was increased from 0.025 to 0.15, the average heat transfer decreased exhibiting an inverse relationship with the amplitude or the height of roughness.

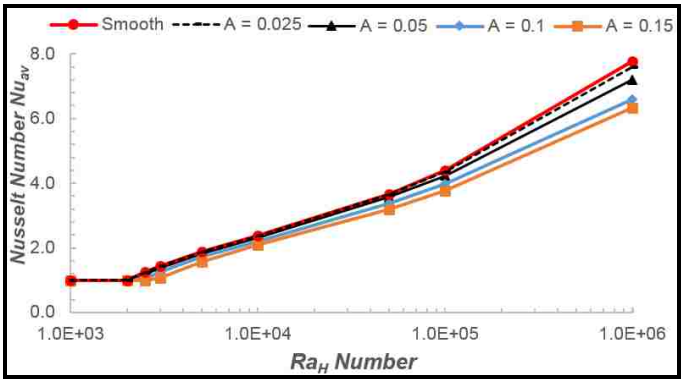

Figure 3-1: Variation of Average Nusselt Number in Smooth and Rough Cavity for Roughness at Bottom Hot Wall

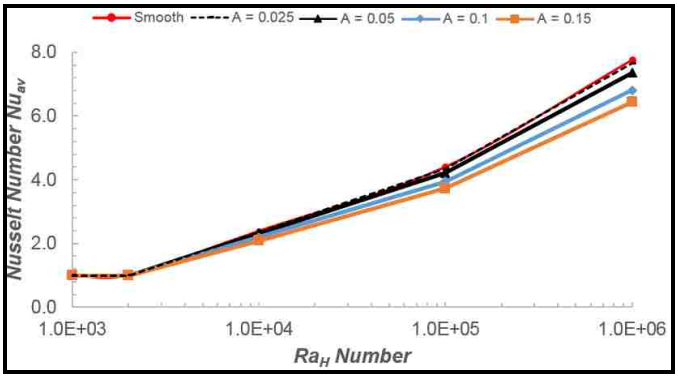

Figure 3-2: Variation of Average Nusselt Number in Smooth and Rough Cavity for Roughness at Top or Cold Wall

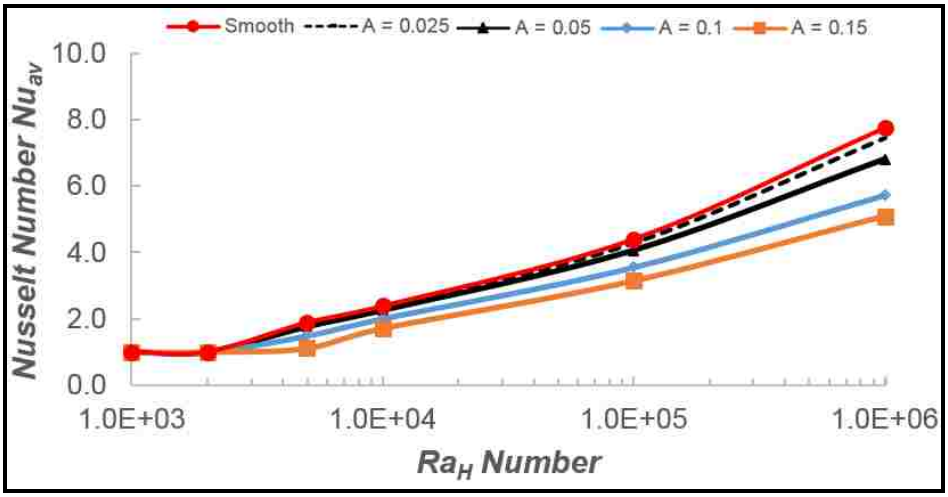

Figure 3-3: Variation of Average Nusselt Number in Smooth and Rough Cavity for Roughness at both Bottom/Hot and Cold/Top Walls

An earlier experimental study performed by Graaf and Held [86] found that in air layer in a cavity heated at the bottom, fluid layers remains stagnant until Ra number reached 2000. As Ra number is increased beyond 2000, convection sets in. This was also shown in Figure 2-6. When roughness elements were introduced in cavity, the effective or average distance between hot and cold walls decreased, hence it caused a delay in onset of natural convection and the heat transfer is through conduction. Same results are reported by the Amin [28] with rectangular roughness and ElSherbiny et al. [26] with bottom surface with V-grooves. A close look at Figure 3-1 and Figure 3-3exhibited that as the amplitude of the roughness is increased, the onset of convection is further delayed approximately up to Ra number 2.5x103 in case of bottom roughness and 5x103 in case of roughness present on both the hot and the cold walls. This delay in the convective motion may cause a decrease in the average heat transfer.

From Figure 3-1 and Figure 3-3, it can be observed that when the roughness only present on a bottom wall or a top wall, the average heat transfer was slightly different for different amplitude for Ra number < 10^5. But this was not the case when roughness was present on both a hot and a cold wall. As Ra number was increased after approximately

$2x10^3$, difference in the average heat transfer for different amplitude increased but not for Amplitude of 0.025 and 0.05. The Average *Nu* in smooth and a cavity with the roughness amplitude of 0.025 is approximately same. This showed that a dimensionless roughness amplitude of 0.025 does not have a significant effects on the average heat transfer and fluid flow as compared to a smooth cavity. Kandlikar [42], Wang [87] and Chengbin et al. [64] reported similar results that dimensionless roughness height of < 0.05 has negligible or no significant effects on heat transfer and fluid flow.

Shakerin et al. [62] performed experimental study by introducing a conducting rectangular roughness elements on hot vertical wall in a square cavity. They concluded that a single perfectly conducting roughness element is a poor fin, as addition of the heat transfer area due to the presence of roughness element in laminar region does not affect the average heat transfer because of a decrease in velocity. In the similar manner, when sinusoidal elements were introduced on hot wall in a cavity heated from below, the surface area for heat transfer is enhanced. But this addition of the heat transfer area caused deceleration in fluid flow and hence reduced heat transfer. As it was reported by Zhang et al. [64] that presence of roughness increased pressure drop. Also, this enhanced area in the cavity caused a reduction in the volume of fluid which was a heat transfer medium. Therefore, a decrease in the heat transfer may be due to reduction in the volume of fluid due to the presence of the roughness as suggested by the Amin [47].

Another phenomenon that can significantly alter the average heat transfer rate in rough cavity was presence of "recirculation" or "eddies" in the space between roughness elements or in shadows of roughness elements. Sowjanya and Jie [65] reported that detachment and re-attachment of fluid is influenced by the presence of vortices between rough grooves and spacing between these grooves. As in the present case, the frequency or spacing between rough elements was constant throughout this study for a fixed amplitude, local recirculation was not observed up to the Ra number of 10^4 as can be seen in Figure 3-4 and Figure 3-5 for amplitude ≤ 0.1. As Ra number was increased, strong recirculation was formed in the wake or shadows of the roughness elements. This recirculation caused detachment of fluid from hot wall. These vortices were trapped among the roughness elements and cause outer fluid detachment from wall. This phenomenon may cause a significant decrease in heat transfer from a hot wall to a cold

wall. Similar results were also reported by Prétot et al.[33] observed during his experimental and numerical studies.

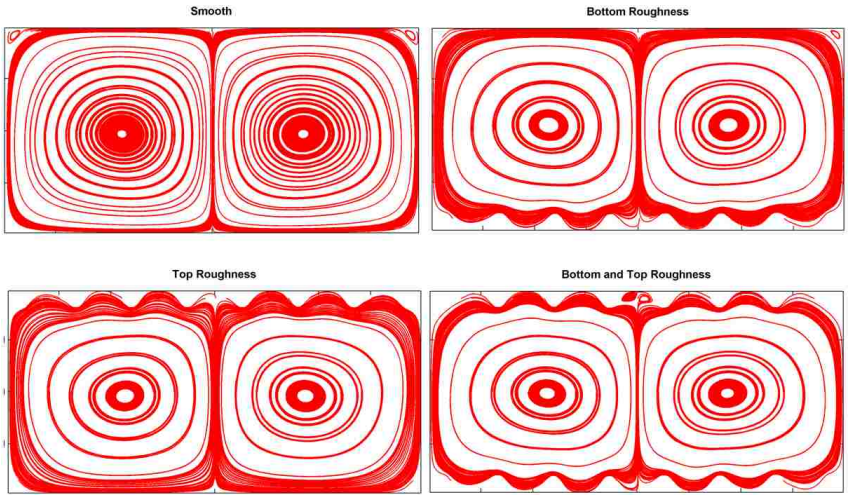

Figure 3-4: Streamlines for Ra-10^4 in Smooth and Rough Cavities at Amplitude = 0.1

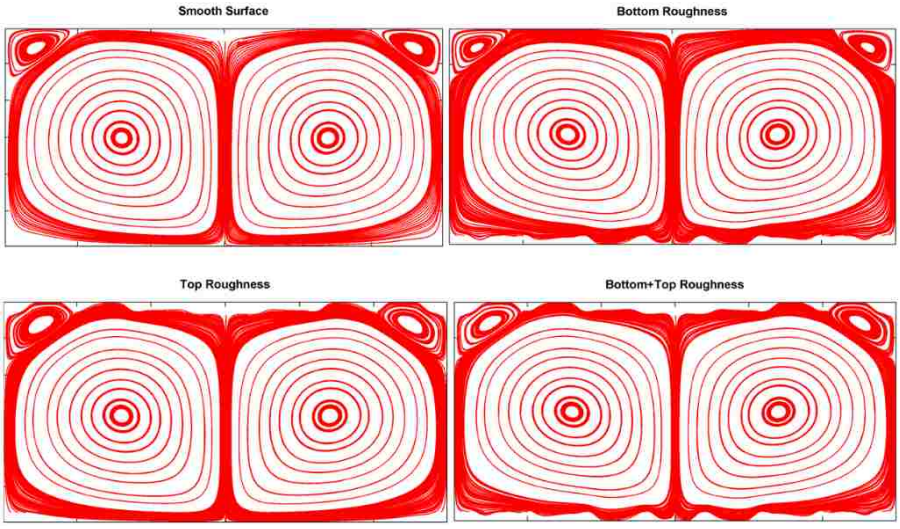

Figure 3-5: Streamlines for Ra-10^6 in Smooth and Rough Cavities at Amplitude = 0.05

Figure 3-6 and Figure 3-8, showed a relationship of the average heat transfer to the variation of roughness amplitude. For Ra number 10^4 and 10^5, the average heat transfer was same in both cases of top and bottom roughness and more as compared to the roughness at both hot and cold walls simultaneously. The degradation in the average heat transfer in case of roughness presence on both walls was as expected. But in case of the Ra number 10^6, heat transfer in case of top roughness was slightly more as compared to bottom roughness case. A possible reason behind this slight increase was, when the roughness was present on a bottom hot wall, generation of the recirculation or eddies caused a fluid detachment as discussed earlier and hence degrade the average heat transfer. Whereas, in case of the roughness on a cold or a top wall only, eddies were formed and caused local fluid detachment and deceleration but not the heat transfer and hence less effect compared to roughness on a hot wall. Moreover, behavior of average *Nu* was linear with amplitude. As amplitude of roughness was increased, Nu was decreased. This decrease in Nu due to an increase in the amplitude was discussed above in detail. Similar results were reported by the experimental and numerical study performed by Prètot et al. [33]

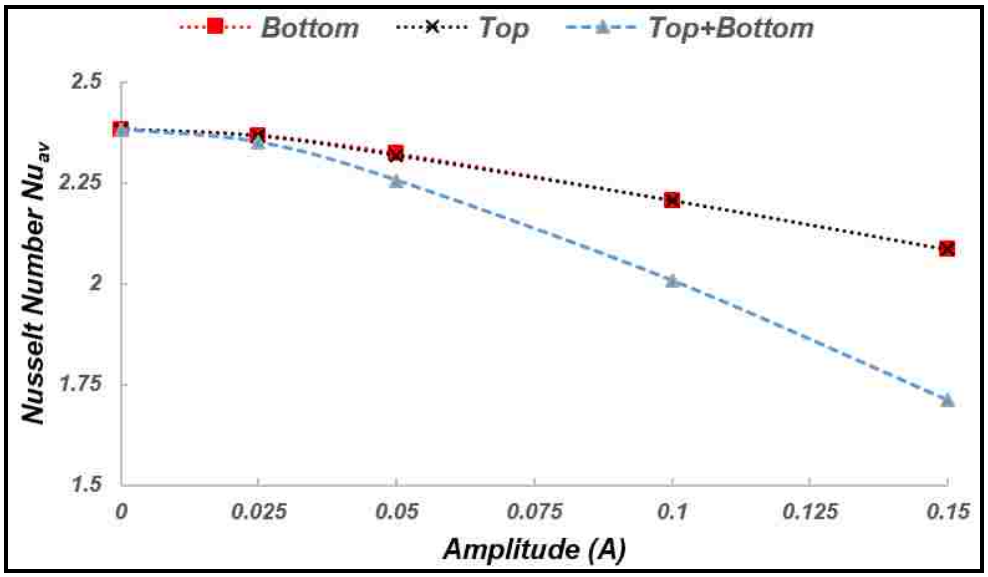

Figure 3-6: Variation of Average Nusselt Number with Roughness Amplitude for Ra = 10^4

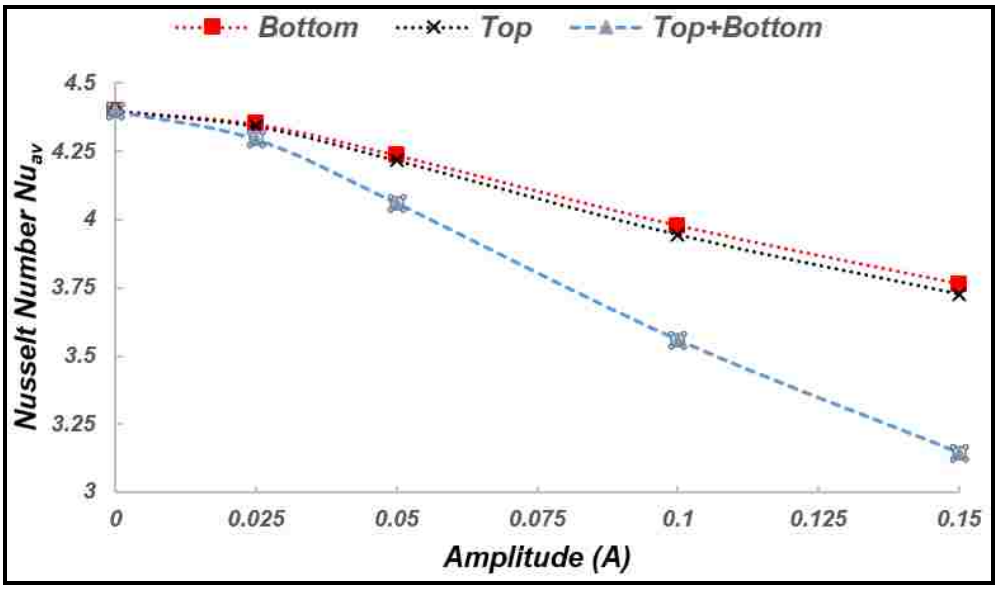

Figure 3-7: Variation of Average Nusselt Number with Roughness Amplitude for Ra = 10^5

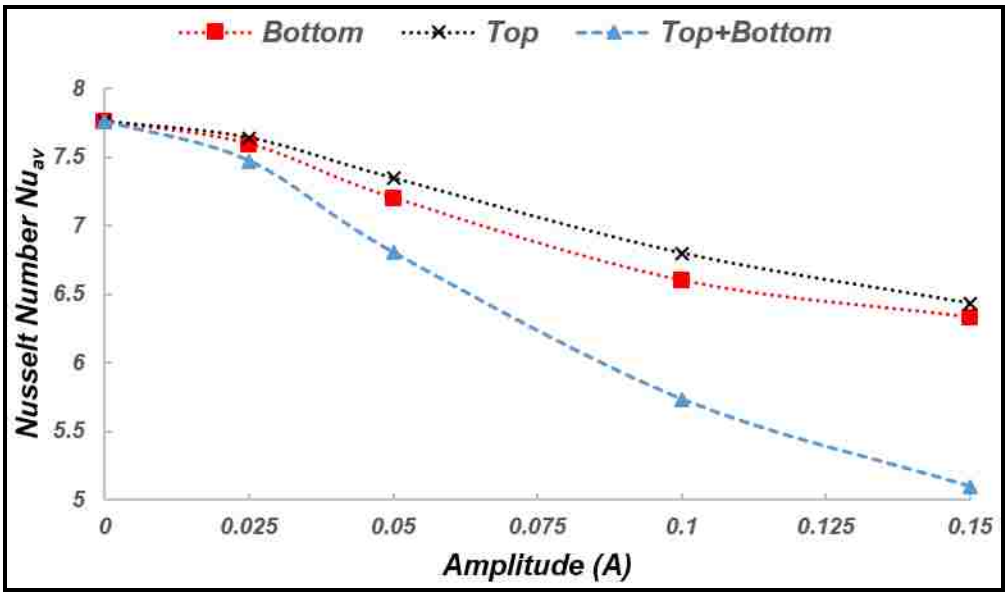

Figure 3-8: Variation of Average Nusselt Number with Roughness Amplitude for Ra = 10^6

3.2 Fluid flow and thermal fields

Fluid flow in the presence of the roughness was significantly affected as shown in Figure 3-9 - Figure 3-11. A comparison of streamlines behavior under different roughness amplitude and Ra number was compared with same Ra number in a smooth cavity. In a smooth cavity with no roughness, two vortices were formed on top corners. These vortices were also observed in rough cavity with no large size variation unless roughness was present on a top wall. When roughness was introduced at a top wall, and a top and a bottom walls, vortices formed in corner were enlarged or flattered. Also, for whole range of the Ra number and the amplitude of roughness elements, flow was bi-cellular for present study. This bi-cellular flow divided the both smooth and rough cavity into two symmetric halves. Two oppositely moving cells were formed due to movement of fluid along adiabatic side walls to top wall.

In Figure 3-4 and Figure 3-5, it was shown that for $Ra \leq 10^4$, and even at very high Ra number of 10^6 but with the roughness amplitude ≤ 0.05, velocity streamlines behaves in the same manner as in a smooth cavity. No eddies or vortices were formed in wake regions of roughness elements in this range of Ra number and the roughness amplitude. Therefore, we observed that for the roughness amplitude close to 0.025, the average Nu was almost same as in the case of a smooth cavity. For large roughness amplitude of ≥ 0.05, and Ra number $> 10^4$, eddies or vortices were formed in the shadows of the roughness elements and got stronger as the amplitude and Ra number increases as shown in Figure 3-9 - Figure 3-11. As compared to study performed by Das and Mahmud [34], no local eddies formation was observed because the whole wall was sinusoidal instead of the presence of a sinusoidal elements on a flat or a smooth surface as in present case. Also, ElSherbiny et al. [26] did not report such type of eddies formation during his experiments with V-corrugated elements. The streamlines above peaks of roughness elements were almost parallel except near the sinusoidal elements. This recirculation phenomenon causes detachment of core flow with wall and hence the average heat transfer decreased when roughness present on hot wall.

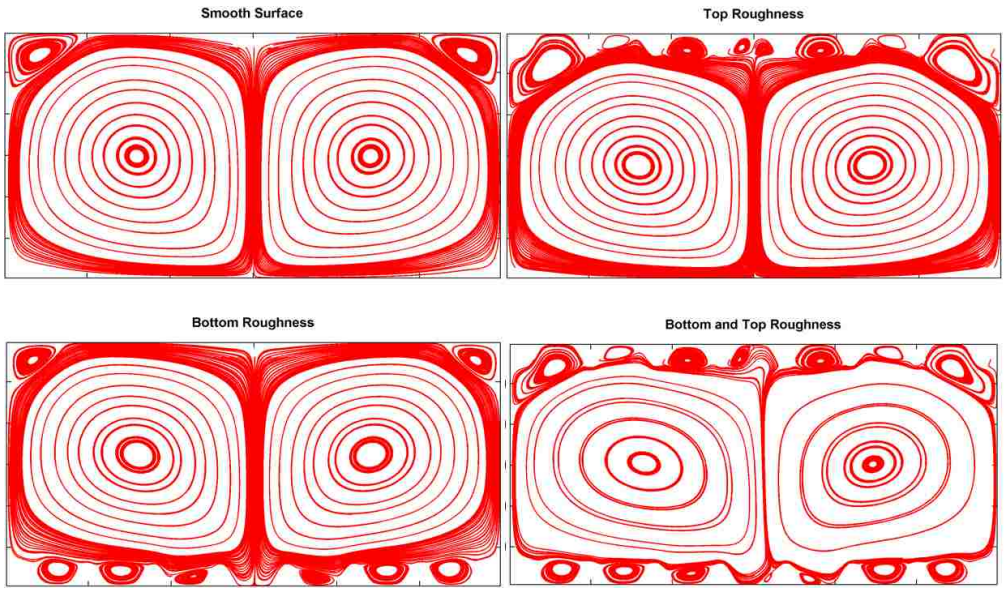

Figure 3-9: Streamlines for Ra=10^6 and Amplitude 0.1 for Smooth and Rough Cavities

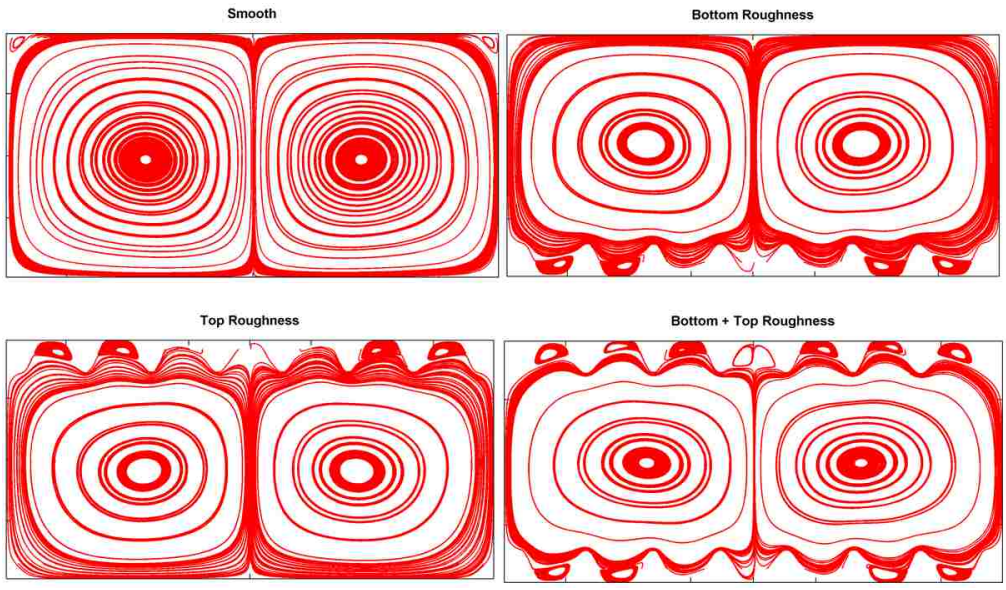

Figure 3-10: Streamlines for Ra=10^4 and Amplitude 0.15 for Smooth and Rough Cavities

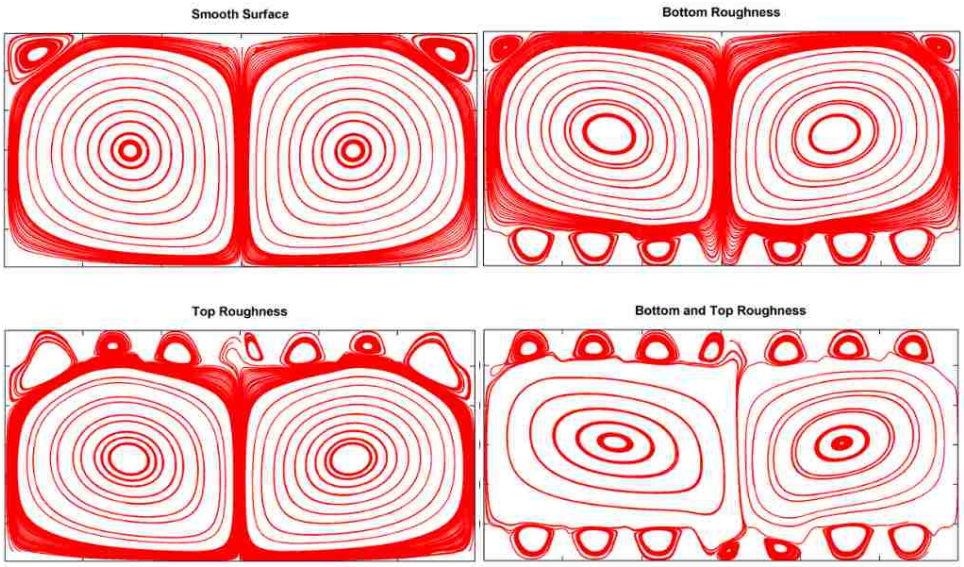

Figure 3-11: Streamlines for Ra=10^6 and Amplitude 0.15 for Smooth and Rough Cavities

Isotherms for the different Ra number and the roughness amplitude were shown in Figure 3-12 - Figure 3-17. Thermal fields for Ra number $\leq 10^4$, behaved in same manner (results are not provided here). At low Ra number, the thermal strata was oriented in such a way that these isotherms looks like to generate from hot wall and trending towards adiabatic wall to top cold wall. The stratification was quite laminar. This was because at lower Ra number, buoyancy force was not too strong. But as Ra number was increased beyond 104, isotherms started swirling towards the center of cavity along a top wall and were divided into two parts in opposite direction. Due to an increase in Ra number, and hence generation of strong buoyancy force, isotherms were further distorted as shown in Figure 3-12 - Figure 3-17, It was evident from the behavior of isotherms that as Ra number increased, isotherms were getting closer towards a hot and a cold wall. A further increase in Ra number and also the amplitude of roughness causes the confinement and constriction of isotherms in wakes or shadows of the roughness elements. This also showed dominance of the convective heat transfer in the cavity. In case of Ra number 10^6, for all cases of the roughness amplitude and even in a smooth cavity, isotherms were

confined in top corners more as compared to bottom. This was also in line with formation of local vortices at top corners even in a smooth cavity at Ra number of 10^6. Also, an increase in height or the amplitude of the roughness elements showed more confinement and constriction of isothermal lines.

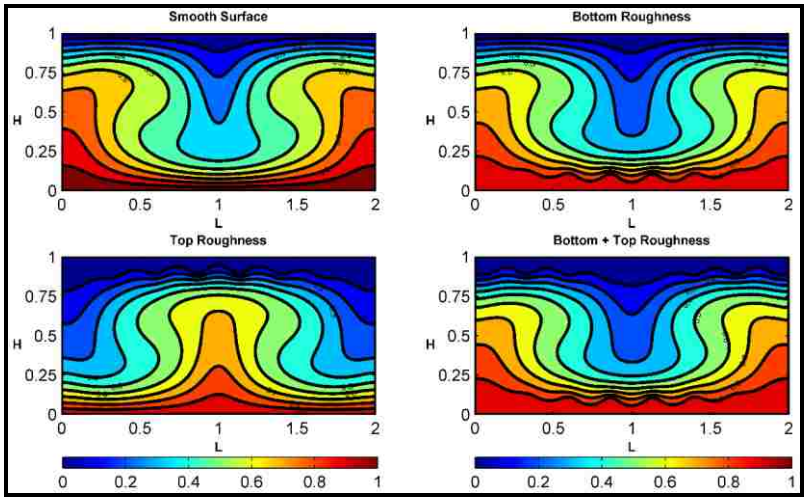

Figure 3-12: Isotherms Behavior at Ra = 10^4 amplitude 0.1 in Smooth and Rough Cavity

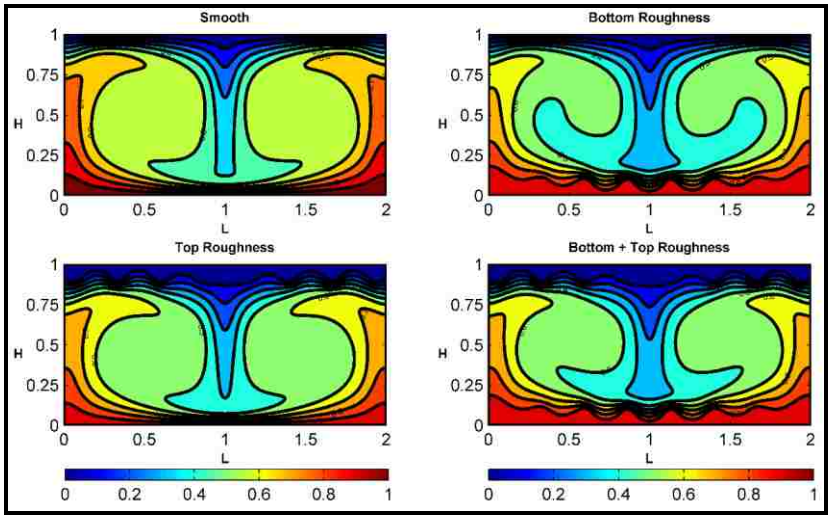

Figure 3-13: Isotherms Behavior at Ra = 10^5 amplitude 0.1 in Smooth and Rough Cavity

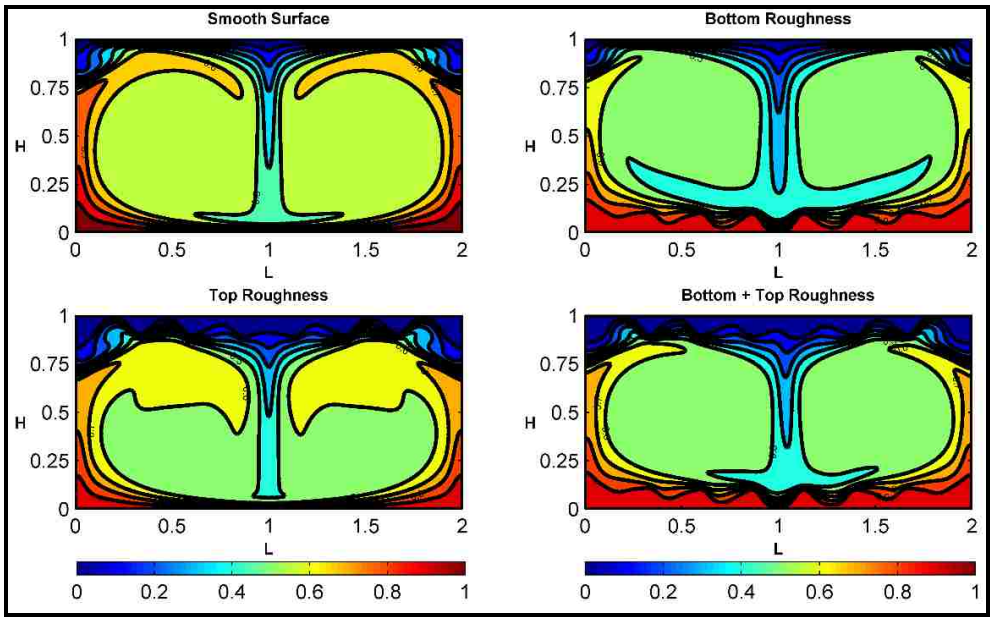

Figure 3-14: Isotherms Behavior at Ra = 10^6 amplitude 0.1 in Smooth and Rough Cavity

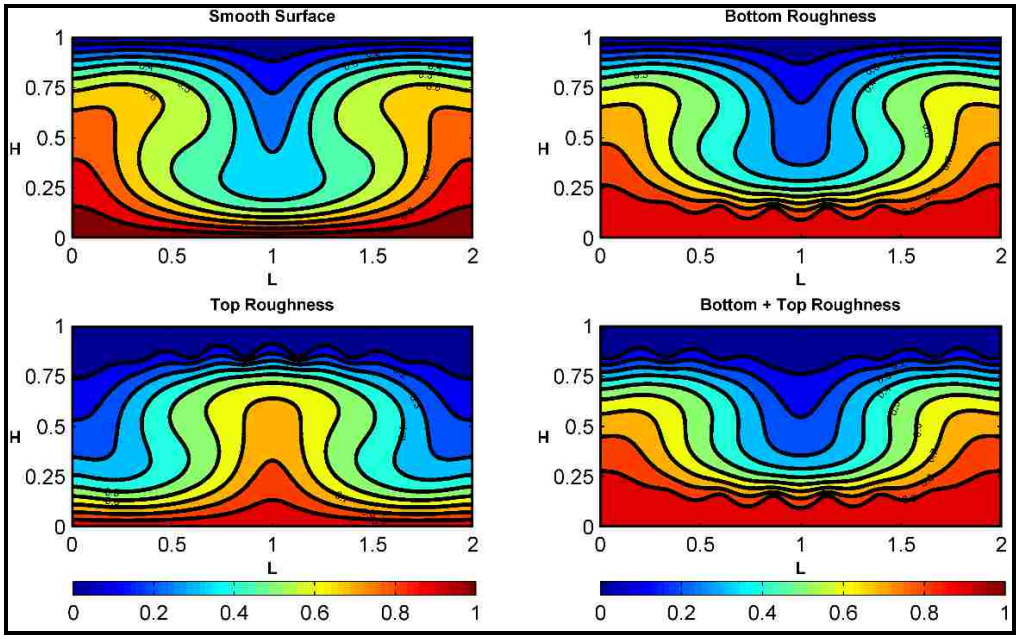

Figure 3-15: Isotherms Behavior at Ra = 10^4 amplitude 0.15 in Smooth and Rough Cavity

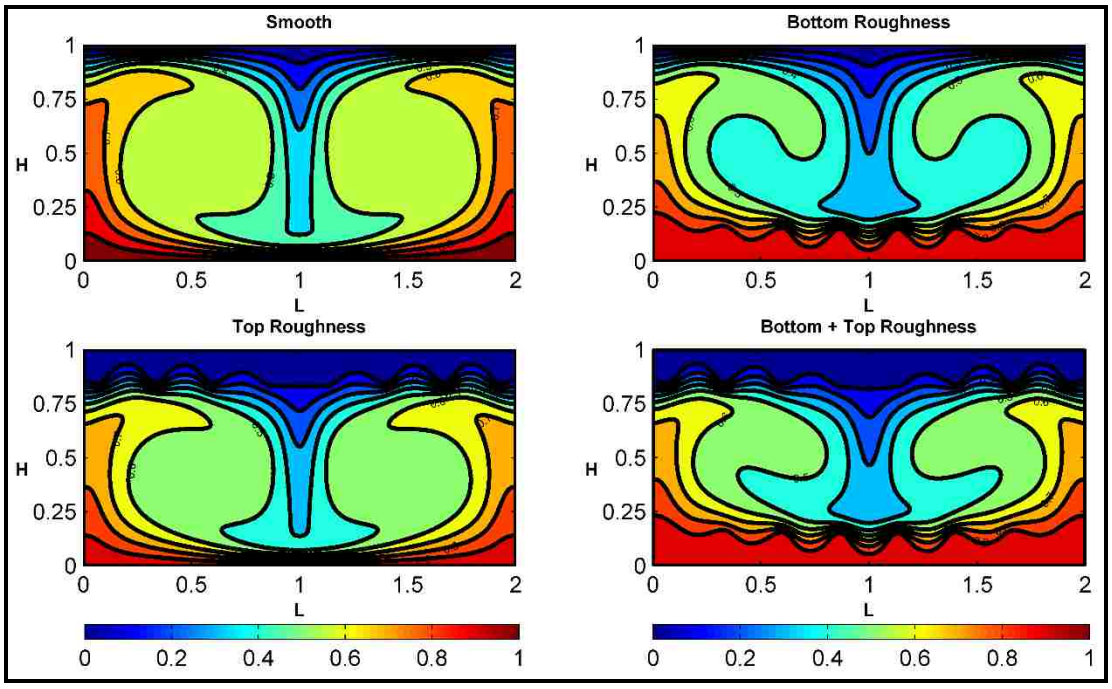

Figure 3-16: Isotherms Behavior at Ra = 10^5 amplitude 0.15 in Smooth and Rough Cavity

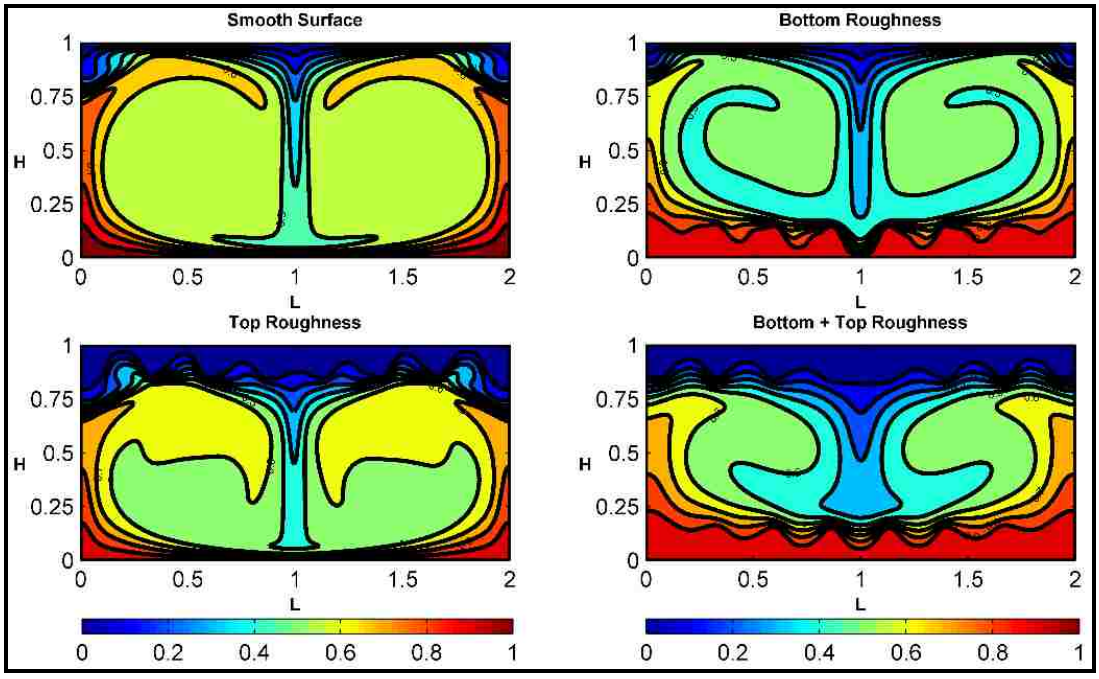

Figure 3-17: Isotherms Behavior at Ra = 10^6 amplitude 0.15 in Smooth and Rough Cavity

4. Conclusion

In the present study, a numerical algorithm based on single relaxation time BGK model of LBM was developed to analyze the effects of the amplitude of the sinusoidal roughness elements on the thermal and hydrodynamic behavior of a Newtonian fluid in laminar region. Dimensionless amplitude of the roughness was varied from very small of 0.015 to 0.15 while keeping frequency constant and locating roughness elements on a bottom or a hot, a cold or a top, and both the hot and cold walls. The present model based on LBM remained stable while simulations were carried out up to Ra 10^6.

The presence of the roughness in rectangular cavity significantly affect the fluid flow and the heat transfer. The average heat transfer decreased as the amplitude of a sinusoidal roughness elements increased in all cases. Decrease in the average heat transfer was more in case of the roughness present on both the hot and cold walls as compared to only on a cold or a hot wall. Also, decrease in the average heat transfer in case of the roughness present on a hot wall was more as compared to the roughness present on a cold wall.

A very small roughness with dimensionless amplitude of approximately 0.025, has negligible or no significant effects on the average heat transfer and fluid flow. Effects of the roughness were more pronounced at higher amplitude.

Local recirculation or eddies were formed in wake of roughness elements and caused a degradation in the average heat transfer fluid detachment from a hot wall. Incorporation of the roughness elements caused a decrease in effective separation between cold and hot walls, and a reduction in the volume of fluid as compared to a smooth cavity, which may play a role in degradation of heat transfer.

References

[1] Gebhart B., Jaluria Y., Mahajan R.L., Sammakia B., Buoyancy-induced flows and transport, 1988.

[2] Amin M.R., The effect of adiabatic wall roughness elements on natural convection heat transfer in vertical enclosures, International journal of heat and mass transfer, 34 (1991) 2691-2701.

[3] Shaw H.-J., Chen C.o.-K., Cleaver J., Cubic spline numerical solution for two-dimensional natural convection in a partially divided enclosure, Numerical Heat Transfer, Part A: Applications, 12 (1987) 439-455.

[4] Anderson R., Bohn M., Heat transfer enhancement in natural convection enclosure flow, Journal of heat transfer, 108 (1986) 330-336.

[5] Schulz T., Westinghouse AP1000 advanced passive plant, Nuclear Engineering and Design, 236 (2006) 1547-1557.

[6] Lommers L., Shahrokhi F., Mayer III J., Southworth F., AREVA HTR concept for near-term deployment, Nuclear Engineering and Design, 251 (2012) 292-296.

[7] Qiu X.-L., Xia K.-Q., Tong P., Experimental study of velocity boundary layer near a rough conducting surface in turbulent natural convection, Journal of Turbulence, (2005).

[8] Croce G., D'agaro P., Nonino C., Three-dimensional roughness effect on microchannel heat transfer and pressure drop, International Journal of Heat and Mass Transfer, 50 (2007) 5249-5259.

[9] Bejan A., Kraus A.D., Heat transfer handbook, John Wiley & Sons, 2003.

[10] Ozisik M.N., Heat transfer: a basic approach, (1985).

[11] Ostrach S., Natural convection in enclosures, Journal of Heat Transfer, 110 (1988) 1175-1190.

[12] Elsherbiny S., Hollands K., Raithby G., Free convection across inclined air layers with one surface V-corrugated, Journal of Heat Transfer, 100 (1978) 410-415.

[13] Bajorek S., Lloyd J., Experimental investigation of natural convection in partitioned enclosures, Journal of Heat Transfer, 104 (1982) 527-532.

[14] Lin N.N., Bejan A., Natural convection in a partially divided enclosure, International journal of heat and mass transfer, 26 (1983) 1867-1878.

[15] Shakerin S., Bohn M., Loehrke R., Natural convection in an enclosure with discrete roughness elements on a vertical heated wall, International journal of heat and mass transfer, 31 (1988) 1423-1430.

[16] Yucel N., Ozdem A.H., Natural convection in partially divided square enclosures, Heat and Mass Transfer, 40 (2003) 167-175.

[17] Saidi C., Legay-Desesquelles F., Prunet-Foch B., Laminar flow past a sinusoidal cavity, International journal of heat and mass transfer, 30 (1987) 649-661.

[18] Ruhul Amin M., Natural convection heat transfer and fluid flow in an enclosure cooled at the top and heated at the bottom with roughness elements, International journal of heat and mass transfer, 36 (1993) 2707-2710.

[19] Ruhul Amin M., Natural convection heat transfer in enclosures fitted with a periodic array of hot roughness elements at the bottom, International journal of heat and mass transfer, 36 (1993) 755-763.

[20] Wang G.v., Vanka S., Convective heat transfer in periodic wavy passages, International Journal of Heat and Mass Transfer, 38 (1995) 3219-3230.
[21] Adjlout L., Imine O., Azzi A., Belkadi M., Laminar natural convection in an inclined cavity with a wavy wall, International Journal of Heat and Mass Transfer, 45 (2002) 2141-2152.
[22] Ashjaee M., Amiri M., Rostami J., A correlation for free convection heat transfer from vertical wavy surfaces, Heat and Mass Transfer, 44 (2007) 101-111.
[23] Pretot S., Zeghmati B., Caminat P., Influence of surface roughness on natural convection above a horizontal plate, Advances in Engineering Software, 31 (2000) 793-801.
[24] Das P.K., Mahmud S., Numerical investigation of natural convection inside a wavy enclosure, International Journal of Thermal Sciences, 42 (2003) 397-406.
[25] Hasan M.N., Saha S., Saha S.C., Effects of corrugation frequency and aspect ratio on natural convection within an enclosure having sinusoidal corrugation over a heated top surface, International Communications in Heat and Mass Transfer, 39 (2012) 368-377.
[26] Meyer L., Thermohydraulic characteristics of single rods with three-dimensional roughness, International Journal of Heat and Mass Transfer, 25 (1982) 1043-1058.
[27] O'Hanley H., Coyle C., Buongiorno J., McKrell T., Hu L.-W., Rubner M., Cohen R., Separate effects of surface roughness, wettability, and porosity on the boiling critical heat flux, Applied Physics Letters, 103 (2013) 024102.
[28] Chang J., You S., Enhanced boiling heat transfer from microporous surfaces: effects of a coating composition and method, International Journal of Heat and Mass Transfer, 40 (1997) 4449-4460.
[29] Rohsenow W.M., Hartnett J.P., Ganic E.N., Handbook of heat transfer applications, New York, McGraw-Hill Book Co., 1985, 973 p. No individual items are abstracted in this volume., 1 (1985).
[30] Dixit H., Babu V., Simulation of high Rayleigh number natural convection in a square cavity using the lattice Boltzmann method, International journal of heat and mass transfer, 49 (2006) 727-739.
[31] Yang X., Shi B., Chai Z., Generalized modification in the lattice Bhatnagar-Gross-Krook model for incompressible Navier-Stokes equations and convection-diffusion equations, Physical Review E, 90 (2014) 013309.
[32] Welty J.R., Wicks C.E., Rorrer G., Wilson R.E., Fundamentals of momentum, heat, and mass transfer, John Wiley & Sons, 2009.
[33] Mohamad A., Lattice Boltzmann Method, Springer, 2011.
[34] Xu K., Lui S.H., Rayleigh-Bénard simulation using the gas-kinetic Bhatnagar-Gross-Krook scheme in the incompressible limit, Physical Review E, 60 (1999) 464.
[35] Sukop M.C., Thorne D.T., Lattice Boltzmann modeling: an introduction for geoscientists and engineers, Springer, 2007.
[36] Guo Z., Shu C., Lattice boltzmann method and its applications in engineering (advances in computational fluid dynamics), World Scientific Publishing Company, 2013.
[37] Mohamad A., Kuzmin A., A critical evaluation of force term in lattice Boltzmann method, natural convection problem, International Journal of Heat and Mass Transfer, 53 (2010) 990-996.

[38] de Vahl Davis G., Jones I., Natural convection in a square cavity: a comparison exercise, International Journal for numerical methods in fluids, 3 (1983) 227-248.
[39] Hollands K., Raithby G., Konicek L., Correlation equations for free convection heat transfer in horizontal layers of air and water, International Journal of Heat and Mass Transfer, 18 (1975) 879-884.
[40] Shan X., Simulation of Rayleigh-Bénard convection using a lattice Boltzmann method, Physical Review E, 55 (1997) 2780.
[41] Taylor J.B., Carrano A.L., Kandlikar S.G., Characterization of the effect of surface roughness and texture on fluid flow—past, present, and future, International journal of thermal sciences, 45 (2006) 962-968.
[42] Kandlikar S.G., Exploring Roughness Effect on Laminar Internal Flow–Are We Ready for Change?, Nanoscale and Microscale Thermophysical Engineering, 12 (2008) 61-82.
[43] De Graaf J., Van der Held E., The relation between the heat transfer and the convection phenomena in enclosed plane air layers, Applied Scientific Research, Section A, 3 (1953) 393-409.
[44] Wang H., Iovenitti P., Harvey E., Masood S., Numerical investigation of mixing in microchannels with patterned grooves, Journal of Micromechanics and Microengineering, 13 (2003) 801.
[45] Zhang C., Chen Y., Shi M., Effects of roughness elements on laminar flow and heat transfer in microchannels, Chemical Engineering and Processing: Process Intensification, 49 (2010) 1188-1192.
[46] Vijiapurapu S., Cui J., Performance of turbulence models for flows through rough pipes, Applied Mathematical Modelling, 34 (2010) 1458-1466.

III. NATURAL CONVECTION HEAT TRANSFER IN A SQUARE CAVITY WITH SINUSOIDAL ROUGHNESS ELEMENTS

M. Yousaf, and S. Usman

ABSTRACT: Natural convection in a two-dimensional square cavity in the presence of roughness on vertical walls was studied numerically. A single relaxation time Bhatnagr-Gross and Krook (BGK) model of Lattice Boltzmann method (LBM) was utilized to solve coupled momentum and energy equations. Validation of computational algorithm was performed against benchmark solutions, and a good agreement was found. Numerical study was performed for a range of Rayleigh number from 10^3 to 10^6 for a Newtonian fluid of Prandtl number 1.0. The sinusoidal roughness elements were located on a hot, and both the hot and cold walls simultaneously with varying number of elements and the dimensionless amplitude. Hydrodynamic and thermal behavior of fluid in the presence of roughness was analyzed in form of isotherms, velocity streamlines, and the average heat transfer. Results based on this numerical study showed that the sinusoidal roughness considerably affect the hydrodynamic and thermal behavior of fluid in a square cavity. A dimensionless amplitude of sinusoidal roughness elements approximately equal to 0.025 has no significant effects on the average heat transfer. The maximum reduction in the average heat transfer was calculated to be 28% when the sinusoidal roughness elements were located on both the hot and cold walls simultaneously.

Keywords: Natural convection, Square cavity, Surface roughness, Laminar, Heat transfer

1. Introduction

Enhancement of heat transfer with constant temperature difference between hot and cold walls is one of the main aim of heat transfer research. Surface roughness is considered as one of the possible method to augment heat transfer [16]. Heat transfer through natural convection from vertical walls with some sort of roughness present, came across in many applications like electronic equipment, solar collectors, energy systems for buildings, safety of nuclear reactors, and thermal storage tanks for fluid etc. [56, 73, 77]. If surface roughness can cause a significant enhancement in heat transfer, it will be more appealing solution as compared to the incorporation of fins on vertical walls [88]. Natural convection in bounded and unbounded geometries is the most commonly studied aspect of heat transfer. But study of natural convection in the presence of complex geometries has not been studied at large. Moreover, the results reported by these studies are conflicting [88]. Therefore, a fundamental study is necessitated for a better understanding of the role of surface roughness during natural convection.

Buoyancy induced natural convection in a square cavity with smooth walls has been extensively studied theoretically, experimentally, and numerically for decades and detailed analysis are available in literature [50, 66, 71-73]. But studies of the natural convection heat transfer in square and rectangular enclosures in the presence of partitions, and surface roughness are limited to some shapes of partitions, and roughness elements. Bajorek and Llyod [74] experimentally studied the effects of an insulated rectangular partition located on the horizontal adiabatic wall in a square cavity. They used air and carbon dioxide as working fluid in the range of Gr from $1.7x10^5$ to $3.0x10^6$. They observed a decrease in the heat transfer from 12 to 21 percent in the presence of partitions as compared to a smooth cavity. Kaviany [89] numerically studied the influence of a cylindrical protuberance present on an adiabatic horizontal wall in the presence of isothermal vertical walls in a square cavity with air as working fluid. He used a finite difference based method for numerical study. The range of Ra number explored was up to 10^4. By varying the radius of protuberance, a decrease in the average and local heat transfer was observed.

Anderson and Bohn [68] studied the effects of square roughness elements on the heat transfer in a cubical cavity using water as a working fluid. They observed an

increase in the average heat transfer up to 15 percent at $3.3x10^{10}$ with no enhancement for $Ra_L < 2.2x10^{10}$. Moreover, an increase in the local heat transfer was found to be up to 40 percent. Shaw et al. [67] numerically studied the effects of partitions present on the adiabatic horizontal wall with isothermal vertical walls using cubic spline method in a laminar region. They found that the increase in partition height resulted a decrease in the average heat transfer and significantly influence flow behavior inside cavity.

Shakerin et al. [62] studied the role of rectangular roughness elements in a square cavity experimentally using dye flow visualization technique and numerically using finite difference method. They introduced a single and double rectangular roughness elements by varying spacing between them in a square cavity on isothermal vertical walls and adiabatic horizontal walls. An increase of up to 12 percent in the average heat transfer was observed as compared to a smooth cavity for a single roughness element. For double roughness elements, the increase was up to 16 percent. They concluded that addition in the surface area due to the roughness on isothermal wall was balanced by the obstruction caused in velocity, as increase in the average Nu was much smaller as compared to increase in the surface area due to the presence of the roughness. They did not report formation of eddies in the wakes of the roughness elements. Moreover, they found that single roughness element was a poor fin and spacing between elements may significantly affect the average heat transfer.

Acharya and Jetli [90] numerically studied the role of partition in a laminar and turbulent region in a square cavity by varying position and height of partition. They concluded that the height of partition significantly influence the heat transfer as compared to position of partition. Amin [28] used a finite element based computational code NACHOS to study natural convection in a square cavity with rectangular roughness elements. He considered a fluid of Pr number 10 and variable amplitude and spacing between the roughness elements. He observed that the presence of roughness on bottom isothermal wall causes a delay in the onset of convection in enclosure. Also, he concluded that the average heat transfer increased at low Ra number of $2x10^3$ while it decreased at Ra number $3x10^4$. A maximum decrease was found to be 61 percent at Ra number $3x10^4$. Yucel and Ozdem [76] numerically investigated the role of adiabatic and fully conducting multiple partitions on horizontal walls with air as working fluid. They

used finite difference method based computational code by varying boundary conditions of horizontal walls as adiabatic and conducting while keeping vertical walls as isothermal throughout the study. They observed that average Nu decreased in both cases either insulated or conducting horizontal walls or partitions and also due to increase in the height of partitions.

Shi and Khodadadi [91] performed a numerical study to observe the role of a thin fin on an isothermal vertical wall in a square enclosure in a laminar flow region of a fluid of Pr number 0.7. They used finite difference method based approach and concluded that average Nu always degraded in the presence of thin fin with variation of position and length. Hasan et al. [36] studied effects of wavy top horizontal wall in a cavity of different aspect ratio (H/L) from 0.5 to 2.0. They utilized finite element based approach with air as a working fluid. They varied the frequency of corrugation. Vertical walls were kept isothermal with bottom horizontal wall as adiabatic and wavy wall at uniform heat flux. They observed that for small aspect ratio, average Nu decreased up to Ra number < 10^4, when the Ra was increase past 10^4, Nu increased. Moreover, they concluded that an increase in corrugation of top wall enhances convective heat transfer.

Besides traditional numerical schemes illustrated above based on finite volume, finite difference, and finite element method, Lattice Boltzmann method has obtained a significant success in solving Navier-Stokes and energy equations in computational fluid dynamics [7, 53]. Lattice Boltzmann method (LBM) was originated from lattice gas automata. In the last two decades, LBM extensively used in the study of complex fluid flow systems for single and multi-phases [44, 55]. Mohamad and Kuzmin [49] studied natural convection in a square cavity by using a simple LBM to analyze different force incorporation schemes. Dixit and Babu [53] utilized non-uniform mesh to observe thermal and fluid flow behavior using BGK model of LBM in a square cavity up to 10^{10} for a fluid of Pr number 1.0. Yang et al. [55] modified BGK model of LBM to enhance its numerical stability. They studied natural convection in a square cavity up to Ra number 10^{12} by introducing a correction parameter with air as a working fluid.

Most of the experimental and numerical studies discussed above, investigated the natural convection in a square cavity with rectangular or square roughness elements, partitions or fins on isothermal or adiabatic walls. However, reports on buoyancy induced

natural convection in a square cavity with sinusoidal roughness elements on isothermal vertical walls in a laminar region of fluid flow are rare. Based on the literature survey, for natural convection with rectangular and square roughness elements, the observations are contradicting. At present, no rational conclusion can be drawn without fully understanding the role of many different shapes of roughness. Therefore, in the present study, the effect of frequency and dimensionless amplitude of sinusoidal roughness elements on the hot, and both the hot and cold walls simultaneously has been investigated. Numerical study was performed by using single relaxation time Bhatnagr-Gross and Krook (BGK) model of Lattice Boltzmann method (LBM) for a Newtonian fluid of Prandtl number 1.0 in a two-dimensional square cavity. The range of Ra number explored was 10^3 to 10^6 for a differentially heated rough square cavity.

Nomenclature

A	Dimensionless Amplitude (h/H)	T_{ref}	Reference Temperature (K)
g	Gravitational acceleration (ms^{-2})	ts	Time step
H	Height of cavity (m)	U	Horizontal velocity component (ms^{-1})
h	Height of Roughness Element (m)	V	Vertical velocity component (ms^{-1})
K	Thermal conductivity ($Wm^{-1}k^{-1}$)	x	Coordinate parallel to the wall (m)
L	Length of cavity (m)	y	Coordinate normal to the wall (m)
lu	Lattice unit		
Nu	Nusselt number	**Greek symbols**	
n	Number of Roughness Elements		
Pr	Prandtl number	α	Molecular thermal diffusivity (m^2s^{-1})
Ra	Rayleigh Number	β	Coefficient of thermal expansion (K^{-1})
ΔT	Temperature difference (K)	θ	Dimensionless temperature
T_c	Temperature of cold wall (K)	ν	Molecular kinematic viscosity (m^2s^{-1})
T_h	Temperature of hot wall (K)	ρ	Density ($Kg.m^{-3}$)

2. Numerical analysis

Numerical study was carried out by utilizing a single relaxation time BGK model of LBM in a two-dimensional square cavity with length '*L*' and height '*H*'. A Newtonian fluid with Pr number 1.0 was studied during this numerical experiment for Ra number 10^3 to 10^6. Sinusoidal roughness elements of variable frequency and dimensionless amplitude ($A=h/H$) were located on the hot, and both the hot and cold walls simultaneously. Dimensionless amplitude (A) was varied from 0.025 to 0.15, and number of roughness elements from 02 to 10. The choice of the smallest dimensionless amplitude of 0.025 was made in order to investigate any small effect due to the presence of roughness. The geometry considered in the present case is shown in the Figure 2-1 with corresponding boundary conditions on walls with roughness present on both walls. Sinusoidal roughness elements were at same boundary conditions as corresponding vertical walls. Different cases were studied separately by locating the roughness elements on vertical isothermal walls of a square cavity by varying the amplitude and number of roughness elements. The fluid was considered radiatively non-participating medium [28].

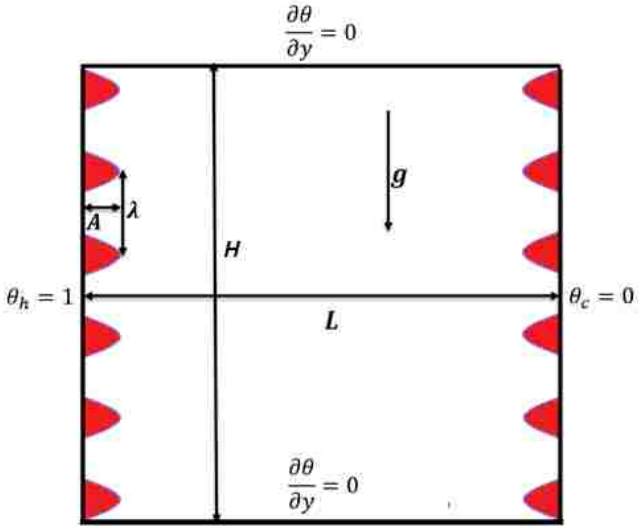

Figure 2-1: Schematic of a Square Cavity with Sinusoidal Roughness Elements

Navier-Stokes and energy equations were coupled using Boussinesq approximations. All properties were considered constant except density which was varying with temperature as shown in Equation 1 [50].

$$\rho - \rho_{\infty} = \rho_{\infty} g \beta \Delta T \tag{1}$$

The dimensionless number and temperature used during the present study are given by following relations [2, 50].

$$Ra_{L} = \frac{g \beta \Delta T H^{3}}{\upsilon \alpha} \tag{2}$$

$$P_{r} = \frac{\upsilon}{\alpha} \tag{3}$$

$$\theta = \frac{T - T_{ref}}{T_{h} - T_{c}} \tag{4}$$

Here, T_{ref} was mean or average temperature of both isothermal walls. Average heat transfer throughout this study was quantified using Nusselt number (Nu) [34, 45] on isothermal walls and in the entire flow domain;

$$Nu_{av} = 1 + \frac{< U . \theta > H}{k \Delta \theta} \tag{5}$$

$$Nu_{av} = \frac{H}{L} \int_{0}^{L} \left(\frac{\partial \theta}{\partial x} \right) dy \tag{6}$$

Where '< >' denoted quantity averaged over entire fluid volume, $\Delta\theta$ is dimensionless temperature difference between hot and cold walls, 'U' was vertical velocity component, and  term was dimensionless temperature gradient normal to hot/cold wall.

Isothermal boundary conditions are implemented on vertical walls of cavity with roughness elements at same boundary condition as wall. Adiabatic or insulated boundary conditions are used for horizontal walls of square cavity.

Bottom wall: $\theta_h = 1$, and top wall: $\theta_c = 0$

Whereas, horizontal walls:  are assumed adiabatic or insulated.

For velocity, no-slip boundary condition is applied on solid nodes in the cavity and walls;

At all walls: U = V = 0, no slip boundary conditions for velocity.

2.1 Lattice Boltzmann method

Lattice Boltzmann method based numerical techniques lie in between macro scale numerical approaches based on finite volume, finite element, and finite difference method, and micro scale approach using molecular dynamics and is known as mesoscale method. In the LBM based numerical studies, a hypothetical particle given by Boltzmann equation is solved in order to extract information for macro scale velocity and density [2]. LBM has proven the ability to simulate single and multi-phase phenomenon of fluid flow and heat transfer, evaporation, condensation, phase separation, and buoyancy induced flows and heat transfer problems [7]. LBM was first introduced in 1980s, and basically originated from lattice gas automata which is used in simulating fluid motion by particles inside it moving and colliding on regular lattices [44, 55]. As compared to other numerical methods, LBM has many advantages: ease of implementation particularly for complex boundaries, easy to simulate multi-phase and multi component systems, and easy on parallel computing [2, 7]. Besides some significant advantages, LBM still have some numerical stability issues to resolve for highly turbulent flows. Efforts are being made to improve this problem [55]. For a complete detail of a LBM models presented to date, reader is referred to Sukop and Thorne [7], Mohamad [2], Yang et al.[55], as present study is performed by using well-established single relaxation time BGK model of LBM due to its simplicity and wide application for study of fluid flows [55].

A standard nine velocity component model D2Q9, and five component model D2Q5 for temperature was used to solve coupled momentum and energy equations in the present study [7]. A brief overview is presented here. Two separate distribution functions are used to solve density or velocity and temperature given as ‘f’ and ‘g’ respectively [49]. A fundamental discretized equation used to solve distribution function ‘f’ and ‘g’ is shown in Equation 7[2].

$$f_i(x + e_i\Delta t, t + \Delta t) - f_i(x,t) = -\frac{\left(f_i(x,t) - f_i^{eq}(x,t)\right)}{\tau} + F_{ext}\Delta t \tag{7}$$

Here, ‘τ’ is relaxation time for momentum and energy equations, ‘F_{ext}’ is external force which in present case is due to buoyancy, and ‘ei’ and ‘Δt’ are lattice velocity and time respectively. Relaxation time constant can be calculated using following equations

for both energy and momentum equations respectively by thermal diffusivity and kinematic viscosity.

$$\alpha = \frac{1}{3}\left(\tau_{energy} - \frac{1}{2}\right) \qquad \upsilon = \frac{1}{3}\left(\tau_{f} - \frac{1}{2}\right) \tag{8}$$

Buoyancy, the only external force in the present study is incorporated in solution of momentum equation by using following relation;

$$F_{ext} = \rho_0 g \beta \tau_{f} \left(T - T_{ref}\right) \tag{9}$$

Equilibrium distribution function for momentum and energy equations are;

$$f_i^{eq} = w_i \rho \left(1 + 3\left(c_i.u\right) + 4.5\left(c_i.u\right)^2 - 1.5\left(u.u\right)\right) \tag{10}$$

W_i = 4/9, 1/9, 1/9, 1/9, 1/9, 1/36, 1/36, 1/36, 1/36, respectively for i= 0 to 8.

$$g_i^{eq} = w_j T \left(1 + 3\left(c_i.u\right)\right) \tag{11}$$

W_j = 1/3, 1/6, 1/6, 1/6, 1/6, for j= 0 to 4 respectively.

Macroscopic quantities of interests like density, velocity, and temperature can be calculated using distribution function by;

$$\rho = \sum_{i=0}^{8} f_i \quad u = \frac{1}{\rho}\sum_{i=0}^{8} c_i f_i \quad \text{and} \qquad T = \frac{1}{e}\sum_{i=0}^{4} g_i \tag{12}$$

Computational code can produce reliable and accurate results if proper boundary conditions are implemented. These boundary conditions play a significant role in the stability and accuracy of numerical scheme [4]. In LBM based numerical simulations, it is necessary to transform density, velocity, and temperature boundary conditions which conforms at mesoscale level for a distribution function. In present study, no-slip boundary conditions for velocity are implemented through well-known bounce back scheme. For a second order accuracy, we used a mid-plane bounce back scheme for all solid nodes present in the flow domain. Densities are bounced back from solid nodes and collision computation omitted. A complete detail to implement this type of boundary conditions is illustrated by Sukop and Thorne [7] with some additional detail are presented in Mohamad [2] and Guo and Shu [4]. Isothermal and insulated boundary conditions are implemented in terms of distribution function as given by Mohamad

[2]and Sukop and Thorne [7] for vertical and horizontal walls. The sinusoidal roughness elements are at same boundary condition as corresponding vertical or isothermal wall of cavity.

2.2 Benchmarking

Numerical investigation of thermal and hydrodynamic behavior of Newtonian fluid in a two-dimensional square cavity with and without roughness present was performed using a computational code based on single relaxation time BGK model of LBM. Accuracy of numerical results produced by computational code was verified for both smooth and rough cavities in two steps. In first step, numerical simulations were performed for a smooth square cavity shown in Figure 2-1 without roughness present on either wall with three different mesh sizes. The results produced with different size of meshes are shown in Table 2-1 and compared with benchmark solution of Davis [56]. It is clear that with finer mesh size improved results are produced. The maximum error as compared to benchmark solution was 0.84% and minimum error was 0.21%. This comparison showed that results produced with present computational code can be considered mesh independent and within range of good accuracy. Mesh size used for Ra number 10^4 was 350x350 to ensure better accuracy and larger mesh size was utilized for larger Ra number.

Table 2-1: Values of Average Nu for Grid Independence Study

Ra	H	Present	Davis [56] % Error
10^4	200	2.2241	0.8426
	250	2.2306	0.5528
	350	2.2381	0.2185

In the second step, results produced with present computational code with a smooth, and differentially heated cavity have been compared with previous studies. Simulations were performed in the range of Ra number 10^3 to 10^6. Present numerical results along with other benchmark solutions performed using different numerical

schemes are shown in Table 2-2. Comparison with different solutions showed that present results are in good agreement with previous studies. Based on grid independence study and comparison with benchmark solutions for smooth cavity, results produced can be considered as grid independent and accurate.

Table 2-2: Comparison of Present Values of Average Nu with Benchmark Solutions

Ra	**10^3**	**10^4**	**10^5**	**10^6**	**10^7**	**Method**
Present	1.1128	2.2381	4.5198	8.8021	16.31	BGK LBM
Davis [56]	1.118	2.243	4.519	8.8	-	Finite Difference
Yan et al. [55]	1.115	2.247	4.544	8.813	16.260	Modified LBM
Hortmann et al. [92]	-	2.2447	4.5216	8.8251	-	Finite Volume
Mayne et al. [93]	1.1149	2.2593	4.4832	8.8811	16.3869	Finite Element
Quérè et al. [94]	1.1178	2.245	4.522	-	-	Pseudo Spectral
Mezrhab et al. [95]	1.112	2.241	4.519	8.817	16.510	MRT LBM

In the next step, a comparison of numerical results produced by present computational code using lattice Boltzmann method was made with Shaw et al. [67], who used a pseudo spectral numerical scheme for a cavity shown in Figure 2-2 with partitions of dimensionless height (h/H) equal to 0.5 at center of bottom insulated wall. The boundary conditions are also mentioned in the diagram showing the geometry. This was performed to further make sure that computational code is working well.

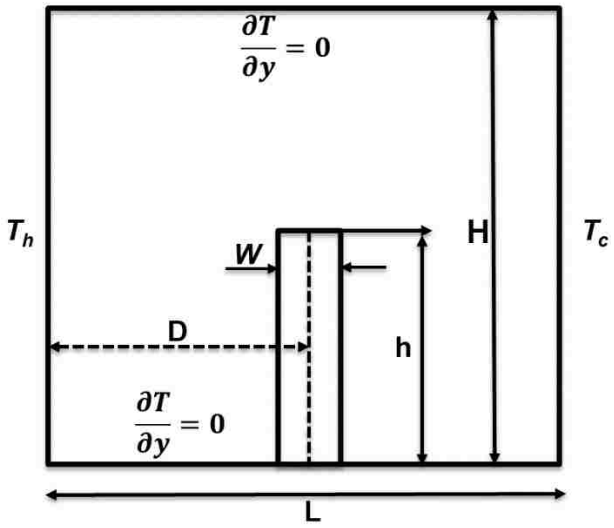

Figure 2-2: A Square Cavity with Partitions

Simulations were run for Ra number 10^4 to 10^6 in a two-dimensional square cavity. Values of average Nu were plotted against previous studies performed by Shaw et al. as shown in Figure 2-3. Our results were in good agreement with previous studies.

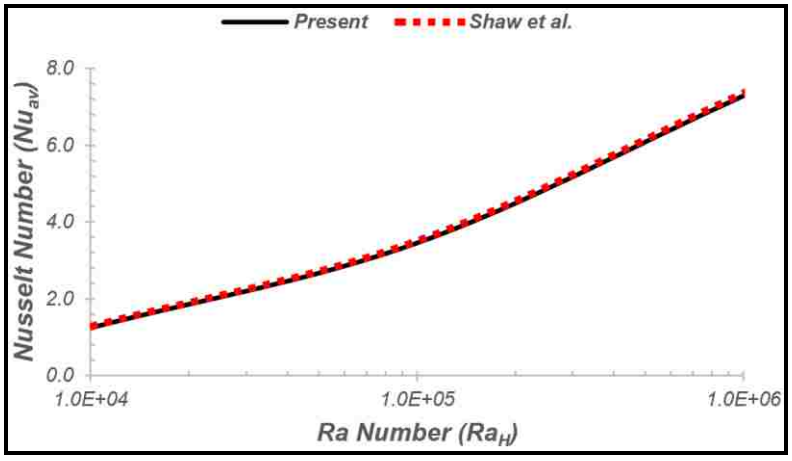

Figure 2-3: A Comparison of Present Values of Average Nu with Shaw et al. [67]

3. Results and discussion

An algorithm based on a single relaxation time BGK model of LBM was developed to analyze the heat transfer and fluid flow in a two-dimensional square cavity. After code validation, simulations were conducted by incorporating the sinusoidal roughness on different walls. The range of Ra number examined was from 10^3 to 10^6 for a Newtonian fluid of Pr number 1.0. Several simulations were performed, but only significant results are reported here. Numerical study was conducted by varying dimensionless amplitude and number of the roughness elements. The dimensionless amplitude was varied from 0.025 to 0.15, while the number of elements were varied from 2 to 10. The sinusoidal roughness elements were introduced on: a hot wall, and both the hot and cold walls simultaneously. These sinusoidal roughness elements were in phase when located on both the hot and cold walls simultaneously.

3.1 Heat transfer

The main purpose of the present study was to analyze the effects of the roughness elements in a differentially heated square cavity by varying the amplitude and frequency. The numerical results reported here were compared to that of a smooth cavity. This was done in order to analyze the role of sinusoidal roughness elements. Amount of the average heat transfer was quantified in terms of average Nu number in the entire flow domain. The heat transfer was taking place from hot vertical wall to cold while the horizontal walls were insulated. Several factors affecting fluid flow and the heat transfer in the presence of roughness are identified and discussed later. The comparison was also made to the previous studies conducted with different shapes of the roughness elements.

In the first step, sinusoidal roughness elements were introduced on a hot wall. The amplitude of the roughness elements was varied from 0.025 to 0.15 while the number of elements were fixed to 10. Figure 3-1 shows the variation of average heat transfer with the amplitude variation. The average heat transfer decreased as the amplitude of the roughness elements was increased. It is clear from Figure 3-1, that an amplitude of roughness approximately 0.025 does not significantly affect the amount of the heat transfer as compared to a smooth cavity. This aspect of the roughness elements having amplitude of 0.025 was further explored by varying number of elements from 2 to 10, while keeping the amplitude constant. The results are shown in the Figure 3-2. The

average heat transfer started deviating in the presence of roughness elements when Ra number was greater than $5x10^4$. The maximum decrease in the average heat transfer was calculated to be 3.8% at Ra number 10^6 as compared to a smooth cavity. This showed that a small dimensionless amplitude of the sinusoidal roughness elements of approximately equal to 0.025 does not significantly affect the amount of the average heat transfer.

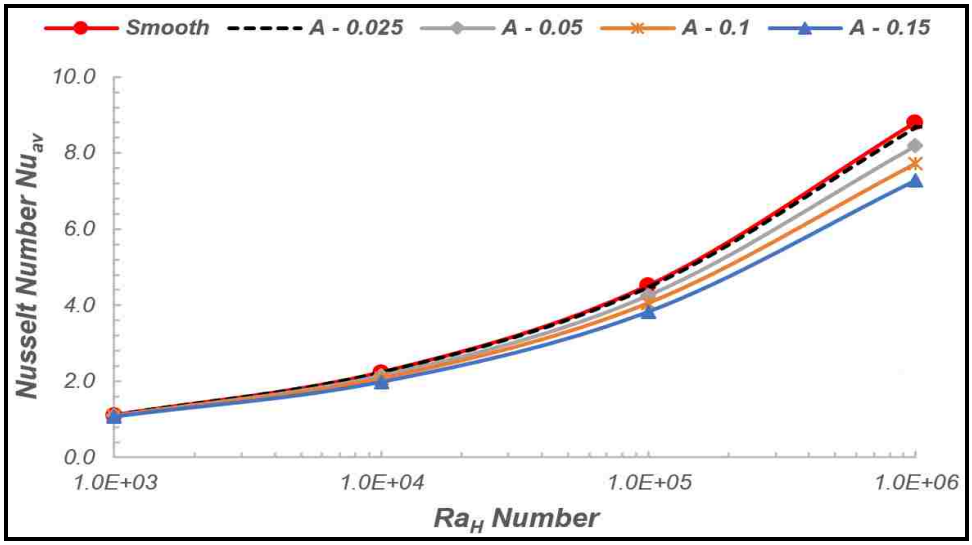

Figure 3-1: Variation of Average Nu with Roughness on a Hot Wall with Number of Roughness Elements - 10 and Amplitude Variation

The average heat transfer for all cases remained similar to that of the smooth case for Ra number up to 10^4 as shown in Figure 3-1. But when Ra number was increased beyond 10^4, the average value of Nu started deviating from a smooth cavity. This deviation was observed to be increasing with increasing Ra number and the amplitude of the roughness elements. The maximum decrease in the average heat transfer was 17.3% at Ra number 10^6 and at an amplitude of 0.15.

Figure 3-3 shows the variation of the average Nu with varying number of the roughness elements while keeping the dimensionless amplitude constant at 0.1. The change in the average Nu was minimal for all cases of number of roughness elements up to Ra number of 10^4. It can be observed that as the number of roughness elements was increased, the average heat transfer decreased.

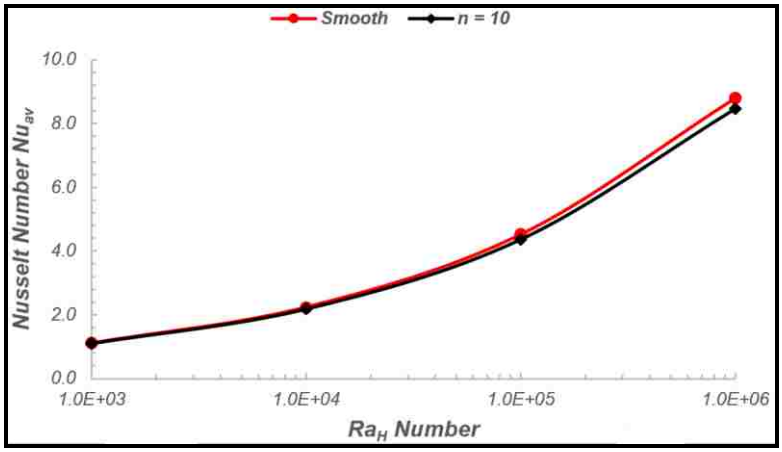

Figure 3-2: Average Nu with A - 0.025 and Varying Number of Roughness Elements

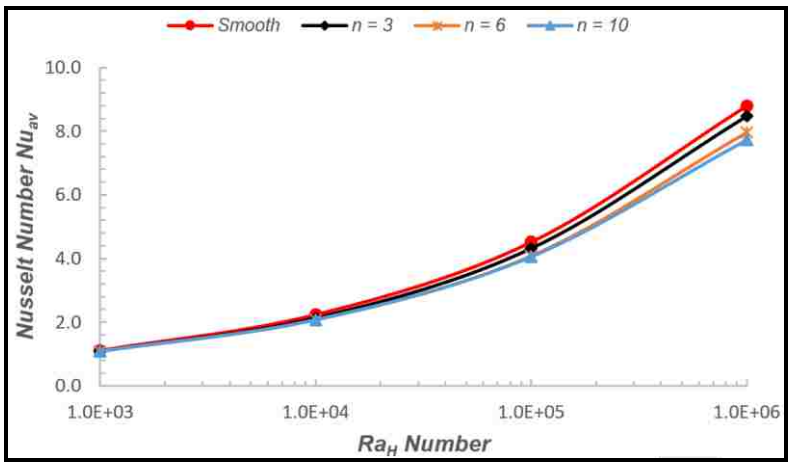

Figure 3-3: Variation of Average Nu with Roughness on a Hot Wall at an Amplitude A - 0.1, and Varying Number of the Roughness Elements

The deviation from the smooth surface was observed to increase with an increase in number of the roughness elements. Similar behavior was seen for the variation of roughness amplitude, that is the deviation was a function of the roughness amplitude. The maximum decrease in the average heat transfer as compared to smooth case was observed to be 12.25% at Ra number 10^6 and number of the roughness elements equal to 10.

In the next step, sinusoidal roughness elements were introduced on both the hot and cold walls exactly aligned with one another. The roughness elements were in phase while on both the hot and cold walls. The amplitude of the roughness elements was varied from 0.025 to 0.15 while keeping the number of roughness elements fixed equal to 6. The variation of average heat transfer both for smooth and rough cavities is shown in Figure 3-4. The decrease in the average heat transfer in case of dimensionless amplitude equal to 0.025 was calculated to be 6.8%. The reduction in the average value of Nu for the case of roughness present only on a hot wall was approximately 3.8%. The comparison of the roughness on both vertical walls for an amplitude of 0.025 simultaneously showed that decrease in the average heat transfer doubles as compared to the case of the roughness present on both walls was slightly lower than the smooth case.

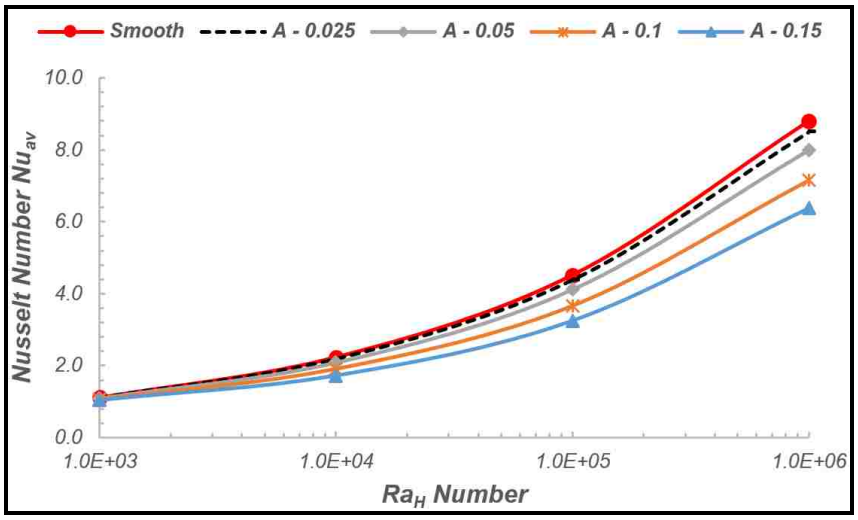

Figure 3-4: Average Nu for Roughness on Both Hot and Cold wall with Number of Elements - 6 and Varying Amplitude

The average heat transfer decreased with the increase in the dimensionless amplitude of the roughness elements. The average value of Nu started deviating from smooth case value at small Ra number of approximately equal to $3x10^3$. This deviation increased with increase in the dimensionless amplitude except for amplitude of 0.025. The maximum reduction in the average heat transfer in the presence of 6 roughness elements on both the hot and cold walls simultaneously with varying amplitude was 28% at Ra number equal to 10^5. This reduction in the average heat transfer was almost twice as compared to the 10 roughness element of same amplitude present only on a hot wall. This showed that if the number of elements were to increase, the average transfer will further deteriorate.

Figure 3-1-Figure 3-4 show the behavior of average Nu with variation of the amplitude of roughness elements for two cases: roughness present on a hot wall, and the roughness present on both the hot and cold walls simultaneously. Increasing the amplitude or the number of the roughness elements resulted in a decrease of average heat transfer for all cases shown in Figure 3-1-Figure 3-4. The present results were compared with previous studies conducted with different shapes of roughness elements. Amin [28] examined the role of isothermal rectangular roughness elements on the heat transfer in a square cavity and found a decrease in the heat transfer. In the present study, as the amplitude of roughness elements was increased while keeping the number of elements constant, the average or effective distance between the cold and hot wall decreased. This decrease in the effective distance between the two walls caused a decrease in average Ra number. The decrease in the average Ra number in turn resulted in a decrease of average heat transfer. This effect was more pronounced when the roughness was present on both the hot and cold walls simultaneously. As the amplitude of roughness was increased, the average Nu further decreased showing an inverse relationship between the average Nu and the roughness amplitude.

Amin [47] performed numerical study for different aspect ratio enclosures and concluded that the presence of the roughness elements causes a reduction in the volume of fluid of fluid within the cavity. This reduction in the fluid volume may cause a reduction in the average heat transfer. This aspect was considered by comparing the reduction of average heat transfer in the case of the roughness present on a hot wall and

on the both the hot and cold walls simultaneously. When the roughness was present on the both walls, the decrease in the average heat transfer was approximately twice than when the roughness was only present on a hot wall. This showed that reduction in the volume of fluid due to the presence of the roughness may cause a reduction in the average heat transfer.

Shakerin et al. [62] experimentally analyzed the effects of rectangular roughness elements on the vertical isothermal wall in a square cavity. They observed an enhancement in the average heat transfer along the hot wall due to addition in the heat transfer area with incorporation of roughness. They further concluded that increase in the heat transfer was counter balanced by the reduction in the velocity of fluid caused by the roughness elements presence. In the present case, when number of roughness elements were increased from 02 to 10, average heat transfer decreased. Heat is transferred due to the motion of fluid inside the cavity during natural convection. At higher fluid velocities, more heat would be transferred from hot to cold wall with insulated horizontal walls. Results showed that the presence of roughness elements hindered or caused an obstruction to the fluid flow and hence resulted in reduction of the average heat transfer.

The majority of the previous studies performed with partitions in a square cavity in a laminar region did not mention eddy formation or flow recirculation. Similarly, studies conducted with roughness in square cavities by Amin [28] and Shakerin et al. [62] did not report on the formation of eddies or vortices in the wakes of roughness elements even at Ra number equal to 10^6. Present study was conducted up to Ra number equal to 10^6 when the sinusoidal roughness elements were present on the vertical walls. Formation of eddies or vortices in the wakes of roughness elements was observed when the roughness was present on a hot wall only and on both the hot and cold walls simultaneously. In case of roughness present on the hot wall only, eddies were observed when the amplitude of the roughness was increased to 0.05 and above with number of roughness elements equal to 10. Prétot et al. [33] reported that eddies were observed when amplitude of the roughness elements was increased. Also, with increase in the amplitude of the sinusoidal elements, a decrease resulted in the average heat transfer. Vijiapurapu and Cui [65] reported of eddies or vortices formation in the wakes or shadows of roughness elements cause a detachment and re-attachment of fluid from the

wall. This reattachment depends on spacing between roughness elements. In present case, when the roughness elements were equal to 2, no formation of eddies was observed. When the number of elements were increased to 6 and 10 in case of roughness on a hot wall only, formation of eddies was observed. When the number of the roughness elements was equal to 6, eddies formation was observed even at Ra number equal to 10^4 at an amplitude of 0.1 and 0.15. This formation of eddies or vortices in the wake of roughness elements may cause a significant reduction in the average heat transfer during the natural convection phenomenon.

3.2 Stream function and isothermal lines

Fluid flow was significantly affected due to the presence of the sinusoidal roughness elements. In a differentially heated square cavity with vertical walls isothermal and horizontal walls insulated, the gain and loss in the velocity occurs along the hot and cold walls respectively. The fluid flows upward along vertical hot wall and downward along cold wall. The central part of the cavity vary its shape with variation of Ra number. For small Ra number, conduction remains dominant as compared to convection. The fluid close to hot wall being less dense started rising upward and then towards the cold wall along insulated wall. When the Ra number was increased, it cause an increase in the buoyancy force and hence in the velocity of fluid. The central part of cavity remains dominated by conduction, whereas, convection shrinks towards isothermal walls. Streamlines for the rough cavity are reported along with smooth cavity to make a better comparison.

Figure 3-5 - Figure 3-7 show the behavior of fluid flow when the number of roughness elements was fixed to 10 and the amplitude was varied from 0.05 to 0.15. At Ra number less than 104, the streamlines behaves in same manner as in a smooth cavity. But when Ra number was increased to 104 and above, buoyancy force increased, and hence velocity of the fluid increased. Some interesting features of eddies or vortices formation in the interstices of the roughness elements were observed when the amplitude was increased to 0.05 and above. These eddies were observed at Ra number equal to 104, and became flattered or elongated with increase in the amplitude. The number of eddies formed in the wakes of the roughness elements also increased with increase in the amplitude as shown in the Figure 3-5. These vortices or eddies disappeared when Ra

number was increased to 10^5 at an amplitude of 0.05, but for amplitude of 0.1 and 0.15 at same Ra number these eddies were still present. Eddies or vortices started shrinking in the size with increase in Ra after 10^4, and some small eddies were observed at Ra number equal to 10^6 with an amplitude of 0.1 and 0.15. When the roughness elements were located on both the hot and cold walls, formation of eddies was also observed at Ra number equal to 10^4. Eddies were observed in the wakes of the roughness elements along hot wall but after H/2 in both cases of '*A*' equal to 0.05 and above, and at Ra number equal to 10^4 as shown in the Figure 3-10. This showed that formation of eddies was related to the magnitude of the velocity, because the velocities at lower half of the hot wall were lower than at the upper half of the wall. The fluid in the central part behaves in almost same manner as it was in case of smooth cavity. As seen in Figure 3-5, the position of the core area recirculation was also same as in smooth cavity. The velocity streamlines were parallel to peaks of the roughness elements in all cases of rough cavities.

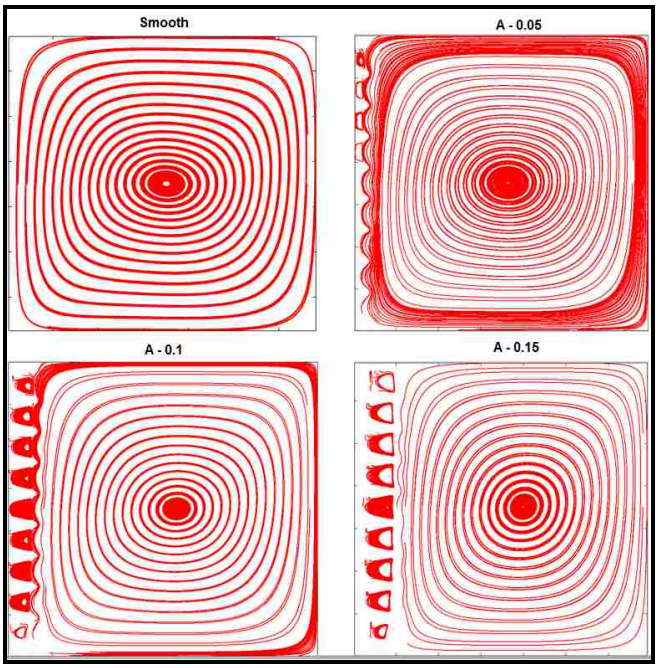

Figure 3-5: Streamlines at Ra-10^4, Number of Roughness Elements -10 and Variable Amplitude

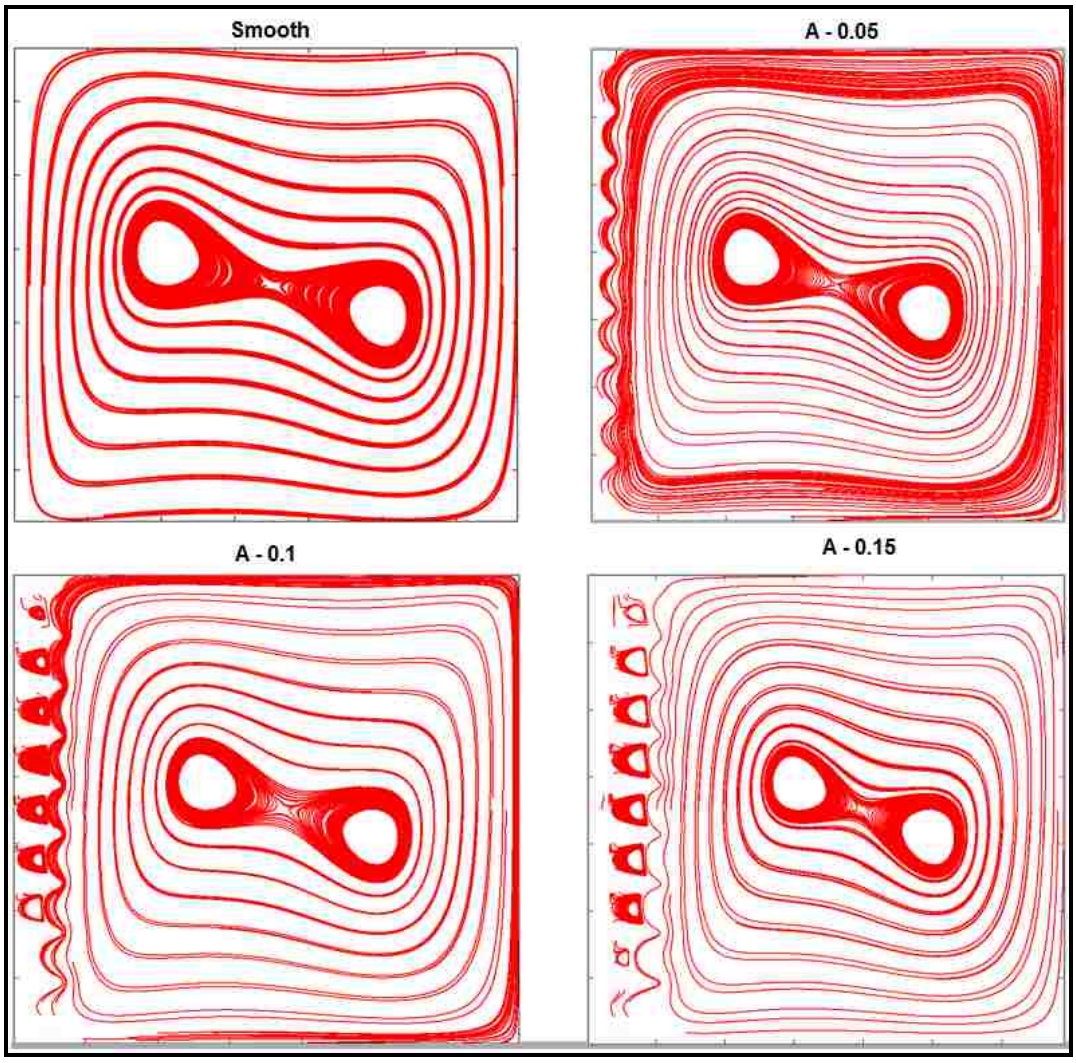

Figure 3-6: Streamlines at Ra-10^5, Number of Roughness Elements -10 and Variable Amplitude

Similarly Figure 3-8 and Figure 3-9 show the streamlines for smooth and rough cavities having different number of the roughness elements while keeping the amplitude constant equal to 0.1. At Ra number equal to 10^4, streamlines remains parallel to peaks of the roughness elements except for number of the roughness elements equal to 2. Due to large spacing between two roughness elements, reattachment of the fluid took place. This showed that reattachment of the fluid in a rough cavity depends on the spacing between

two roughness elements. Eddies formation was observed when number of roughness elements were increased to 6 and 10. At an amplitude of 0.1 and number of elements equal to 6, eddies were present on upper half of the hot wall. A further increase in the number of roughness elements to 10, eddies were observed along the entire hot wall.

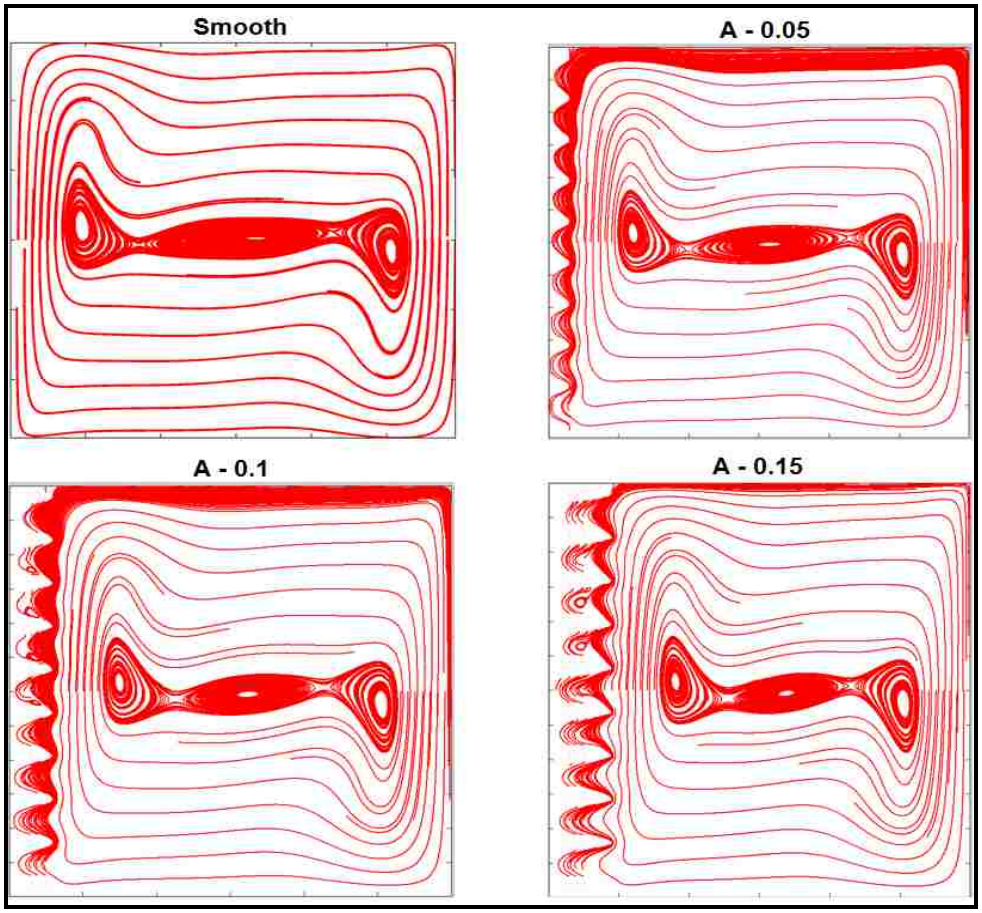

Figure 3-7: Streamlines at Ra-10^6, Number of Roughness Elements -10 and Variable Amplitude

When Ra number was increased to 10^6, behavior of streamlines was not significantly different from smooth cavity except for roughness elements equal to 10.

Local recirculation in the central part of the cavity with roughness elements equal to 2 was slightly shifted upward along the hot wall as compared to the smooth cavity. But the number and shape of the core area recirculation remains same as in smooth case. Some eddies were observed in the upper half of the hot wall at Ra number equal to 10^6 when number of elements were 10. But no eddies or vortices were present when the roughness elements were equal to 6.

Sinusoidal roughness elements were introduced on both the hot and cold walls with varying amplitude from 0.05 to 0.15 while number of elements were fixed to 6. Figure 3-10 - Figure 3-12 shows the behavior of fluid flow for different Ra numbers and different number of elements. Unlike the case with an amplitude of 0.05 and number of elements equal to 10 and Ra number 10^4, no eddies formation was observed at an amplitude of 0.05 and number of elements equal to 6 at same Ra number. When the amplitude was increased to 0.15, these eddies flattered or elongated and increased in number.

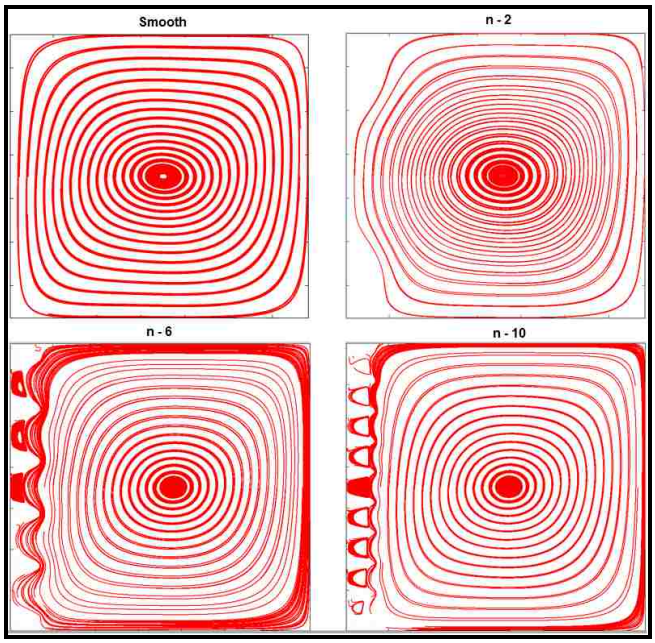

Figure 3-8: Streamlines at Ra-10^4 and Variation in Number of Roughness Elements with Constant Amplitude A - 0.1

Interestingly, when Ra number was increased to 10^5 and 10^6, no eddies were observed even at larger amplitude of 0.15. The local flow recirculation in the central part at an amplitude of 0.15 and Ra number 10^6, shrinks in size. Streamlines behavior was same as in the smooth cavity except shrinking in the central area due to the presence of roughness elements. The eddies or vortices were present in the wakes of the roughness elements at Ra number equal to 10^4, but disappear or shrink in the size and number at Ra number 10^6. This difference may be due to the following reason. At lower Ra number equal to 10^4, weak or less buoyancy effects and lower velocity, the fluid was trapped in the wakes of the roughness elements. But when the Ra number was increased beyond 10^4, resulting in strong buoyancy and hence increase in the velocity, the fluid was swept away from the wakes, and so on.

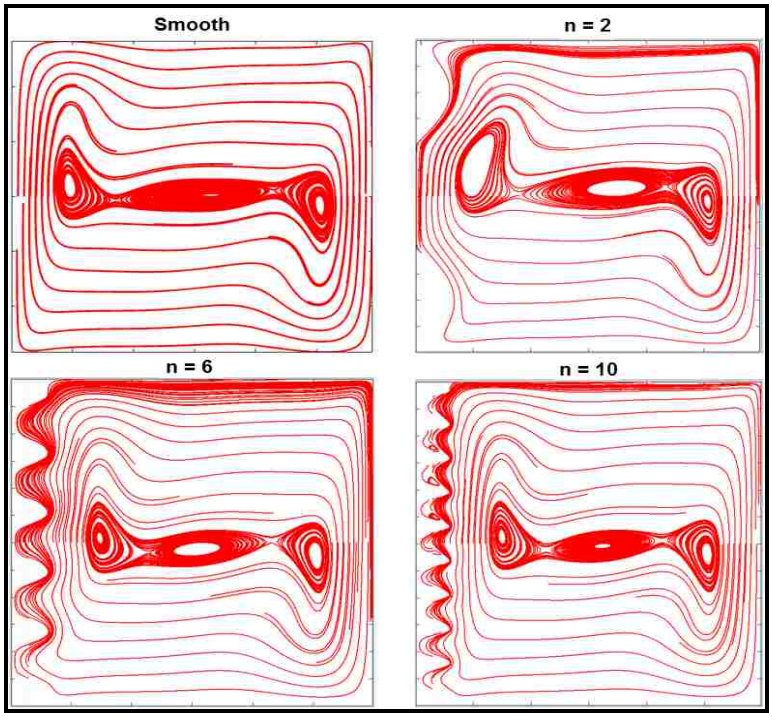

Figure 3-9: Streamlines at Ra-10^6 and Variation in Number of Roughness Elements with Constant Amplitude A - 0.1

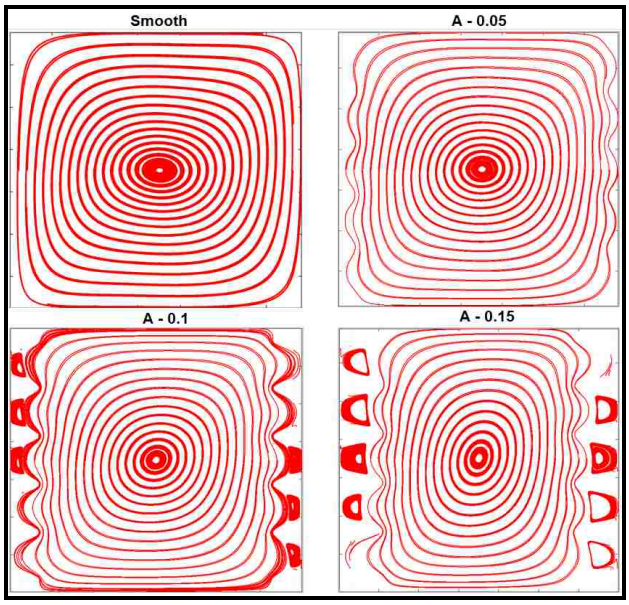

Figure 3-10: Streamlines at Ra - 10^4 with Variation in Amplitude and Constant Number of Elements – 6

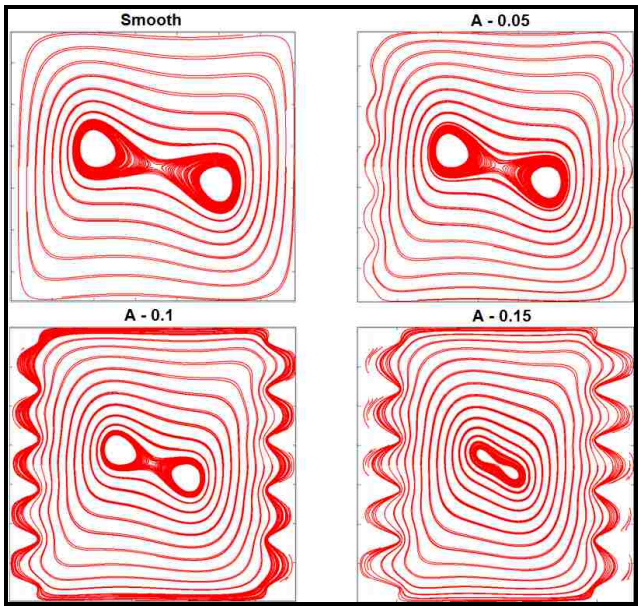

Figure 3-11: Streamlines at Ra - 10^5 with Variation in Amplitude and Constant Number of Elements – 6

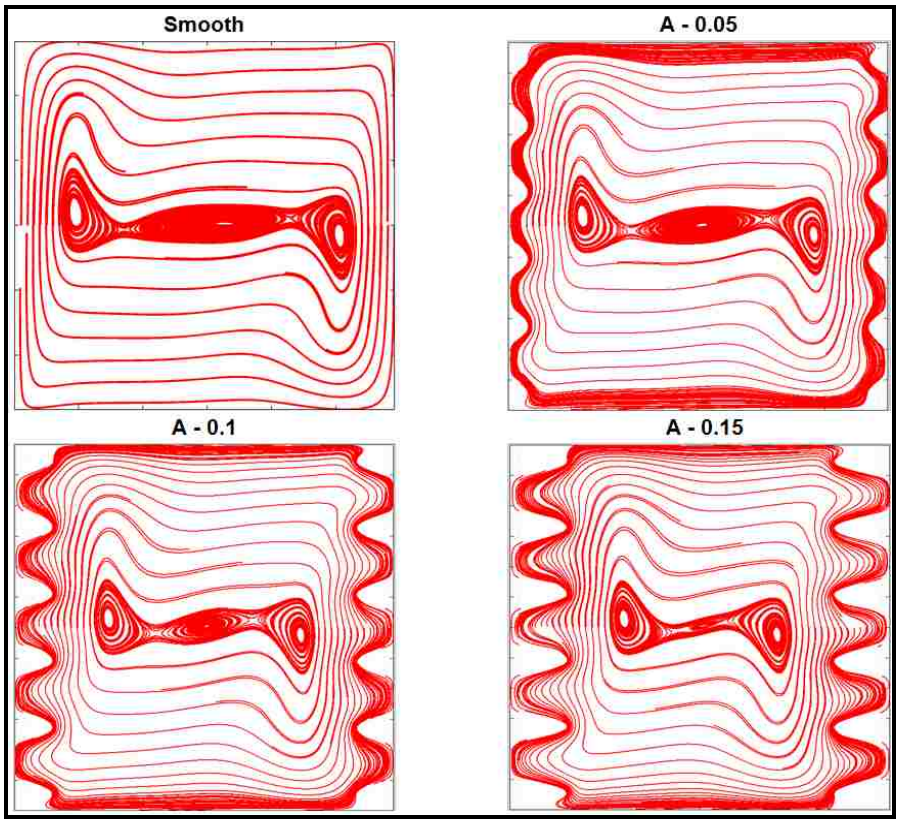

Figure 3-12: Streamlines at Ra – 10^6 with Variation in Amplitude and Number of Elements – 6

Thermal behavior of a Newtonian fluid of Pr number 1.0 in presence of roughness elements is presented in Figure 3-13 - Figure 3-17. Some selected cases are shown here for a better comparison with smooth cavity. The contours of dimensionless temperature in the range of 0 to 1 are shown to make better analysis. For Ra number < 10^4, behavior of isotherm was same as in a smooth cavity. At lower Ra number of 10^4, with weak buoyancy force, isotherms slightly distorted along hot and the cold walls. The stratification or distortion was almost same in all cases of rough and smooth cavity. No constriction of isotherms was observed at Ra number 10^4. But when Ra number was increased, and hence buoyancy force increased, isotherms started shrinking towards the hot and cold walls. This behavior is same as in smooth cavity. But in the presence of the roughness elements, isotherms constriction or density in the wakes of roughness elements

increased with increase of Ra number above 10^4. Isotherms at the tip of the roughness elements were parallel.

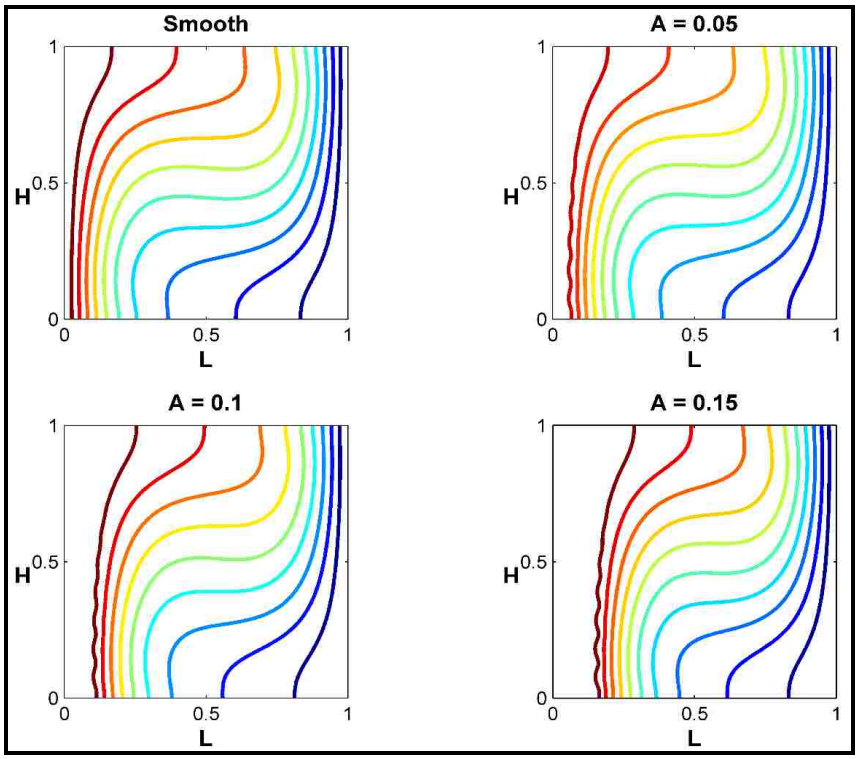

Figure 3-13: Isotherms at 10^4 with Constant Roughness Elements –10 and Variation of Amplitude

When the sinusoidal roughness elements were located on both the hot and cold walls simultaneously, the stratification of isotherms slightly differed from the smooth cavity. This may be due to the presence of the roughness elements and hence, shrinking of the central area. Isotherms are showing a mirror like behavior in the rough cavities. Density of isotherms was more at bottom of the hot wall compared to top and similarly, density of isotherms was more at top of the cold wall than bottom. When the Ra number was increased to 10^5 and 10^6, the isotherms moved towards the hot and cold walls. This

shift of isotherms showed the strong presence of convection as compared to conduction. The isotherms in the central part of the core were straight showing a strength of conduction in the core or central area. Also, with increase in Ra number and hence buoyancy force, constriction of isotherms was observed in same manner as in the case of roughness present on a hot wall only. Isotherms density or constriction was more in the bottom of the hot wall than top and similarly, at top of the cold wall than at bottom.

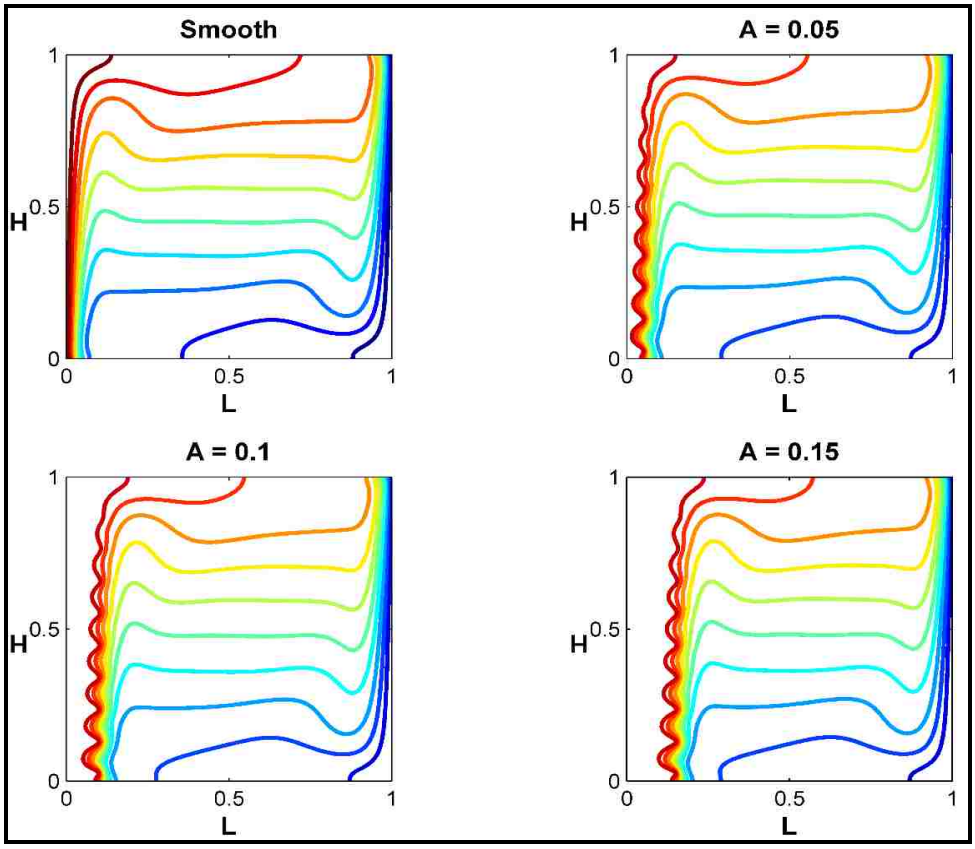

Figure 3-14: Isotherms at 10^6 with Constant Roughness Elements –10 and Variation of Amplitude

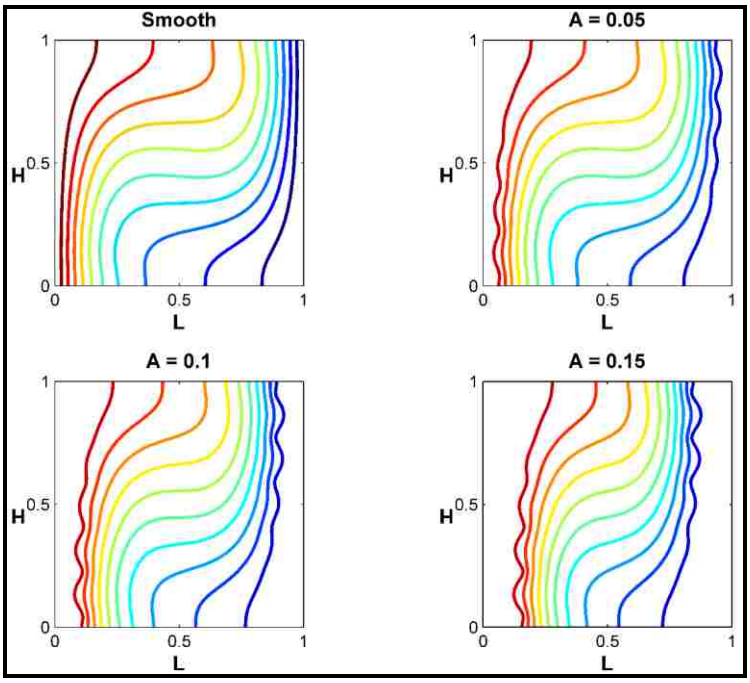

Figure 3-15: Isotherms at Ra-10^4 with Constant Roughness Elements - 6 and Variation of Amplitude

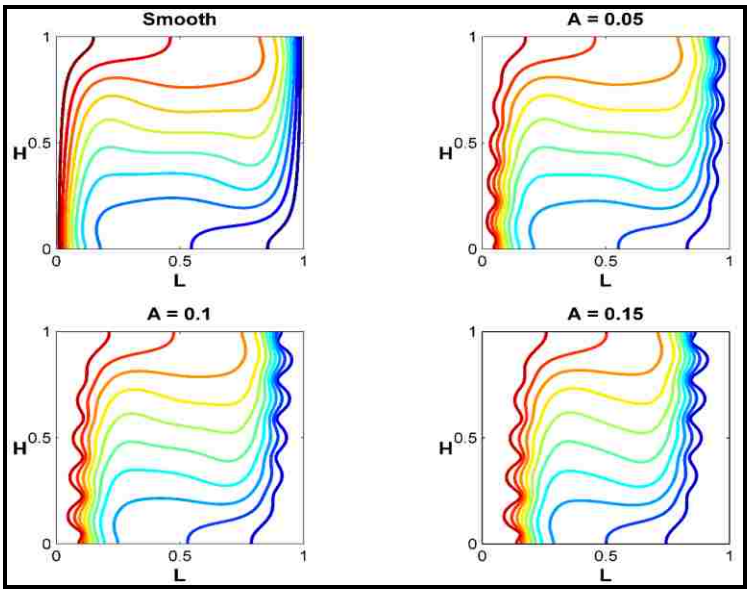

Figure 3-16: Isotherms at Ra-10^5 with Constant Roughness Elements – 6 and Variation of Amplitude

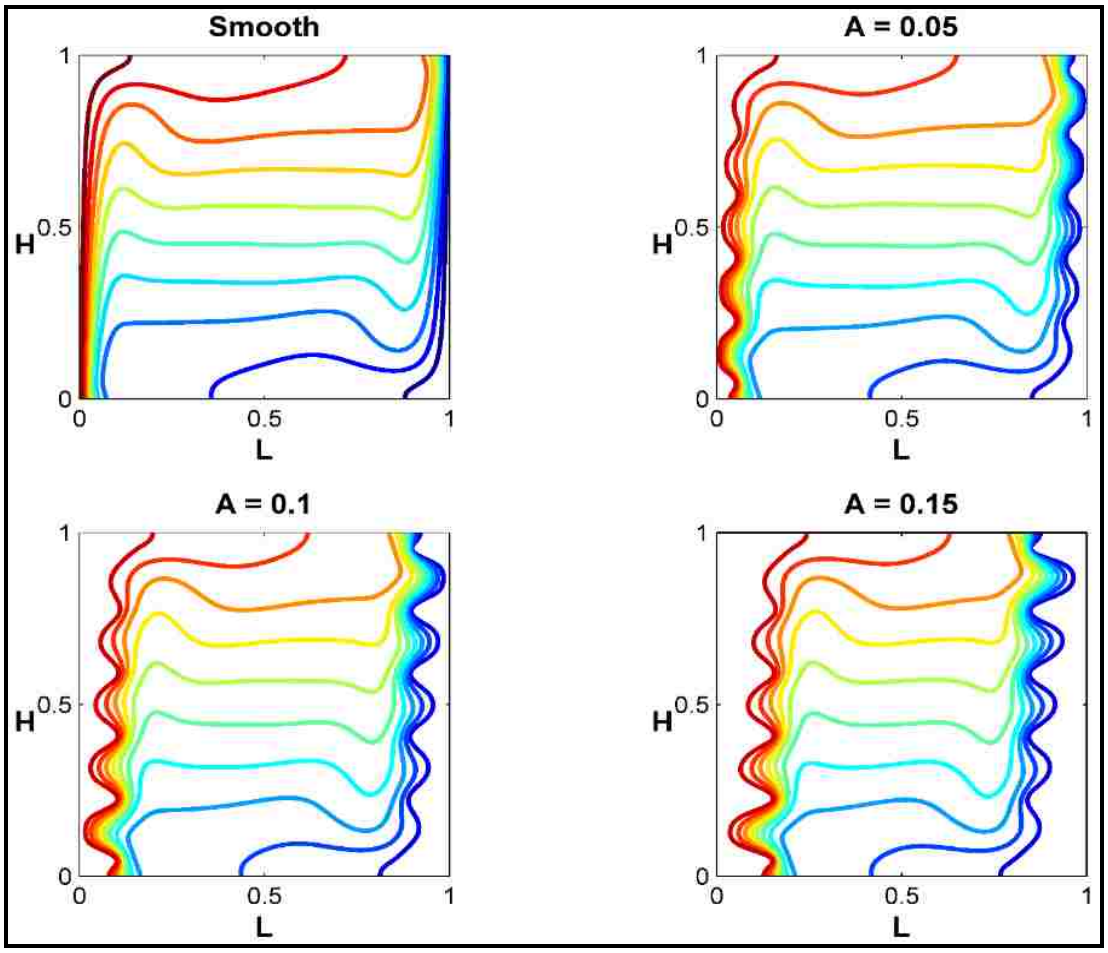

Figure 3-17: Isotherms at Ra-10^6 with Constant Roughness Elements – 6 and Variation of Amplitude

4. Conclusion

A numerical algorithm was developed based on a single relaxation time BGK model of LBM to analyze the role of the sinusoidal roughness elements on the thermal and hydrodynamic behavior of a fluid in laminar region. Two-dimensional studies were conducted in a square cavity by varying the dimensionless amplitude of the roughness from very small value of 0.025 to 0.15 while keeping frequency constant, and vice versa. The sinusoidal roughness elements were located on a hot, and both the hot and cold walls.

1. The maximum reduction in the average heat transfer when the roughness was located at a hot wall was calculated to be 17% when the amplitude was varied while keeping number of elements equal to 10 and at Ra number 10^6.
2. When the number of the roughness elements were varied while keeping dimensionless amplitude constant equal to 0.1, the maximum decrease in the average heat transfer was calculated to be 12.25% at Ra number 10^6 as compared to a smooth cavity.
3. Eddies formation was observed at Ra number equal to 10^4 with a small amplitude of 0.05 with number of roughness elements equal to 10 while varying the dimensionless amplitude if the roughness elements.
4. The maximum reduction in the average heat transfer was calculated to be 28% at Ra number equal to 10^5 when the sinusoidal roughness elements were located at both the hot and cold walls.
5. For both walls with roughness, eddies formation was observed even at Ra number 10^4 while no such phenomenon of eddies formation was observed at $Ra > 10^4$.
6. The effective distance between isothermal walls, reduction in the volume of the fluid, and formation of eddies or vortices in the wakes of the sinusoidal roughness elements may be the main factors affecting fluid flow and average heat transfer in the presence of the roughness in a square cavity.

References

[1] Versteeg H.K., Malalasekera W., An introduction to computational fluid dynamics: the finite volume method, Pearson Education, 2007.
[2] Mohamad A., Lattice Boltzmann Method, Springer, 2011.
[3] Chung T., Computational fluid dynamics, Cambridge university press, 2010.
[4] Guo Z., Shu C., Lattice boltzmann method and its applications in engineering (advances in computational fluid dynamics), World Scientific Publishing Company, 2013.
[5] McNamara G.R., Zanetti G., Use of the Boltzmann equation to simulate lattice-gas automata, Physical Review Letters, 61 (1988) 2332.
[6] He X., Chen S., Doolen G.D., A novel thermal model for the lattice Boltzmann method in incompressible limit, Journal of Computational Physics, 146 (1998) 282-300.
[7] Sukop M.C., Thorne D.T., Lattice Boltzmann modeling: an introduction for geoscientists and engineers, Springer, 2007.
[8] Le Gal P., Croquette V., Appearance of a square pattern in a Rayleigh–Bénard experiment, Physics of Fluids (1958-1988), 31 (1988) 3440-3442.
[9] Getling A.V., Rayleigh-Bénard Convection, World Scientific, 1998.
[10] Bénard H., Les tourbillons cellulaires dans une nappe liquide.-Méthodes optiques d'observation et d'enregistrement, J. Phys. Theor. Appl., 10 (1901) 254-266.
[11] Rayleigh L., LIX. On convection currents in a horizontal layer of fluid, when the higher temperature is on the under side, The London, Edinburgh, and Dublin Philosophical Magazine and Journal of Science, 32 (1916) 529-546.
[12] Latif M., Heat convection, in, Berlin: Springer-Verlag, 2006.
[13] Turgut O., Onur N., An experimental and three-dimensional numerical study of natural convection heat transfer between two horizontal parallel plates, International communications in heat and mass transfer, 34 (2007) 644-652.
[14] Stringano G., Pascazio G., Verzicco R., Turbulent thermal convection over grooved plates, Journal of Fluid Mechanics, 557 (2006) 307-336.
[15] Rohsenow W.M., Hartnett J.P., Ganic E.N., Handbook of heat transfer applications, New York, McGraw-Hill Book Co., 1985, 973 p. No individual items are abstracted in this volume., 1 (1985).
[16] Shishkina O., Wagner C., Modelling the influence of wall roughness on heat transfer in thermal convection, Journal of Fluid Mechanics, 686 (2011) 568-582.
[17] Ahlers G., Experiments with Rayleigh-Bénard convection, in: Dynamics of Spatio-Temporal Cellular Structures, Springer, 2006, pp. 67-94.
[18] Chu T., Goldstein R., Turbulent convection in a horizontal layer of water, Journal of Fluid Mechanics, 60 (1973) 141-159.
[19] Deardorff J.W., A numerical study of two-dimensional parallel-plate convection, Journal of the Atmospheric Sciences, 21 (1964) 419-438.
[20] Bodenschatz E., Pesch W., Ahlers G., Recent developments in Rayleigh-Bénard convection, Annual review of fluid mechanics, 32 (2000) 709-778.
[21] Siggia E.D., High Rayleigh number convection, Annual review of fluid mechanics, 26 (1994) 137-168.

[22] Koschmieder E., Pallas S., Heat transfer through a shallow, horizontal convecting fluid layer, International Journal of Heat and Mass Transfer, 17 (1974) 991-1002.
[23] Malkus J.S., Witt G., The evolution of a convective element: A numerical calculation, The atmosphere and the sea in motion, (1959) 425-439.
[24] Praslov R., On the effects of surface roughness on natural convection heat transfer from horizontal cylinders to air, Inzhenerno Fizicheskii Zhurnal (in Russian), 4 (1961) 3-7.
[25] Chinnappa J., Free convection in air between a 60 vee-corrugated plate and a flat plate, International Journal of Heat and Mass Transfer, 13 (1970) 117-123.
[26] Elsherbiny S., Hollands K., Raithby G., Free convection across inclined air layers with one surface V-corrugated, Journal of Heat Transfer, 100 (1978) 410-415.
[27] Saidi C., Legay-Desesquelles F., Prunet-Foch B., Laminar flow past a sinusoidal cavity, International journal of heat and mass transfer, 30 (1987) 649-661.
[28] Ruhul Amin M., Natural convection heat transfer and fluid flow in an enclosure cooled at the top and heated at the bottom with roughness elements, International journal of heat and mass transfer, 36 (1993) 2707-2710.
[29] Shen Y., Tong P., Xia K.-Q., Turbulent convection over rough surfaces, Physical review letters, 76 (1996) 908.
[30] Villermaux E., Transfer at rough sheared interfaces, Physical review letters, 81 (1998) 4859.
[31] Du Y.-B., Tong P., Enhanced heat transport in turbulent convection over a rough surface, Physical review letters, 81 (1998) 987.
[32] Ciliberto S., Laroche C., Random roughness of boundary increases the turbulent convection scaling exponent, Physical review letters, 82 (1999) 3998.
[33] Pretot S., Zeghmati B., Caminat P., Influence of surface roughness on natural convection above a horizontal plate, Advances in Engineering Software, 31 (2000) 793-801.
[34] Das P.K., Mahmud S., Numerical investigation of natural convection inside a wavy enclosure, International Journal of Thermal Sciences, 42 (2003) 397-406.
[35] Tisserand J.-C., Creyssels M., Gasteuil Y., Pabiou H., Gibert M., Castaing B., Chillà F., Comparison between rough and smooth plates within the same Rayleigh–Bénard cell, Physics of Fluids (1994-present), 23 (2011) 015105.
[36] Hasan M.N., Saha S., Saha S.C., Effects of corrugation frequency and aspect ratio on natural convection within an enclosure having sinusoidal corrugation over a heated top surface, International Communications in Heat and Mass Transfer, 39 (2012) 368-377.
[37] Penner S., Seiser R., Schultz K., Steps toward passively safe, proliferation-resistant nuclear power, Progress in Energy and Combustion Science, 34 (2008) 275-287.
[38] Schulz T., Westinghouse AP1000 advanced passive plant, Nuclear Engineering and Design, 236 (2006) 1547-1557.
[39] Lommers L., Shahrokhi F., Mayer III J., Southworth F., AREVA HTR concept for near-term deployment, Nuclear Engineering and Design, 251 (2012) 292-296.
[40] Donne M.D., Meyer L., Turbulent convective heat transfer from rough surfaces with two-dimensional rectangular ribs, international Journal of Heat and Mass transfer, 20 (1977) 583-620.

[41] Firth R., Meyer L., A comparison of the heat transfer and friction factor performance of four different types of artificially roughened surface, International Journal of Heat and Mass Transfer, 26 (1983) 175-183.
[42] Kandlikar S.G., Exploring Roughness Effect on Laminar Internal Flow–Are We Ready for Change?, Nanoscale and Microscale Thermophysical Engineering, 12 (2008) 61-82.
[43] Du Y.-B., Tong P., Turbulent thermal convection in a cell with ordered rough boundaries, Journal of Fluid Mechanics, 407 (2000) 57-84.
[44] Shan X., Simulation of Rayleigh-Bénard convection using a lattice Boltzmann method, Physical Review E, 55 (1997) 2780.
[45] Xu K., Lui S.H., Rayleigh-Bénard simulation using the gas-kinetic Bhatnagar-Gross-Krook scheme in the incompressible limit, Physical Review E, 60 (1999) 464.
[46] Zhou Y., Zhang R., Staroselsky I., Chen H., Numerical simulation of laminar and turbulent buoyancy-driven flows using a lattice Boltzmann based algorithm, International Journal of Heat and Mass Transfer, 47 (2004) 4869-4879.
[47] Amin M.R., The effect of adiabatic wall roughness elements on natural convection heat transfer in vertical enclosures, International journal of heat and mass transfer, 34 (1991) 2691-2701.
[48] Welty J.R., Wicks C.E., Rorrer G., Wilson R.E., Fundamentals of momentum, heat, and mass transfer, John Wiley & Sons, 2009.
[49] Mohamad A., Kuzmin A., A critical evaluation of force term in lattice Boltzmann method, natural convection problem, International Journal of Heat and Mass Transfer, 53 (2010) 990-996.
[50] Jiji L.M., Jiji L.M., Heat convection, Springer, 2006.
[51] Wang J., Wang D., Lallemand P., Luo L.-S., Lattice Boltzmann simulations of thermal convective flows in two dimensions, Computers & Mathematics with Applications, 65 (2013) 262-286.
[52] Eggels J., Somers J., Numerical simulation of free convective flow using the lattice-Boltzmann scheme, International Journal of Heat and Fluid Flow, 16 (1995) 357-364.
[53] Dixit H., Babu V., Simulation of high Rayleigh number natural convection in a square cavity using the lattice Boltzmann method, International journal of heat and mass transfer, 49 (2006) 727-739.
[54] Zou Q., He X., On pressure and velocity boundary conditions for the lattice Boltzmann BGK model, Physics of Fluids (1994-present), 9 (1997) 1591-1598.
[55] Yang X., Shi B., Chai Z., Generalized modification in the lattice Bhatnagar-Gross-Krook model for incompressible Navier-Stokes equations and convection-diffusion equations, Physical Review E, 90 (2014) 013309.
[56] de Vahl Davis G., Natural convection of air in a square cavity: a bench mark numerical solution, International Journal for Numerical Methods in Fluids, 3 (1983) 249-264.
[57] Clever R., Busse F., Transition to time-dependent convection, J. Fluid Mech, 65 (1974) 625-645.
[58] Nag A., Sarkar A., Sastri V., Natural convection in a differentially heated square cavity with a horizontal partition plate on the hot wall, Computer methods in applied mechanics and engineering, 110 (1993) 143-156.

[59] de Vahl Davis G., Jones I., Natural convection in a square cavity: a comparison exercise, International Journal for numerical methods in fluids, 3 (1983) 227-248.
[60] Kao P.-H., Yang R.-J., Simulating oscillatory flows in Rayleigh–Benard convection using the lattice Boltzmann method, International Journal of Heat and Mass Transfer, 50 (2007) 3315-3328.
[61] Tanda G., Natural convection heat transfer in vertical channels with and without transverse square ribs, International journal of heat and mass transfer, 40 (1997) 2173-2185.
[62] Shakerin S., Bohn M., Loehrke R., Natural convection in an enclosure with discrete roughness elements on a vertical heated wall, International journal of heat and mass transfer, 31 (1988) 1423-1430.
[63] Ji Y., Yuan K., Chung J., Numerical simulation of wall roughness on gaseous flow and heat transfer in a microchannel, International journal of heat and mass transfer, 49 (2006) 1329-1339.
[64] Zhang C., Chen Y., Shi M., Effects of roughness elements on laminar flow and heat transfer in microchannels, Chemical Engineering and Processing: Process Intensification, 49 (2010) 1188-1192.
[65] Vijiapurapu S., Cui J., Performance of turbulence models for flows through rough pipes, Applied Mathematical Modelling, 34 (2010) 1458-1466.
[66] Gebhart B., Jaluria Y., Mahajan R.L., Sammakia B., Buoyancy-induced flows and transport, 1988.
[67] Shaw H.-J., Chen C.o.-K., Cleaver J., Cubic spline numerical solution for two-dimensional natural convection in a partially divided enclosure, Numerical Heat Transfer, Part A: Applications, 12 (1987) 439-455.
[68] Anderson R., Bohn M., Heat transfer enhancement in natural convection enclosure flow, Journal of heat transfer, 108 (1986) 330-336.
[69] Qiu X.-L., Xia K.-Q., Tong P., Experimental study of velocity boundary layer near a rough conducting surface in turbulent natural convection, Journal of Turbulence, (2005).
[70] Croce G., D'agaro P., Nonino C., Three-dimensional roughness effect on microchannel heat transfer and pressure drop, International Journal of Heat and Mass Transfer, 50 (2007) 5249-5259.
[71] Bejan A., Kraus A.D., Heat transfer handbook, John Wiley & Sons, 2003.
[72] Ozisik M.N., Heat transfer: a basic approach, (1985).
[73] Ostrach S., Natural convection in enclosures, Journal of Heat Transfer, 110 (1988) 1175-1190.
[74] Bajorek S., Lloyd J., Experimental investigation of natural convection in partitioned enclosures, Journal of Heat Transfer, 104 (1982) 527-532.
[75] Lin N.N., Bejan A., Natural convection in a partially divided enclosure, International journal of heat and mass transfer, 26 (1983) 1867-1878.
[76] Yucel N., Ozdem A.H., Natural convection in partially divided square enclosures, Heat and Mass Transfer, 40 (2003) 167-175.
[77] Ruhul Amin M., Natural convection heat transfer in enclosures fitted with a periodic array of hot roughness elements at the bottom, International journal of heat and mass transfer, 36 (1993) 755-763.

[78] Wang G.v., Vanka S., Convective heat transfer in periodic wavy passages, International Journal of Heat and Mass Transfer, 38 (1995) 3219-3230.
[79] Adjlout L., Imine O., Azzi A., Belkadi M., Laminar natural convection in an inclined cavity with a wavy wall, International Journal of Heat and Mass Transfer, 45 (2002) 2141-2152.
[80] Ashjaee M., Amiri M., Rostami J., A correlation for free convection heat transfer from vertical wavy surfaces, Heat and Mass Transfer, 44 (2007) 101-111.
[81] Meyer L., Thermohydraulic characteristics of single rods with three-dimensional roughness, International Journal of Heat and Mass Transfer, 25 (1982) 1043-1058.
[82] O'Hanley H., Coyle C., Buongiorno J., McKrell T., Hu L.-W., Rubner M., Cohen R., Separate effects of surface roughness, wettability, and porosity on the boiling critical heat flux, Applied Physics Letters, 103 (2013) 024102.
[83] Chang J., You S., Enhanced boiling heat transfer from microporous surfaces: effects of a coating composition and method, International Journal of Heat and Mass Transfer, 40 (1997) 4449-4460.
[84] Hollands K., Raithby G., Konicek L., Correlation equations for free convection heat transfer in horizontal layers of air and water, International Journal of Heat and Mass Transfer, 18 (1975) 879-884.
[85] Taylor J.B., Carrano A.L., Kandlikar S.G., Characterization of the effect of surface roughness and texture on fluid flow—past, present, and future, International journal of thermal sciences, 45 (2006) 962-968.
[86] De Graaf J., Van der Held E., The relation between the heat transfer and the convection phenomena in enclosed plane air layers, Applied Scientific Research, Section A, 3 (1953) 393-409.
[87] Wang H., Iovenitti P., Harvey E., Masood S., Numerical investigation of mixing in microchannels with patterned grooves, Journal of Micromechanics and Microengineering, 13 (2003) 801.
[88] Bhavnani S., Bergles A., Natural convection heat transfer from sinusoidal wavy surfaces, Wärme-und Stoffübertragung, 26 (1991) 341-349.
[89] Kaviany M., Effect of a protuberance on thermal convection in a square cavity, Journal of heat transfer, 106 (1984) 830-834.
[90] Acharya S., Jetli R., Heat transfer due to buoyancy in a partially divided square box, International journal of heat and mass transfer, 33 (1990) 931-942.
[91] Shi X., Khodadadi J., Laminar natural convection heat transfer in a differentially heated square cavity due to a thin fin on the hot wall, Journal of Heat Transfer, 125 (2003) 624-634.
[92] Hortmann M., Peric "M, Scheuerer G (1990) Finite volume multigrid prediction of laminar natural convection: Benchmark solutions, Int J Numer Meth Fluids, 11 189-207.
[93] Mayne D.A., Usmani A.S., Crapper M., h-adaptive finite element solution of high Rayleigh number thermally driven cavity problem, International Journal of Numerical Methods for Heat & Fluid Flow, 10 (2000) 598-615.
[94] Le Quéré P., De Roquefortt T.A., Computation of natural convection in two-dimensional cavities with Chebyshev polynomials, Journal of Computational Physics, 57 (1985) 210-228.

[95] Mezrhab A., Moussaoui M.A., Jami M., Naji H., Bouzidi M.h., Double MRT thermal lattice Boltzmann method for simulating convective flows, Physics Letters A, 374 (2010) 3499-3507.

SECTION

2. CONCLUSION

The present study was conducted using an algorithm based on a single relaxation time BGK model of LBM for different cases. The range of Ra number from 10^3 to 10^6 was explored for a Newtonian fluid of Pr number 1.0. The significant conclusions gathered from this study are following:

- A numerical scheme based on single relaxation time BGK model of LBM was found stable up to Ra number of $5x10^5$ and $1x10^6$ for cavities heated at bottom
- In the absence of any perturbation, no transition was observed up to Ra number $1x10^5$ in RB convection
- Thermal and mechanical (roughness) perturbations produced almost same results for average heat transfer in RB convection
- Roughness causes a delay in the onset of natural convection in RB convection and Rectangular cavity heated at bottom
- A small roughness of dimensionless amplitude 0.025, does not have significant effects on the average heat transfer and fluid flow in all cases
- Reduction in the average heat Transfer increased with increasing roughness elements amplitude
- Maximum reduction in the average heat transfer was observed when roughness was present on both the hot and cold walls simultaneously
- Amount of average heat transfer reduction was 27%, 41%, and 51% was observed for Square, Rectangular cavity and RB convection respectively
- Most significant factors affecting heat transfer are: formation of eddies, reduction in the fluid volume, variation in the characteristic length, and obstruction in the fluid velocity
- Modified Ra number should include variation in the volume of fluid, characteristic length, and other factors

3. FUTURE WORK

A numerical study was carried out in two-dimensional geometries to investigate the role of surface roughness during natural convection. An algorithm based on a single relaxation time BGK model of LBM was utilized. Initial results reported here with sinusoidal roughness elements, following are future recommendations:

i. A single relaxation time BGK model of LBM need to build to investigate three dimensional roughness elements. Present computational code should be upgraded to run for parallel computing using GPU to analyze large scale systems in the presence of roughness elements.
ii. Experimental studies should be performed to validate the present results and to enhance the range of present simulations.
iii. Simulations should be carried out for turbulent region of flow with sinusoidal roughness elements to make a rationale conclusion regarding the role of sinusoidal roughness elements during natural convection for laminar as well as turbulent region.

VITA

Muhammad Yousaf was born in the city of Gujrat, Punjab, Pakistan. He obtained his B.S. in Physics from University of Engineering and Technology (UET) Lahore in 2005 and joined Institute of Space Technology Lahore as an Assistant Manager (Physics). He was selected for the Pakistan Nuclear Regulatory Authority (PNRA) fellowship for a M.S. in Nuclear Engineering at Pakistan Institute of Engineering & Applied Sciences (PIEAS) Islamabad in 2006. He completed his M.S. in 2008 as a fellow in Nuclear Engineering. After his MS, he was appointed in PNRA as a Scientific Officer in Center for Nuclear Safety. In December, 2010, he was promoted to Senior Scientific Officer and then he resigned to leave for his Ph.D. In spring 2011, he joined Missouri University of Science and Technology, and received his Ph.D. in Nuclear Engineering in May 2016. During his stay at Missouri S & T, he worked as a Graduate Research and Teaching Assistant. He was selected for AREVA Summer fellowship in 2012, and worked on Emergency Core Cooling Systems (ECCS) of High Temperature Reactor (HTR). His research interests are in the areas of Reactor Thermal Hydraulics, Nuclear Reactor Safety, Radiological Engineering, Natural Convection and Passive Safety Systems, and Radiation Detector Dead-time and Spectroscopy.